BEAMFORMING IN THE UPLINK AND DOWNLINK CHANNELS OF A CELLULAR CDMA COMMUNICATION SYSTEM

by

Tao Luo

A thesis submitted to the
Department of Electrical and Computer Engineering
in conformity with the requirements
for the degree of Master of Science.(Engineering)

Queen's University
Kingston, Ontario, Canada
February 1998

Abstract

As the 900MHz cellular subscriber population continues to grow at a rapid pace, service providers have to find new methods of enhancing system capacity and coverage. This is also true for the operators of the recent 1.9 GHz Personal Communications Systems (PCS). An antenna array at the base station may be incorporated in future systems for increasing system capacity. Digital beamforming based on antenna arrays will be one key technique in fulfilling this task. In beamforming, we multiply a complex-valued weighting vector to the outputs of antenna array and sum these outputs to generate a signal for each user. As each user will have a unique weight, we can select the weights to greatly decrease interference from other users, and therefore increase system capacity.

Using a base station antenna array in cellular code-division multiple-access (CDMA) communications systems can potentially increase system capacity several-fold. Beamforming shows great potential for improving signal-to-interference-noise ratios (SINR) which in turn increases cell capacity. To perform optimum SINR beamforming, we need to estimate an array response vector and an interference-noise (IN) covariance matrix. Currently, estimation of the IN covariance matrix for optimum beamforming requires great computational cost. As a result, sub-optimum beamforming (maximum SNR) is used which does not require the IN matrix. However, when the number of users is not very large and the distribution of users is not uniform, there is a large gap between maximum SINR and maximum SNR beamforming performance. We propose a direct signal cancellation method to estimate the interference-noise covariance matrix which increases the SINR and decreases computation compared with previous work in this area. This new algorithm potentially increases system capacity and coverage. Since DOA estimation of mobiles is also improved, the method can

potentially be applied to transmit beamforming in the downlink to further increase system capacity.

The combined effect of estimate error from finite-sample data, interference and thermal noise in a generic DS-CDMA cellular system was analytically determined. We quantify how finite-sample errors in the estimation in both the array response and MAI covariance matrices affect system SINR. As an application of the above results, we consider our proposed optimum beamforming algorithm. We show that finite-sample estimation errors in the array response vector are independent of multi-access interference errors in this algorithm.

In a cellular CDMA communication system, there are two links in the system: the uplink and the downlink. The downlink refers to that from the base station to the mobile. As the capacity is only partially determined by the uplink, we also address the downlink. One expensive solution to improving downlink capacity is to perform beamforming at each mobile [75]. Alternatively, in [71, 52, 51], researchers have shown that capacity can be improved with transmitting antenna array at the base station. In this thesis we consider a transmitting antenna array at the base station and a single antenna at the mobile. In order to perform downlink beamforming, we need to know the downlink channel vectors for all the users in the same cell. For the uplink, the base station can estimate the channel vector for the mobile, there is no such inherent feedback for the downlink. Therefore, the key problem in the downlink is how to estimate downlink channel vector. We present a novel approach for downlink channel estimation through the feedforward method. This has not been proposed for CDMA systems previously. The proposed algorithm estimates downlink channel vectors much more accurately and reduces the amount of transmission overhead. Therefore, the overall system capacity may be increased.

Acknowledgements

I would like to thank my supervisor, Dr. Steven D. Blostein, for his excellent guidance, encouragement and support during my time at Queen's. His guidance makes me go beyond what I might have previously considered my limits and finish this thesis in less than one and half years.

I would like to thank my committee members, Dr. S.G. Akl, Dr. P.J. McLane and Dr. C.Zarowski for carefully reviewing my thesis and providing useful suggestions.

To all of the friends and colleagues I have had over the past year, thanks for all of the good times and assistance, both technical and non-technical. Special thanks for Wan-Yi (Wemby) Shiu for her simulation program and Geoff Colman for his assistance in language usage.

I would like to thank my parents and other family members for their support and encouragement throughout my life.

I would like to thank my wife, Lijia, for her patience, understanding and support through my study here.

This work was supported by the Canadian Institute for Telecommunications Research and the School of Graduate Studies and Research at Queen's University.

Contents

List of Tables

List of Figures

List of Symbols

$\mathbf{E}$	expectation
$\mathbf{R}$	interterference plus noise matrix
φ	angle
rr	scalar signal
F_θ	radiation gain
s	desired signal
d	space between antennas
λ	wavelenght of carrier
$\mathbf{K_{ula}}$	constant
$\mathbf{K_{circular}}$	constant
γ	angle
f	frequency
$d(f)$	doppler spectrum
f_d	doppler frequency
μ	mean value
π	constant
$p(x)$	probability density
$AWGN$	additive white Gaussian noise
R	correlation
ULA	uniformly spaced linear array
$CDMA$	code division multiple access
$\mathbf{E}_b/\mathbf{N}_0$	signal energy to interference plus noise density ration
u	a real variable

$\mathbf{a}_z$	a vector
$\mathbf{b}_z$	a vector
$\mathbf{c}_z$	a vector
$\mathbf{b}_y$	a vector
$\mathbf{c}_y$	a vector
$\mathbf{sen_{matrix}}$	sensitivity of signal to noise ratio with respect to covariance error
$\mathbf{sen_{array}}$	sensitivity of signal to noise ratio with respect to array vector error
$\approx$	approximation
η	small error vector
K	constant
∂	differential symbol
$\mathbf{F}$	matrix
$\mathbf{T}$	transpose of a matrix
$\|\|.\|\|$	Euclidean norm
$\mathbf{d}$	vector
$\mathbf{c}$	perturbed vector
$\mathbf{Tr}$	Trace of matrix
$\mathbf{\Delta}$	error matrix
ε	perturbation matrix
$\mathbf{Q}$	interference plus noise covariance matrix
$\hat{\mathbf{Q}}$	estimated interference plus noise covariance matrix
σ_w	perturbation variance of weights
σ_a	perturbation variance of array vector
δ	Kronecker delta
$\mathbf{BPSK}$	binary phase shift keying
$\mathbf{Var}$	variance
$\mathbf{R}_{in}$	autocorrelation function of interference plus noise
β	distribution symbol
$\mathbf{R}_{na_i}$	autocorrelation function of interference plus noise
ν	constant

ς	constant
$\hat{\eta}$	normalized SINR
$\tilde{\eta}$	normalized SINR
$\widehat{\mathbf{SINR}}$	perturbed SINR due to weights error
$\widetilde{\mathbf{SINR}}$	perturbed SINR due to covariance error and array error
$\overline{\mathbf{SINR}}$	perturbed SINR due to array error
γ	constant
$\mathbf{MAI}$	interference plus noise covariance
$\mathbf{R}_{IN}$	true interference plus noise covariance
cc	a new PN sequence
ξ	consant
ϕ	consant
$\mathbf{R}_{xx}$	autocorrelation function of input signal
$\mathbf{R}_{xx_i}$	autocorrelation function of input signal
$\mathbf{R}_{zz_i}$	post autocorrelation function of despreading signal
$\hat{\mathbf{R}}_{zz_i}$	maximum likelihood estimated post autocorrelation function of despreading signal
$\mathbf{R}_{yy_i}$	post autocorrelation function of despreading signal
$\hat{\mathbf{R}}_{yy_i}$	maximum likelihood estimated post autocorrelation function of despreading signal
$\mathbf{z}$	despreading signal
$\mathbf{y}$	despreading signal
$\mathbf{x}$	spreading signal
$\int$	integration
L	spreading gain
θ	angle of arrival
$\hat{\theta}$	estimated angle of arrival
$\mathcal{N}$	Normal distribution
∞	infinite
p	time limited pulse
T_c	chip period
$\pm$	stacked positive and negative sign

c	Pseudo noise sequence
SINR	Signal to noise plus interference ratio
$\mathbf{SINR}_{max}$	optimum signal to noise plus interference ratio
$\mathbf{SINR}_{imax}$	optimum signal to noise plus interference ratio
IN	interfence plus noise matrix
t	time index
$\mathbf{x}$	uplink baseband received signal
$\mathbf{r}$	received vector signal
$\mathbf{r}_{up}(m)$	uplink received vector signal from mth mobile at the base station
$\mathbf{a}_k(\theta_{k,l}, \omega_{up})$	uplink array response vector for kth user' lth path
$\beta_{up,k,l}(mT_b, \omega_{up})$	uplink channel gain for kth user' lth path
$b_k(mT_b - \tau_{k,l})$	symbol for kth user's lth path
α	complex gain
$\alpha_{k,l}(mT_b, \omega_{up})$	uplink fast fading gain for kth user's lth path
$\Gamma_{k,l}(mT_b)$	shadowing of mth symbol of kth user's lth path
d_k	distance between kth user and the base station
$\theta_{k,l}$	Direction of arrival for lth path of kth user
τ	time delay
$\tau_{k,l}$	relative delay of kth user's lth path
$\tau_{i,j}$	relative delay between ith user and jth user
$\tau_{i,k}$	relative delay between ith user and kth user
$\tau_{i,l}$	relative delay between ith user and lth user
$\tau_{i,i}$	relative delay between ith user itself
T_b	symbol period
ω_{up}	uplink carrier frequency
ω_{down}	downlink carrier frequency
$\hat{n}$	path loss index
$S_{k,l}$	total number of scatters for kth user' lth path
l	path index
K	constant gain
C_i	complex reflection coefficiency of ith scatter

v	speed of the mobile
c	speed of the light
Ω_i	angle between the motion direction of the mobile and the ith local scatter
m	index of the symbol
$\sigma_{up,\beta_{k,l}}$	variance of the uplink channel gain for lth path of kth user
$r_{down,k,l}$	downlink received signal of lth path of kth user
$\mathbf{w}_{k,l}$	weight vector for lth path of kth user
$\mathbf{a}_k(\theta_{k,l}, \omega_{down})$	downlink array response vector for lth path of kth user
$\beta_{down,k,l}(mT_b, \omega_{down})$	downlink channel gain of lth path of kth user
$\alpha_{k,l}(mT_b, \omega_{down})$	downlink fast fading gain of lth path of kth user
$\sigma_{down,\beta_{k,l}}$	variance of the downlink channel gain for lth path of kth user
τ_{max}	maximum delay in the city
$\mathbf{a}$	array response vector
$\hat{\mathbf{a}}$	estimated array response vector
r_k	downlink received signal for kth user
$\mathbf{w}$	weights vector
$\mathbf{w}_i$	weights for ith user
$\hat{\mathbf{w}}_i$	weights for ith user
$\hat{\mathbf{w}}$	perturbated downlink weights
$\tilde{\mathbf{w}}_i$	weights for ith user
$\dot{\mathbf{w}}_i$	weights for ith user
$\mathbf{w}_j$	downlink beamforming weights for jth user
$\mathbf{w}_k$	downlink beamforming weights for kth user
b	symbol for a user
b_k	downlink symbol for kth user
b_l	downlink symbol for lth user
b_j	symbol for jth user
b_i	symbol for ith user
$\mathbf{w}$	downlink beamforming total weights
$\hat{b}_k$	downlink demodulated symbol for kth user

ζ	downlink positive constant
y_k	downlink output of the correlator of kth user
$y_{k,p}$	perturbed downlink output of the correlator of kth user
BER	downlink bit error rate
SNR	signal to noise ratio
$\mathbf{SNR}_k$	downlink signal-to-noise ration for kth user
$\mathbf{SNR}_{k,p}$	perturbed signal to noise ratio for kth user
$\mathbf{SNR}_{PRLS}$	signal to noise ratio due to PRLS
$\widehat{\mathbf{SNR}}_{PRLS}$	simplied signal to noise ratio due to PRLS
ρ_{PRLS}	relative simplied signal to noise ratio due to PRLS
σ^2	downlink thermal noise variance
P	downlink transmitted power
P	power of the signal
P_j	transmitted power for jth user
P_i	transmitted power for ith user
P_l	transmitted power for lth user
N	total number of users
$\mathbf{P}_{ideal}$	downlink ideal scatter matrix
$\mathbf{w}_{ideal}$	downlink ideal weights
$\mathbf{P}_{estimate}$	downlink estimated scatter matrix
$\mathbf{w}_{estimate}$	downlink estimated weights
ρ_{SNR}	downlink signal-to-noise normalization
$\mathbf{n}_k$	downlink noise vector for kth user
ψ_k	downlink noise variance constant
g	downlink ideal scalar channel gain
$\hat{g}$	perturbed downlink ideal scalar channel gain
y_{mmse}	downlink minimum mean square error
$\dagger$	pseudo inverse
n_k	white noise vector for kth user
$\mathbf{n}$	thermal noise vector
$\hat{L}$	index of RLS update

e	error of RLS
ϑ	weighted error
α	forgetting factor
MSE	normalized mean square error
W	weight matrix
F	cross vector
M	number of antenna
e_i	complex scalar
$\dot{e}_i$	supposed complex scalar
A	matrix A
B	matrix B
J	matrix J
D	matrix D
S	inverse of weight matrix
u	matrix u
χ	innovation scalar
ζ	initial scalar value for RLS
G	matrix G
T	matrix T
E	square root of the matrix
U	product of matrix G and E
v_{max}	maximum speed of the mobiles
v_{min}	minimum speed of the mobiles
S	scatter matrix
$\rho_{weight,i}$	weight relative change
$\in$	belong to
C	complex set C
$Range$	Range symbol
$\underline{\mathbf{x}}$	a vector
$\underline{\theta}$	a vector
$\underline{\mathbf{w}}$	null vector

$\forall$	for all
Υ	null space
$\triangleq$	definition symbol
$\mathbf{0}$	null vector
$\mathbf{0}$	null matrix
F_{Total}	total number of symbols for a PRLS period
F_f	number of symbols in feeding forward stage
F_e	number of symbols in PRLS algorithm
F_b	number of symbols in feeding back
F_u	number of symbols in calculating the principal eigenvector
ϖ	pertubation scale factor
$\delta_{\mathbf{w}_i}$	perturbation weight vector
$\delta_{\mathbf{w}_L}$	perturbation weight vector
$\mathbf{I}$	identity matrix
P_{extra}	extra power due to perturbation
ρ_{extra}	relative extra power due to perturbation
κ	a complex constant
$\mathbf{SNR}_{opt}$	ideal signal to noise ratio
b	number of the quantized bits
r	total number of probing signals

Chapter 1

Introduction

1.1 Motivation

The concept of cellular radio can be traced back to the 1960s[31, 12]. At the very beginning, there was no frequency reuse. Each frequency was used only once in the geographical area in the band of 150 or 450 MHz. Later, a paired band of 666 channels in the 800 MHz band range was introduced [15]. Frequency reuse was introduced to improve spectral efficiency by using small cells in the serving area. Frequency-division multiple access (FDMA) implements partial frequency reuse to prevent co-channel interference; time-division multiple access (TDMA) reuses time slots. In order to meet the needs of an ever-accelerating worldwide demand for mobile and personal portable communications, the spread spectrum communication technique was introduced to commercial wireless applications. This makes universal frequency reuse possible. Code-division multiple access (CDMA) was introduced as a strong candidate for the current 900 MHz and future 1.9 GHz personal communications systems (PCS). As CDMA is interference-limited, by suppressing these noise-like interferences, we may improve the system capacity and the quality of the communication system. A detailed tutorial of spread spectrum and CDMA may be found in [16, 35, 58, 59].

Beamforming can be used to suppress interference by using an antenna array at the base station, therefore, increasing the system capacity. Digital beamforming based on the antenna array will be one key technique in fulfilling this task. In beamforming, we apply a complex-valued weighting vector to the outputs of the antenna array and

sum the results to generate a signal for each user. As each user has unique weights, we may select the weights to greatly decrease the interference from other users, and therefore increase system capacity.

The author feels it is more general to study a generic CDMA system instead of going to a specific protocol such as IS-95 [62]. It is desired to use optimum beamforming with low computational complexity to maximize the system capacity and performance. This leads to a novel algorithm for optimum uplink beamforming. In a real system, there are always estimation errors. Analysis of these errors leads to some robust algorithms, therefore improving system capacity. This brings up an original error analysis of those error effects on a DS-CDMA communication system. As the system capacity is only partially determined by the uplink, we need to deal with downlink beamforming as well. This results in a novel downlink beamforming technique in a DS-CDMA communication system.

1.2 Summary of contributions

The following is a brief summary of the contributions made by this thesis. A more detailed summary may be found at the end of the thesis in Section 6.2.

- An original optimum uplink beamforming algorithm employing signal cancellation , is proposed with an improvement in performance both in output signal-to-noise-plus-interference ratio ($SINR$) and direction of arrival (DOA) estimation.

- A theoretical analysis of the signal cancellation method was conducted and compared with the code-filtering method in [51, 49].

- An original analysis of beamforming errors on a DS-CDMA communication system was conducted. Several closed-form expressions of these errors' effects on the output $SINR$ were obtained.

- The above error analysis was applied to the proposed signal cancellation method.

- A novel downlink channel estimation technique was proposed.

- The recursive least-squares (RLS) algorithm was applied to adaptive updating of channel estimates. Further, a perturbed recursive least-squares (PRLS) algorithm was proposed and analyzed.

1.3 Thesis outline

Chapter 2 introduces the basic signal model and channel model that will be used in the rest of the thesis. A signal cancellation method for optimum uplink beamforming is developed in Chapter 3. Chapter 4 deals with error analysis of uplink beamforming and its application. In Chapter 5, we describe a feedforward downlink beamforming technique and its application and analysis. Finally, Chapter 6 summarizes the contributions and future directions.

Chapter 2

DS-CDMA system model

2.1 Introduction

Code-division multiple access (CDMA) is a strong candidate for future personal communications systems (PCS). There are two types of basic CDMA communication systems: one is direct sequence code-division multiple access (DS-CDMA), the other is frequency-hopping code-division multiple access (FH-CDMA). A detailed comparison of these two systems may be found in [8]. FH-CDMA is more suitable for military communications while DS-CDMA is more suitable for commercial communications. This thesis is devoted to a DS-CDMA communication system.

In a DS-CDMA communication system, there exist two communication links: from a mobile to a base station (uplink) and from a base station to a mobile (downlink). The system capacity is defined by both links. Therefore, beamforming should be implemented in both the uplink and downlink to obtain a balanced capacity. In this thesis, we consider a transmitting and receiving antenna array at the base station only. The cost and complexity of implementing an antenna array at the mobile is much greater over-all than that of implementing only at each base station [75].

As beamforming is only concerned with the baseband modulation and demodulation of signals, we need not consider the coding and decoding process although such process should boost the system performance as shown in Figure 2.1 and Figure 2.2.

Therefore, we are only concerned about a simple signal model including spreading and despreading instead of a complex model which includes interleaving, coding,

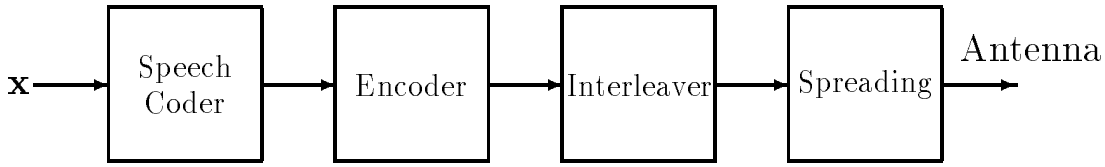

Figure 2.1: Conceptual uplink transmitter model at the mobile

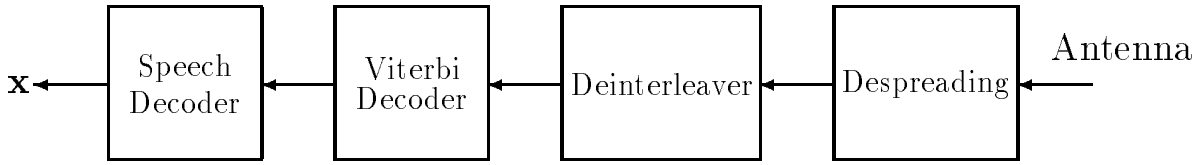

Figure 2.2: Conceptual uplink receiver model at the base station

deinterleaving and decoding.

There are many topologies of antenna arrays available. Without loss in generality, we consider the two most common topologies in the simulations contained in this thesis: uniform linear array (ULA) and circular antenna array.

This chapter describes relevant background material for the following chapters including: basic spreading and despreading processes and the relevant uplink and downlink signal models of a DS-CDMA system, the uplink and downlink channel models and the principle of beamforming using antenna arrays.

A detailed introduction of CDMA may be found in [77, 57]. A comprehensive introduction of the mobile channel model used may be found in [34, 29]. Array signal processing background may be found in [65, 27, 30, 39, 60, 41]. A tutorial introduction to beamforming may be found in [74].

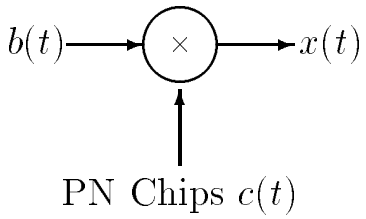

Figure 2.3: Spreading in the uplink

2.2 DS-CDMA uplink and downlink data model

Figure 2.3 shows the spreading process of a generic DS-CDMA communication system. We are concerned with the output of the spreading process. We may reasonably assume that the input to the spreading process is a random variable. As we consider a **BPSK** signal in this thesis, $b(t)$, may only take the value of $+1$ or -1. In Figure 2.3, $c(t)$ is a Pseudo-Noise(PN) sequence taking the value of $+1$ or -1. We address the definition of the PN sequence later. The PN sequence is unique for each user. Suppose the symbol period is T_b and the chip period is T_c. After spreading, the output signal may be written as:

$$\mathbf{x}(t) = \sum_{i=0}^{L-1} \sqrt{P} b(t) c(t - iT_c) \tag{2.1}$$

where P is the power of the signal and

$$L = \frac{T_b}{T_c} \tag{2.2}$$

is termed the processing gain. At the receiver, we simply use the same PN sequence to despread the received signal and integrate over one symbol period T_b as shown in Figure 2.4.

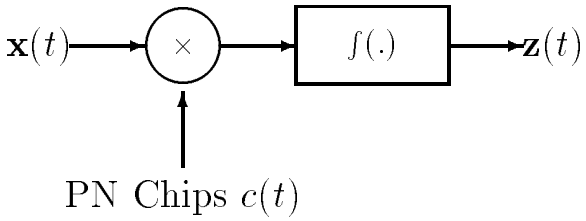

Figure 2.4: Despreading at the base station

There are certain properties of a PN sequence that we have exploited in the signal cancellation algorithm proposed in this thesis. The PN chip sequences are generated by a PN code generator and the desired random sequence should have the following properties [25]:

I Probabilities of "0" and "1" are each $\frac{1}{2}$

II Run lengths(of zeros or ones) are as expected in a coin-flipping experiment; half of all run lengths are unity; one-quarter are of length two; one-eighth are of length 3; a fraction of $\frac{1}{2^n}$ are of length n for all finite n.

III If the random sequence is shifted by any non-zero number of elements, the resulting sequence will have an equal number of agreements and disagreements with the original sequence.

The sequences which satisfy the above three properties are termed Pseudo-Noise sequences. If $c(t)$ is a PN sequence, it is zero mean, i.e.,

$$\mathbf{E}\{c(t)\} = 0 \tag{2.3}$$

Another important property is the cross-correlation between different users' PN sequences. Let $c_i(t)$ and $c_j(t)$ represent the PN sequences of the user i and the user j respectively. We expect the cross-correlation to be as small as possible, ideally, zero, i.e.,

$$\mathbf{E}\{c_i(t)c_j(t)\} = 0 \tag{2.4}$$

However, due to the difference in time delay of different users' signals arriving at the base station,

$$\mathbf{E}\{c_i(t)c_j(t-\tau)\} \neq 0 \tag{2.5}$$

when τ is not a multiple of the chip period T_c. This accounts for the interferences from the other users sharing the same frequency band in the uplink because the uplink uses asynchronous transmission. For the downlink, due to synchronous transmission, the interferences from other users are zero in the same cell when there is no multipath.

Now we examine the autocorrelation function of a PN sequence. It is easy to show

that [55]

$$R(\tau) = \begin{cases} 1 - \frac{|\tau|}{T_c} & \text{if } |\tau| \leq T_c \\ 0 & \text{otherwise} \end{cases} \tag{2.6}$$

A plot of Eq. (2.6) is in Figure 2.5. From Eq. (2.6), we may conclude that

$$\mathbf{E}\{c_i(t)c_i(t-\tau)\} \neq 0 \qquad for\ |\tau| \leq T_c \tag{2.7}$$

Non-zero autocorrelation causes self-interference when the multipaths are present and the relative delays of these multipaths are less than one chip period T_c. If the delay is greater than one chip period, we may treat this as signals originating from a different user in the same cell. A detailed derivation of the crosscorrelation and autocorrelation functions of a PN sequence may be found [72, 73].

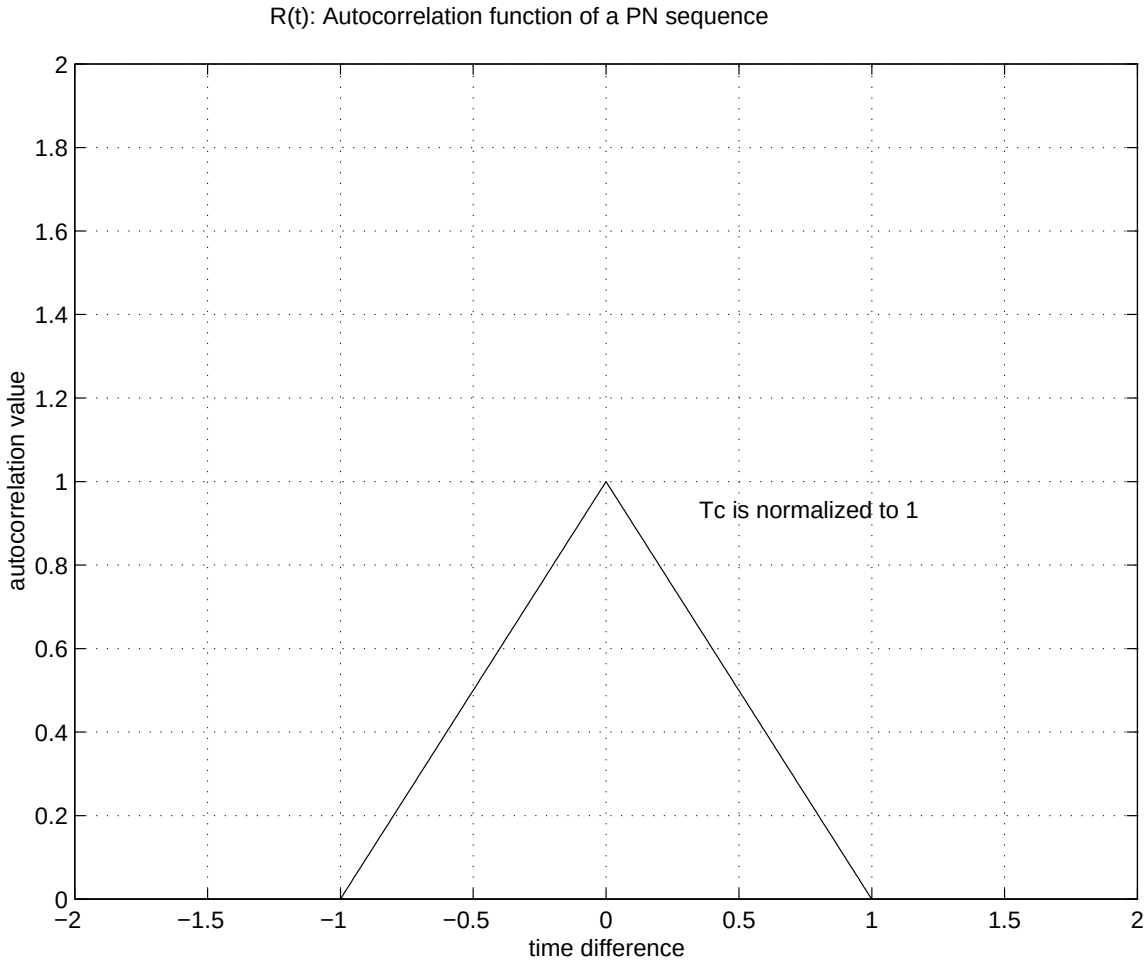

Figure 2.5: Autocorrelation function of a PN sequence

2.3 Channel model in a cellular system

Here we consider a channel model in a cellular communication system. It is different from other communication systems such as satellite communication systems, or military communication systems. In a satellite communication system, our attention is on the large path loss due to the long distance from the mobile to the satellite. An additive white Gaussian noise(AWGN) channel may be suited for this case. In a military communication system, the interference to the desired signal is narrow-band jamming as well as thermal noise. In a cellular CDMA communication system, due to universal reuse of frequencies, each user sharing the same frequency band is a source of interference. Thermal noise is less important here as a cellular CDMA communication system is basically interference-limited. The path loss is less severe because of small cell size. However, small cell size also causes interference to nearby base stations. Cellular systems have been implemented in urban areas with high population density, where tall buildings and trees attenuate the signals to some extent. As the mobile moves, the Doppler effect causes signal carrier frequency expansion as will be described in Section 2.3.3. Also, there are always scatterers around the mobile which cause severe fast fading. In the following sections, we will examine each of these effects.

2.3.1 Path loss in a cellular system

The propagation path between a mobile and a base station is complicated by the antenna height of the base station and mobiles, the carrier frequency used, the terrain, local scatterers around the mobile, large scatterers such as buildings and mountains. The path loss is defined as the difference between the effective power transmitted and average field strength of the received signal. The field strength of the received signal reflects the magnitude of the signal transmitted at the carrier frequency band. There is no closed-form expression available for the actual path loss. Some propagation models have already been developed such as the Egli Model, the Longley-Rice model, the Okumura method and Hata model in [56]. In this thesis, for simplicity, we assume a fourth power loss in proportion to the distance between the base station and the

mobiles.

2.3.2 Shadowing effect

Often, the long-term average of the signal strength varies slowly as well. This is caused by large obstacles between the base station and the mobiles such as high buildings and foliage. This random process is generally assumed to be lognormally distributed or when all the values associated with this random process are measured in decibels, it is a normal distribution. Suppose x is lognormally distributed, then its density function is:

$$p(x) = \begin{cases} \frac{1}{\sqrt{(2\pi\sigma^2)}x} e^{-(\ln x - \mu)^2/2\sigma^2} & \text{if } x \geq 0 \\ 0 & \text{otherwise} \end{cases} \tag{2.8}$$

The typical value of variance σ^2 in dB ranges from $4dB$ to $12dB$. A plot of the distribution function of Eq. (2.8) is in Figure 2.6.

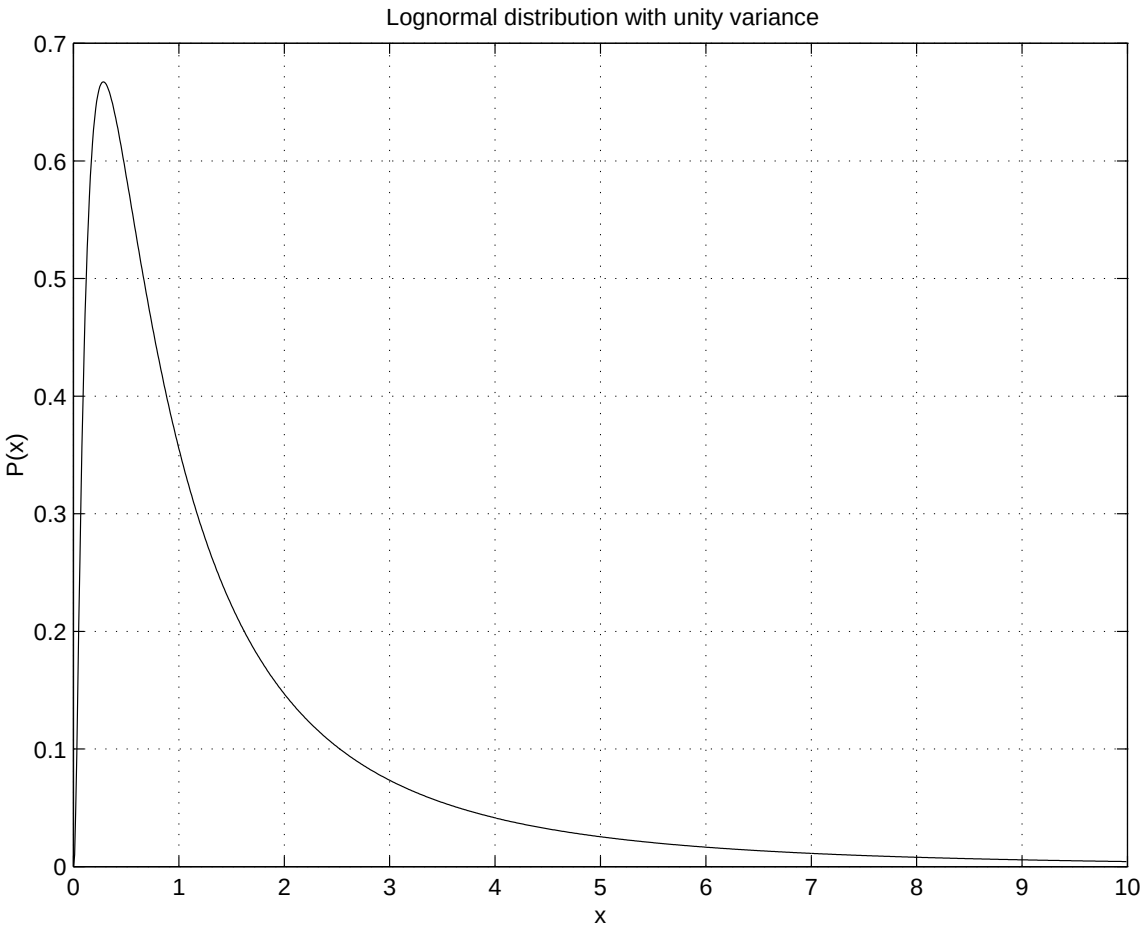

Figure 2.6: Lognormal distribution with unity variance

2.3.3 Fast fading in a cellular system

As there are always some scatterers around the mobiles in an urban area, the magnitude of the signal received by the mobile or by the base station fluctuates. The phase of the received signal changes as well. We use the uplink case for example. Suppose there are a total of $S_{k,l}$ scatterers affecting the lth path of the kth mobile, we may write the complex gain in the direction of θ due to the scatterers and the movement of the mobile as [64]:

$$\alpha(t) = K \sum_{i=1}^{S_{k,l}} C_i e^{j\omega_{up}\frac{v}{c}cos(\Omega_i)t} \tag{2.9}$$

where Ω_i is the angle of local scatterer i with respect to the direction of the mobile velocity vector which is distributed uniformly, C_i is the complex reflection coefficient of the ith local scatterer and exhibits a complex Gaussian distribution, c is the speed of light, K is a constant including the effects of the mobile antenna gain and transmitted power and $f_d = \omega_{up}\frac{v}{c}$ is termed as the maximum Doppler shift. The Doppler effect may be thought of as the spectrum expansion of the carrier frequency. Ideally, for a single frequency carrier, after the channel, the carrier spectrum should consist of two sharp peaks the same as the carrier spectrum before the transmission . Due to the Doppler effect, its spectrum is expanded to

$$d(f) = \begin{cases} \frac{1}{\pi f_d}\frac{1}{\sqrt{1-(f/f_d)^2}} & |f| \leq f_d \\ 0 & \text{otherwise} \end{cases} \tag{2.10}$$

as in Figure 2.7.

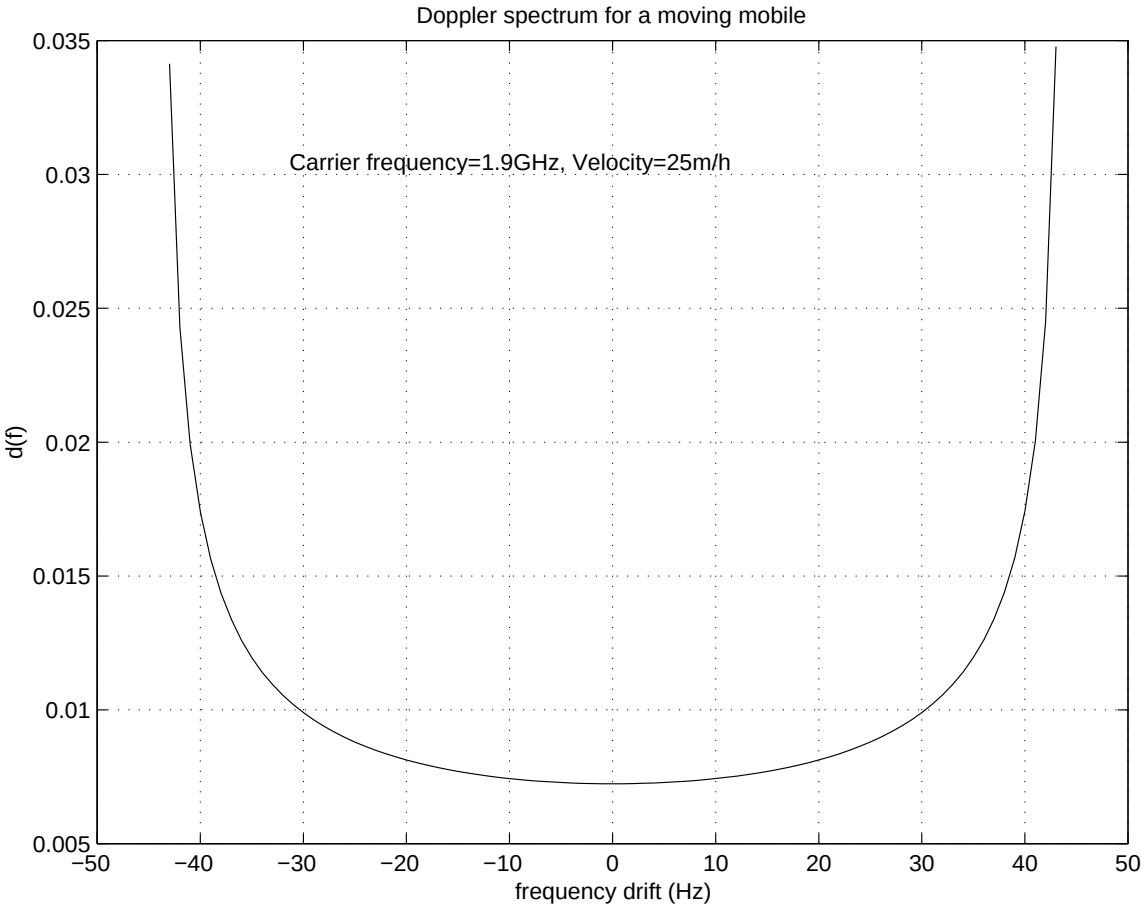

Figure 2.7: Doppler spectrum of a moving mobile

In Chapter 5, we use Eq. (2.9) to derive the relationship between the uplink and downlink channel gain. A typical fast fading channel is plotted in Figure 2.8. We see the channel changes significantly over time. However, as the data rate is high as well, i.e., $9600 bits/sec$, the magnitude of the channel gain is relatively stable for several data symbols as shown in Figures 2.9 and 2.10.

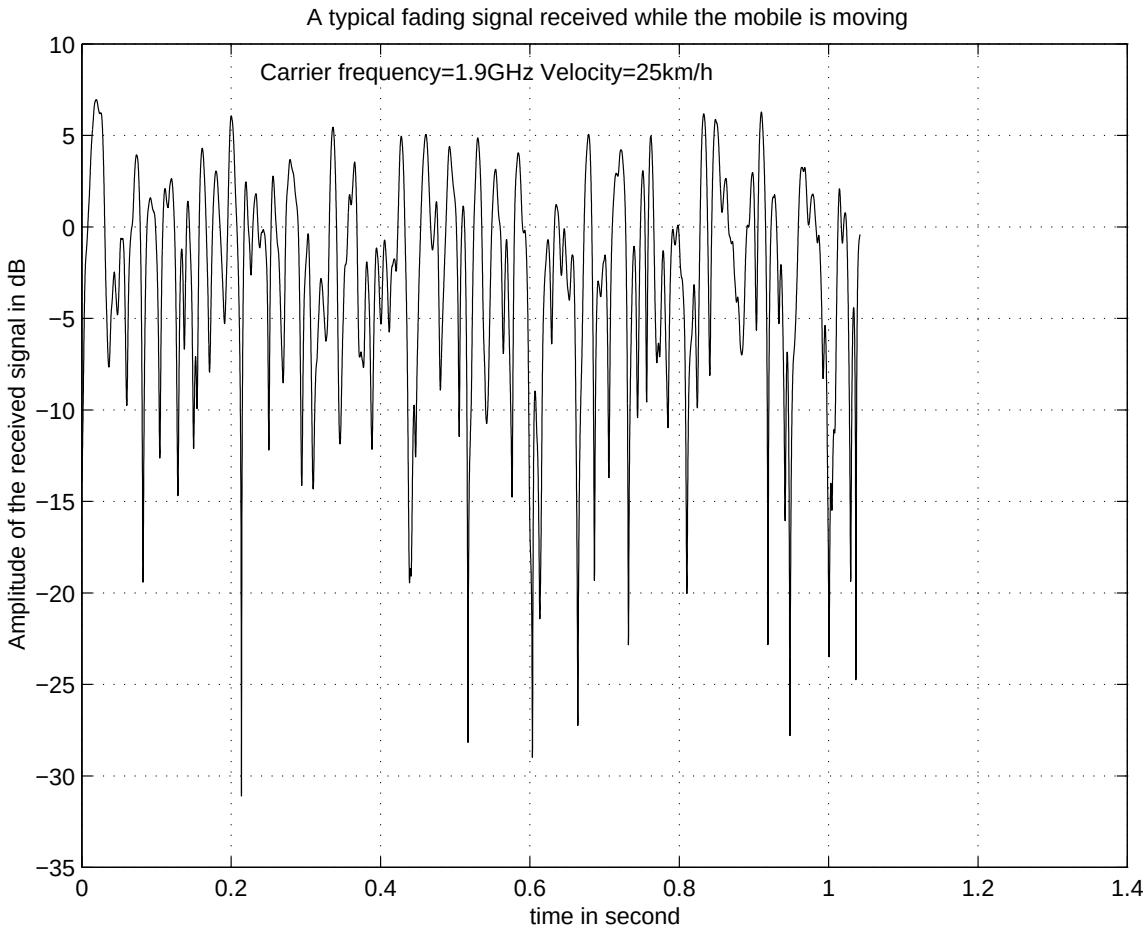

Figure 2.8: A typical fading signal

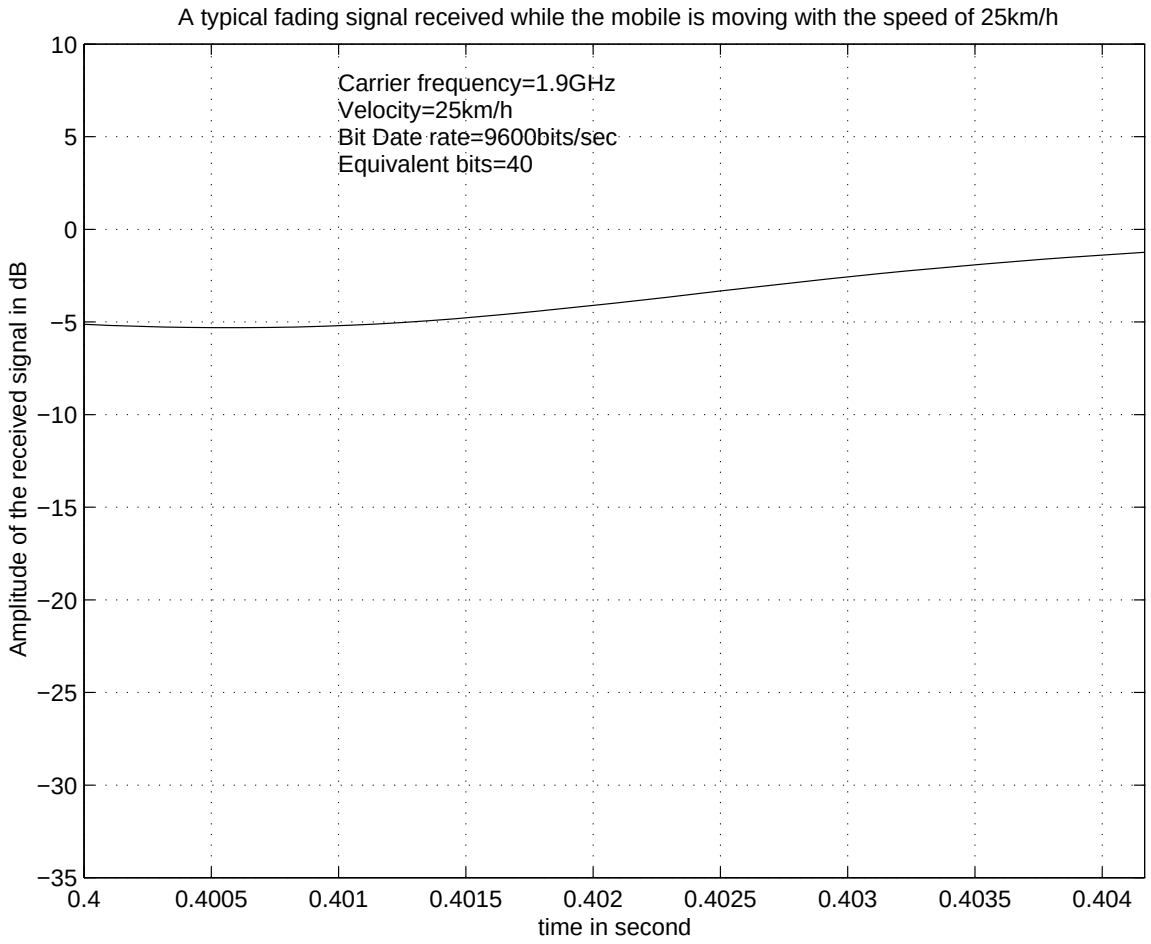

Figure 2.9: An expanded view of the typical fading amplitude: relatively stable variation over several symbols with a speed of 25km/h

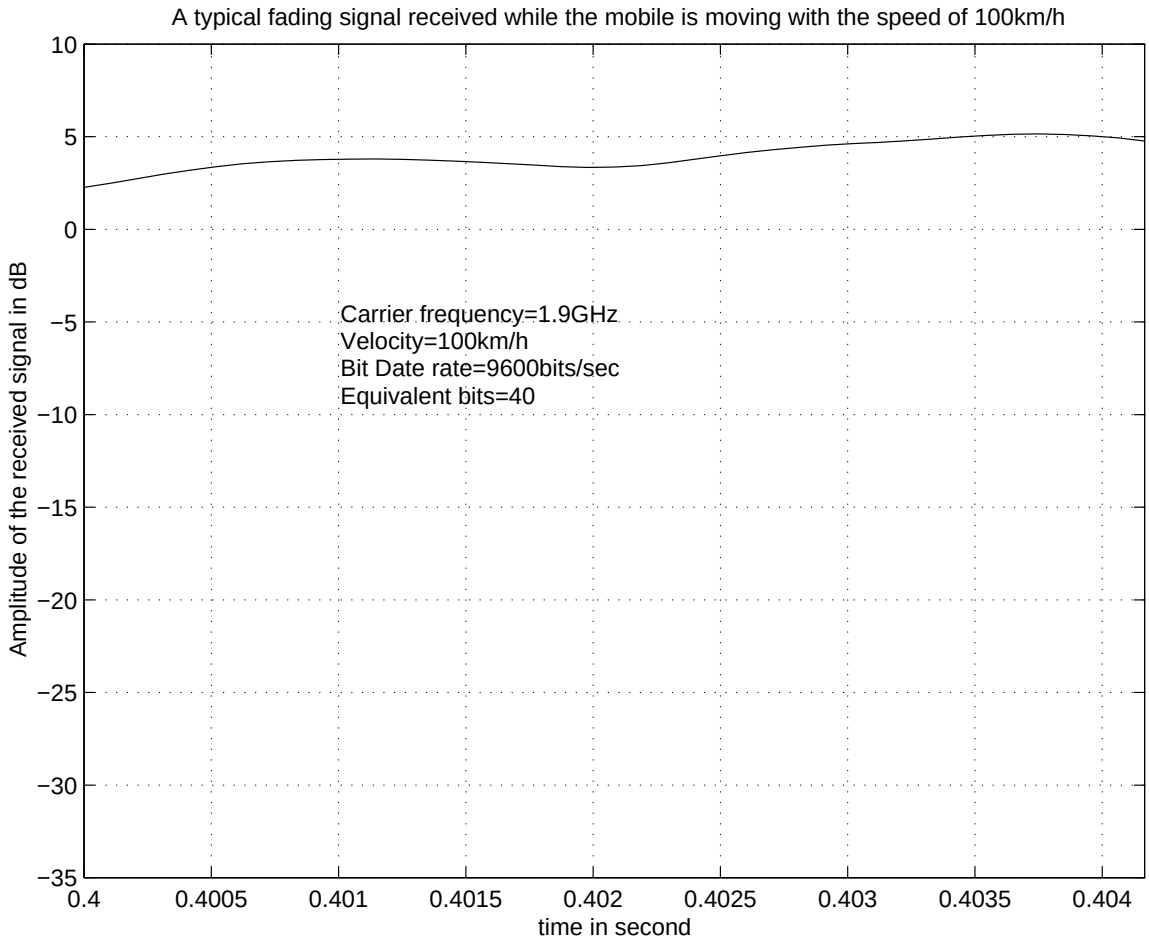

Figure 2.10: An expanded view of the typical fading amplitude: relatively stable variation over several symbols with a speed of 100km/h

2.4 Beamforming and antenna arrays

2.4.1 Multiple antenna array vs a single antenna

In this thesis, we consider a transmitter antenna array and a receiver antenna array at the base station. With careful design, the uplink and downlink may share the same antenna array because the uplink and downlink use different carrier frequencies, therefore their wavelengths are different. In the case of one antenna element, there is only one channel between the base station and the mobile. A multiple-element antenna may be treated as multiple channels in the same frequency band. From the mobile to the base station, it is a single point to multi-point communication; from the base station to the mobile, it is a multi-point to a single point communication as we use an antenna array at the base station and a single antenna at the mobile. A multiple access channel may accommodate more users than one antenna element only. The capacity depends on the relationship of these user signals . When these antenna elements are close to each other, such as one half-wavelength corresponding to the carrier frequency for a single ray, the received signals at the different antenna element may only differ in phase while their magnitudes are nearly the same. This corresponds to perfect statistical correlation. When the antenna elements are far apart from one other, for example, more than 10 wavelengths, the correlation between different antenna elements may be very small [82]. They may be treated as independent channels and the methods exploiting independent signal paths are termed diversity techniques. We consider a closely-spaced antenna array in this thesis. For the case of diversity, the reader may refer to [36, 81, 68, 82, 67]. Due to the local scatterers around the mobiles, there are always many rays arriving at the antenna array from a small angle. The effect of scattering causes magnitude differences in different antenna elements. This cause the difficulty of estimating direction of arrival (DOA) of the mobile in the case of an urban environment. However, in the case of a suburban area or a rural area, scattering may be less of a problem and DOA information may be used in downlink beamforming.

2.4.2 Array response vector

Without loss in generality, we consider a planar array where the centres of all elements lie on a single plane. While we use the uplink for illustration purposes, the analysis also applies to the downlink. As mentioned in Section 2.4.1, we may treat multiple antennas as multiple channel communications. Each channel has a complex gain associated with it. Let $\mathbf{a}_i(\omega_{up}, \theta_i)$ represent the complex gain from the mobile to the ith element of the antenna array, where ω_{up} is the uplink carrier frequency and θ_i is the angle of arrival for the incident ray with respect to the horizontal line. Suppose the array has M elements, we may stack these M complex channel gains to form a vector $\mathbf{a}$,

$$\mathbf{a} = \begin{bmatrix} \mathbf{a}_1(\omega_{up}, \theta_1) \\ \mathbf{a}_2(\omega_{up}, \theta_2) \\ \vdots \\ \mathbf{a}_M(\omega_{up}, \theta_M) \end{bmatrix} \tag{2.11}$$

If the mobile and the base station are far apart compared to the wavelength of the carrier, we may treat incoming rays as planar waves. Later in the thesis, as we use the uniform linear array (ULA) and circular array in simulations, we present their array response vectors here. ULA is a special case of a planar array as the centres of the ULA elements lie along a straight line. We consider the case of a single ray arriving at the antenna array. In Figure 2.11, we have a circular array with M antenna elements. The adjacent elements have one-half wavelength spacing between them. Without loss in generality, we assume that one of the elements is at angle zero with respect to the horizontal line. Therefore, the angles at which the elements are located on the circle are:

$$\gamma_i = (i-1)(\frac{2\pi}{M}) \qquad i = 1, 2 \ldots, M \tag{2.12}$$

It has been shown in [41] that

$$\mathbf{a}_{circular} = \mathbf{K_{circular}} \begin{bmatrix} e^{j\frac{\pi cos(\theta-\gamma_1)}{2sin(\pi/M)}} \\ e^{j\frac{\pi cos(\theta-\gamma_2)}{2sin(\pi/M)}} \\ \vdots \\ e^{j\frac{\pi cos(\theta-\gamma_M)}{2sin(\pi/M)}} \end{bmatrix} \tag{2.13}$$

where $\mathbf{K_{circular}}$ is a constant. For the case of ULA as in Figure 2.12,

$$\mathbf{a}_{ula} = \mathbf{K_{ula}} \begin{bmatrix} 1 \\ e^{j\frac{2\pi}{\lambda}d(M-1)\cos\theta} \\ e^{j\frac{2\pi}{\lambda}2d(M-1)\cos\theta} \\ \vdots \\ e^{j\frac{2\pi}{\lambda}Md(M-1)\cos\theta} \end{bmatrix} \tag{2.14}$$

where $\mathbf{K_{ula}}$ is a constant.

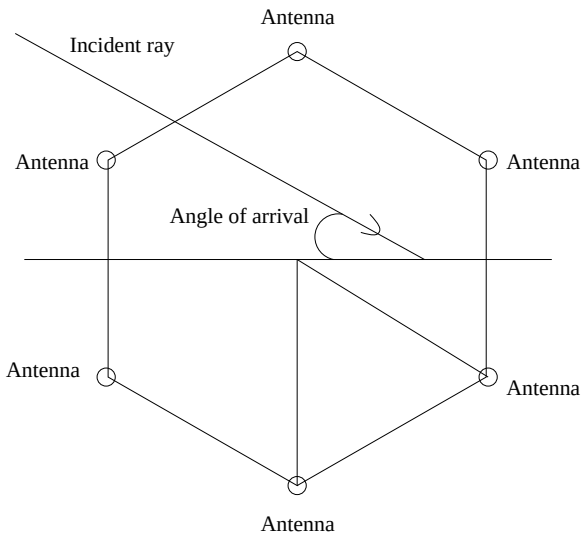

Figure 2.11: Circular antenna array

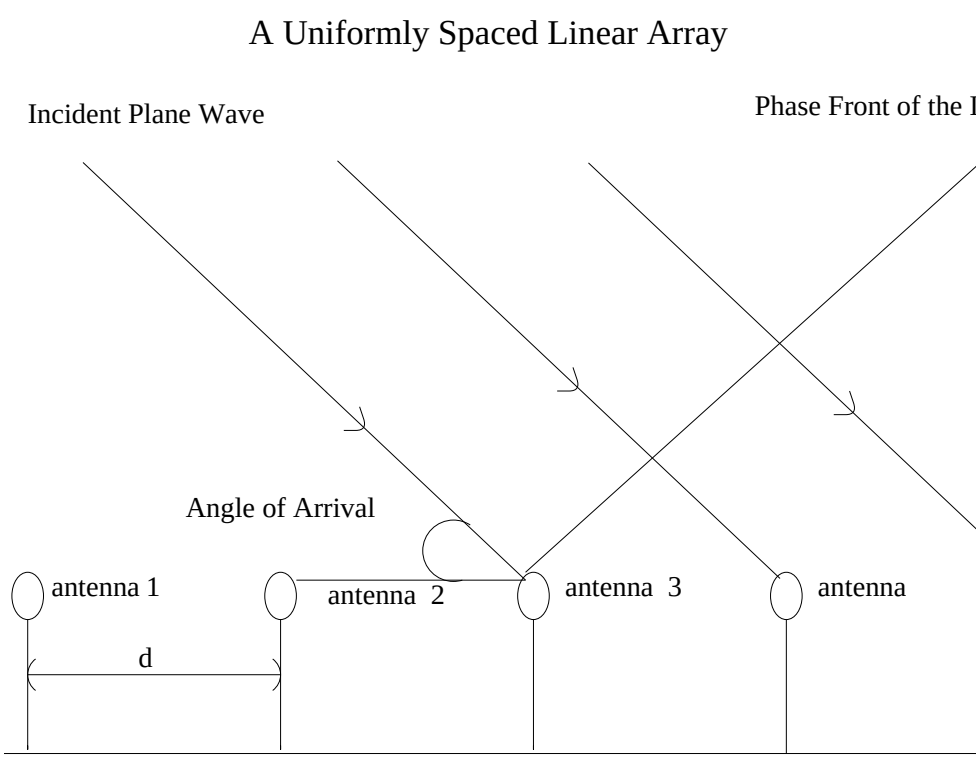

Figure 2.12: An illustration of a plane wave incident on a uniformly spaced linear array

2.4.3 Beamforming

As multiple antennas provide multiple received signals originating from one source, we may combine these to increase the signal-to-noise ratio (SNR). Suppose there is only one mobile in the cell. At the antenna array, there is thermal noise in each antenna element. A reasonable assumption is that the thermal noise is modelled as independent, identically distributed (i.i.d) Gaussian white noise. Let $\mathbf{n}_i(t)$ represent the thermal noise at ith antenna element, we stack $\mathbf{n}_i(t)$ together,

$$\mathbf{n} = \begin{bmatrix} \mathbf{n}_1(t) \\ \mathbf{n}_2(t) \\ \vdots \\ \mathbf{n}_M(t) \end{bmatrix} \tag{2.15}$$

Therefore the received signal may be expressed as

$$\mathbf{r}(t) = s(t)\mathbf{a} + \mathbf{n} \tag{2.16}$$

where $s(t)$ is the desired signal from the mobile. We use a complex-valued vector $\mathbf{w}$ to weight the received signal $\mathbf{r}(t)$,

$$\mathbf{w^H r}(t) = s(t)\mathbf{w^H a} + \mathbf{w^H n} \tag{2.17}$$

It is well-known that choosing that $\mathbf{w} = \mathbf{a}$ maximizes the SNR in Eq. (2.17) [41]. Wa may use radiation pattern F_θ to illustrate this idea. Define

$$F_\theta = |\mathbf{w^H}(\varphi)\mathbf{a}(\theta)| \tag{2.18}$$

For each θ, we vary the φ from $-\pi$ to π and use Eq. (2.13) to calculate $\mathbf{w}(\varphi)$ and $\mathbf{a}(\theta)$ for a circular array. Typical radiation patterns of a circular array are shown in Figures 2.13 and 2.14. Often , a ULA is used in a sector with an angle spread of 120°. Therefore, we change the angle φ from $-\frac{\pi}{3}$ to $\frac{\pi}{3}$. Typical radiation patterns of a ULA are in Figure 2.15 and Figure 2.16.

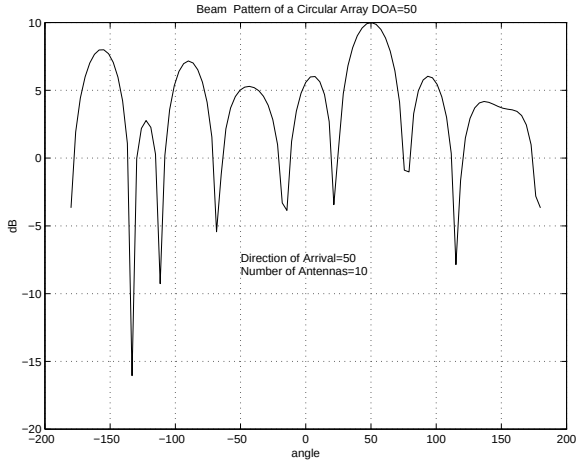

Figure 2.13: Circular array radiation pattern with DOA 50°

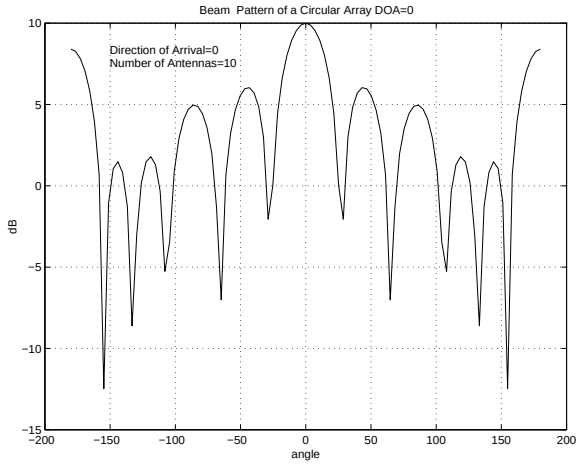

Figure 2.14: Circular array radiation pattern with DOA 0°

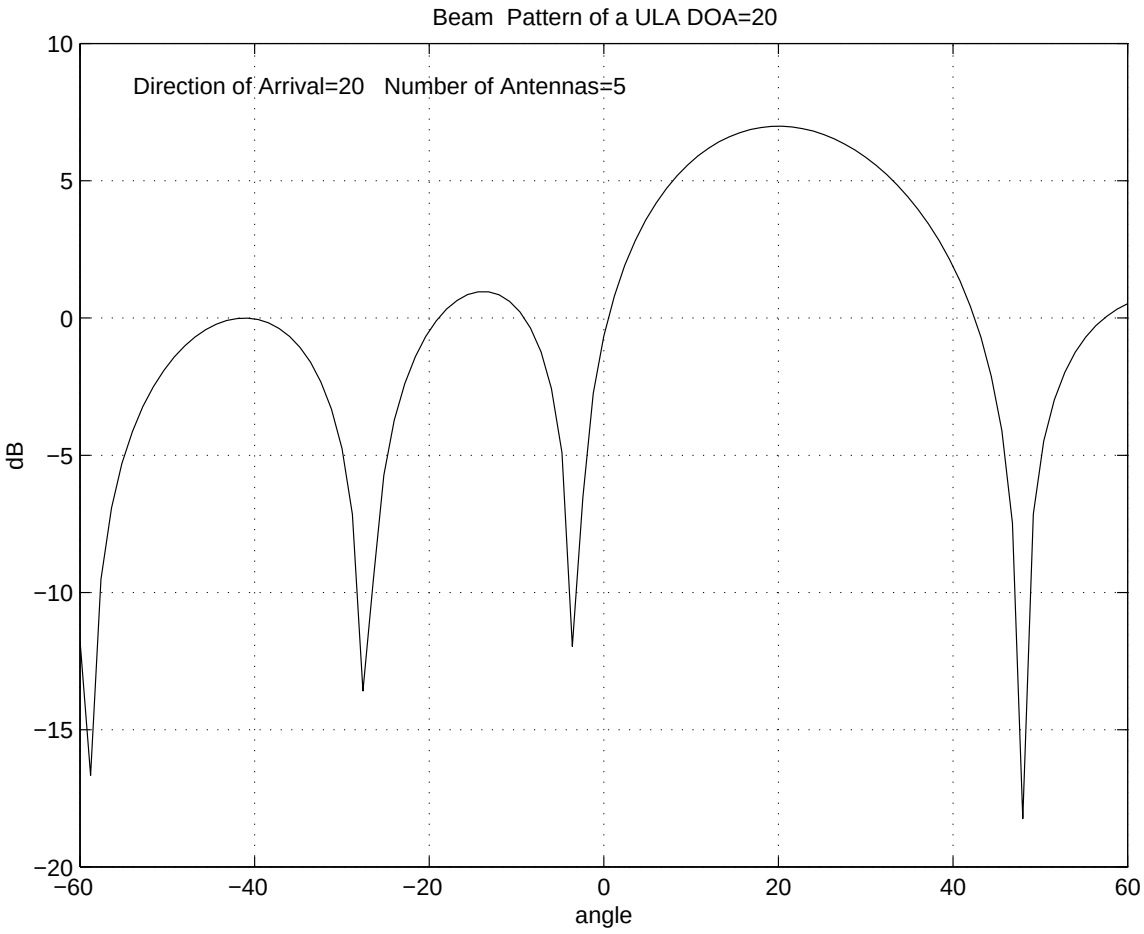

Figure 2.15: ULA radiation pattern with DOA 20°

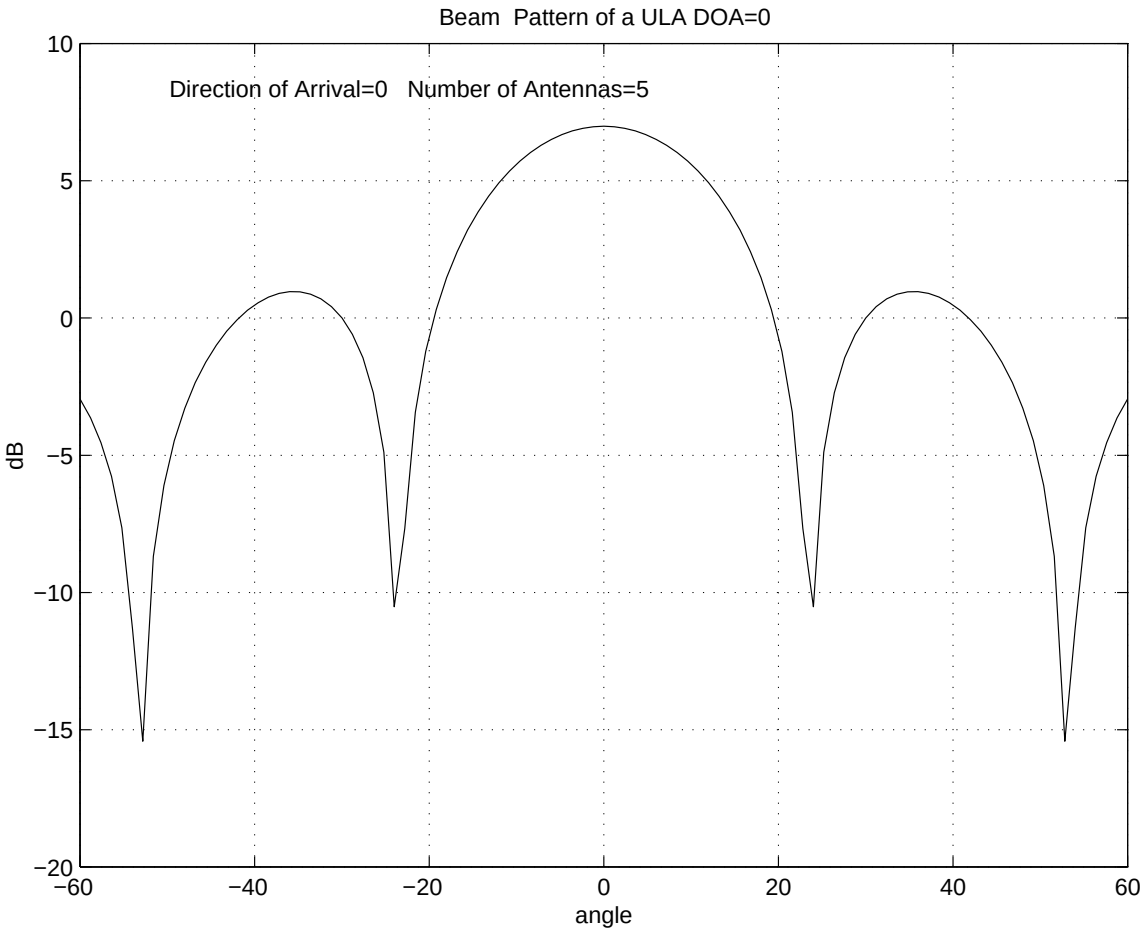

Figure 2.16: ULA radiation pattern with DOA 0°

As shown in Figures 2.13 – 2.16, when $\varphi = \theta$, we obtain maximum F_θ. Now suppose there are N users' signals arriving at the antenna array. Rather than maximizing SNR, we may also form nulls to interferences from these other users. When the number of users, N, exceeds the number of antennas, M, we no longer have enough degrees of freedom (DOF) to form a null in the direction of all the interferences. We maximize the signal-to-interference-plus-noise ratio ($SINR$) to obtain optimum performance as will be presented in Chapter 3. The data model for the multi-user case is

$$\mathbf{w^H r}(t) = s(t)\mathbf{w^H a} + \sum_{i=1}^{N-1} s_i(t)\mathbf{w^H a}_i + \mathbf{w^H n} \tag{2.19}$$

Assume $\mathbf{E}\{|\mathbf{n}|^2\} = \sigma^2$, then the optimum weights to maximize the $SINR$ are [41]

$$\mathbf{w}_{opt} = \gamma \mathbf{R}^{-1}\mathbf{a} \tag{2.20}$$

where γ is a constant which does not affect $SINR$, and can be omitted. From Eq. (2.19), it can be shown that the multi-access interference covariance matrix

$$\begin{aligned} \mathbf{R} &= \mathbf{E}\{|\sum_{i=1}^{N-1} s_i(t)\mathbf{a}_i + \mathbf{n}|^2\} \\ &= \sum_{i=1}^{N-1} P_i \mathbf{a}_i \mathbf{a}_i^{\mathbf{H}} + \sigma^2 \mathbf{I} \end{aligned} \tag{2.21}$$

where $P_i = \mathbf{E}\{|s_i(t)|^2\}$ and $\mathbf{I}$ is the identity matrix. We have assumed that the noise random variables are mutually uncorrelated. In a DS-CDMA system, since the number of users far exceeds the number of antennas, we need not only to maximize the desired signal but also suppress the interference from the other users. Furthermore, the array response vector may only be estimated from the received data. Since the channel changes with time, we need to update the weights over time. We develop these techniques in the following chapters.

2.5 Summary

This chapter presented basic background information relevant to this thesis. DS-CDMA data models and the uplink and downlink channel models were presented. Two basic array patterns, the ULA and Circular Array were introduced. The principle of beamforming antenna arrays was presented.

Chapter 3

Using Signal Cancellation for Optimum Beamforming in a Cellular CDMA System

3.1 Introduction

In Chapter 2, we have shown that maximum signal-to-interference plus noise ($SINR$) beamforming is desirable in cellular code-division multiple-access (CDMA) communications systems employing base station antenna arrays as system capacity may be increased several-fold [51]. Beamforming shows great potential for improving **SINR** which in turn increases cell capacity. To perform optimum **SINR** beamforming, we need to estimate an array response vector and an interference-noise (IN) covariance matrix [41]. Currently, estimation of the IN covariance matrix for optimum beamforming requires great computational cost [51, 49]. As a result, sub-optimum beamforming (maximum **SNR**) is used which does not require the IN matrix . However, when the number of users is not very large and the distribution of users is not uniform, there is a large gap between maximum **SINR** and maximum **SNR** beamforming performance. In this chapter, we propose a direct signal cancellation method to estimate the interference-noise covariance matrix which increases **SINR** and decreases computation compared with [51, 49]. Since DOA estimation of mobiles is also improved, the method can potentially be applied to transmit beamforming in the downlink.

This chapter is organized as follows: Section 3.2 describes our system model and in Section 3.4, our algorithm is compared with [51, 49] through analysis. A comparison of computational requirements between our proposed signal cancellation method and the code-filtering method [51, 49] is presented in Section 3.5. Numerical and simulation results are shown in Section 3.6 and the conclusions are made in Section 3.7.

3.2 System model

Here we consider the reverse (mobile to base station) link with Rayleigh amplitude fading, path loss, shadowing, and perfect power control in a generic cellular CDMA system. First we consider the single path case. Assuming a narrow band signal model, at time t, the baseband signal received at the M-element antenna array for the ith user is:

$$\mathbf{x}_i(t) = \sum_{j=1}^{N} c_j(t-\tau_{i,j}) b_j(t-\tau_{i,j}) \sqrt{P_j(t)} \mathbf{a}_j(t) + \mathbf{n}(t) \tag{3.1}$$

where N is the total number of in-band mobiles, $c_j(t)$ is the pseudo noise (PN) sequence for the jth mobile defined as

$$c_j(t) = \sum_{l=-\infty}^{\infty} c_{j,l} p(t - lT_c) \tag{3.2}$$

where T_c is the chip period and $p(t)$ is the chip pulse assumed to be an arbitrary time-limited waveform. PN chips are modelled as independent and identically distributed (i.i.d) random variables taking values ± 1 with equal probability, $b_j(t)$ is the information bit sequence of the j^{th} mobile, $\tau_{i,j}$ is the differential time delay of the j^{th} mobile relative to that of the i^{th} mobile, vector $\mathbf{n}(t) \sim \mathcal{N}(0, \sigma^2\mathbf{I})$ represents i.i.d Gaussian thermal noise, P_j is the total power received at the base station of the j^{th} mobile, and $\mathbf{a}_j(t)$ is the array response vector of j^{th} mobile whose time-varying DOA is $\theta_j(t)$. Without loss of generality, for all i=1,2,..... N and j=1,2,..... N, we assume self-synchronization, i.e. $\tau_{i,i}$=0, and the signal $b_j(t-\tau_{i,j})$, chips $c_j(t)$ and noise $\mathbf{n}(t)$ are mutually uncorrelated. Chips from users j and k, $c_j(t)$ and $c_k(t)$, are assumed mutually uncorrelated as well as bits $b_j(t-\tau_{i,j})$ and $b_k(t-\tau_{i,k})$ for all k=1,2,.....N and $k \neq j$. The array response vector $\mathbf{a}_j(t)$ is assumed to be unchanged over one

information bit period T_b. The spreading gain L is defined as T_b/T_c. From [49],

$$\mathbf{R}_{xx_i}(t) = P_i \mathbf{a}_i(t)\mathbf{a}_i(t)^{\mathbf{H}} + \sum_{j=1, j\neq i}^{N} P_j \mathbf{a}_j(t)\mathbf{a}_j(t)^{\mathbf{H}} + \sigma^2 \mathbf{I} \tag{3.3}$$

where $\mathbf{x}_i(t)$ is given in Eq. (3.1).

3.3 Signal cancellation algorithm

3.3.1 Code-filtering

Using code-filtering [49], the antenna outputs are correlated with PN codes to yield one sample vector per information bit. At information bit n

$$\begin{aligned} \mathbf{z}_i(n) &= \sqrt{T_b}\sqrt{P_i} b_i(n)\mathbf{a}_i(n) + \frac{1}{\sqrt{T_b}} \int_0^{T_b} \mathbf{n}(t) c_i(t) dt \\ &\quad + \sum_{j=1, j\neq i}^{N} \frac{1}{\sqrt{T_b}} \int_0^{T_b} \sqrt{P_j} b_j(t-\tau_{i,j}) c_j(t-\tau_{i,j}) c_i(t) \mathbf{a}_j(n) dt \end{aligned} \tag{3.4}$$

The post-correlation autocorrelation matrix can be defined as

$$\mathbf{R}_{zz_i}(t) = \frac{1}{T_c} \mathbf{E}\{\mathbf{z}_i(n)\mathbf{z}_i(n)^{\mathbf{H}}\} \tag{3.5}$$

Using the result in [49, 72], we have

$$\mathbf{R}_{zz_i}(n) = L P_i \mathbf{a}_i(n)\mathbf{a}_i(n)^{\mathbf{H}} + \xi \sum_{j=1, j\neq i}^{N} P_j \mathbf{a}_j(n)\mathbf{a}_j(n)^{\mathbf{H}} + \frac{\sigma^2}{T_c}\mathbf{I} \tag{3.6}$$

where ξ is a constant. If the signal is rectangular, ξ will be $\frac{2}{3}$. In reality, the channel is bandlimited, therefore, the assumption of square transmitted pulse shapes do not hold. If this bandlimited channel has an ideal low pass filter characteristics, ξ will be *unity*. However, this constant will not change the output **SINR**.

3.3.2 Signal cancellation

An alternative to code-filtering is now presented. This new algorithm is identical to the code-filtering algorithm if the covariance matrices $\mathbf{R}_{zz_i}$, $\mathbf{R}_{xx_i}$ are known perfectly. However, we will show later that the following algorithm has improved finite-sample

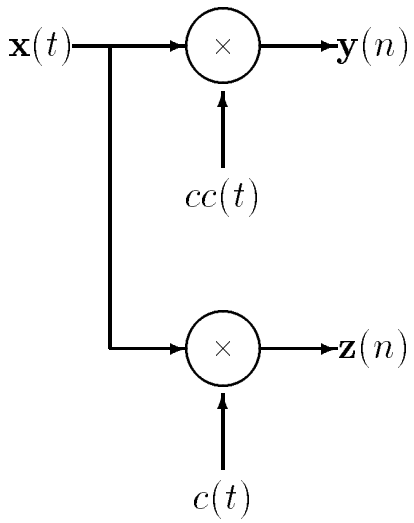

Figure 3.1: Conceptual Signal cancellation algorithm

performance. That is, when $\mathbf{R}_{zz_i}$, $\mathbf{R}_{xx_i}$ are estimated from received data, the following algorithm has improved **SINR** performance as will be shown in Section 3.4. In our proposed algorithm, the value of ξ will not affect the estimation of the array response vector as we use two correlators and their outputs. Whatever the **SINR** is, the MAI is the same for the two correlators and the correlator's outputs will cancel each other perfectly. We notice that in Eq. (3.6), $\mathbf{R}_{zz_i}(n)$ is independent of the PN codes of user i as long as PN codes and information bits are random sequences. In addition to forming $\mathbf{z}_i(n)$, we propose to also despread the array output with the PN code as shown in Figure 3.1:

$$cc_j(t) = \sum_{l=-\infty}^{\infty} (-1)^l c_{j,l} p(t - lT_c) \tag{3.7}$$

It is straightforward to show that $cc_j(t)$ is a random binary sequence where

$$\mathbf{E}\{(-1)^{l+m} c_{j,l} c_{j,m}\} = 0, l \neq m \tag{3.8}$$

If we apply Eq. (3.7) to Eq. (3.4) as a matched filter, we notice that after integration over T_b, the signal term vanishes as long as L is even. In a practical system, it is easily possible to select L as an even number. We obtain as output

$$\begin{aligned} \mathbf{y}_i(n) &= \frac{1}{\sqrt{T_b}} \int_0^{T_b} \mathbf{n}(t) cc_i(t) dt \\ &\quad + \sum_{j=1, j\neq i}^{N} \frac{1}{\sqrt{T_b}} \int_0^{T_b} \sqrt{P_j} b_j(t - \tau_{i,j}) c_j(t - \tau_{i,j}) cc_i(t) \mathbf{a}_j(n) dt \end{aligned} \tag{3.9}$$

Using an analogous definition to Eq. (3.5), we obtain

$$\mathbf{R}_{yy_i}(n) = \xi \sum_{j=1, j\neq i}^{N} P_j \mathbf{a}_j(n)\mathbf{a}_j(n)^{\mathbf{H}} + \frac{\sigma^2}{T_c}\mathbf{I} \tag{3.10}$$

which is the interference and noise portion of Eq. (3.6). Alternatively, in [51, 49], the MAI correlation matrix is estimated as

$$\mathbf{R}_{na_i}(n) = \nu(\mathbf{R}_{xx} - \frac{1}{L}\mathbf{R}_{zz_i}) \tag{3.11}$$

where ν depends on the bandwidth of the channel. However, this constant will not change the output **SINR**.

In [49], the array response vector is estimated as the generalized eigenvector corresponding to the largest eigenvalue of the Hermitian-definite matrix pencil $\mathbf{R}_{zz_i} - \varsigma\mathbf{R}_{xx}$. In [41], it is shown that the beamformer that will maximize the **SINR** has the form $\mathbf{w}_i = \gamma\mathbf{R}_{in}^{-1}\mathbf{a}_i$, where we have dropped the time dependence to simplify notation. γ is a constant which will not affect **SINR** and can be omitted [41]. Using our method, we calculate the optimum weights as

$$\hat{\mathbf{w}}_i = \mathbf{R}_{yy_i}^{-1}\mathbf{a}_i \tag{3.12}$$

while using the method in [51, 49], the weights are given by

$$\tilde{\mathbf{w}}_i = \mathbf{R}_{na_i}^{-1}\mathbf{a}_i \tag{3.13}$$

We should point out that only the phases of $\hat{\mathbf{w}}_i$ and $\tilde{\mathbf{w}}_i$ affect the final **SINR**. For the case of multipath delay spread, generalization of the above is straightforward.

3.4 Finite-sample performance

First, we show that our new method converges to the optimum solution. Define $\mathbf{SINR}_{imax}$ to be the **SINR** for the true array response vector $\mathbf{a}_i$ and true interference-noise covariance matrix $\mathbf{R}_{IN}$. It can be shown that [41]

$$\mathbf{SINR}_{imax} = LP_i\mathbf{a}_i^{\mathbf{H}}\mathbf{R}_{IN}^{-1}\mathbf{a}_i \tag{3.14}$$

To simplify the problem, we assume we have perfect array vector estimates using both methods. Let $\mathbf{SINR}_1$ denote the **SINR** of the proposed method and $\mathbf{SINR}_2$

denote the **SINR** of the proposed method in [49, 51]. Normalizing $\mathbf{SINR}_{imax}$ [41, 60], let

$$\hat{\eta}_i \equiv \frac{\mathbf{SINR}_1}{\mathbf{SINR}_{imax}} = \frac{|\hat{\mathbf{w}}_i^{\mathbf{H}}\mathbf{a}_i|^2}{\hat{\mathbf{w}}_i^{\mathbf{H}}\mathbf{R}_{IN}\hat{\mathbf{w}}_i}\frac{1}{\mathbf{a}_i^{\mathbf{H}}\mathbf{R}_{IN}^{-1}\mathbf{a}_i} \tag{3.15}$$

and

$$\tilde{\eta}_i \equiv \frac{\mathbf{SINR}_2}{\mathbf{SINR}_{imax}} = \frac{|\tilde{\mathbf{w}}_i^{\mathbf{H}}\mathbf{a}_i|^2}{\tilde{\mathbf{w}}_i^{\mathbf{H}}\mathbf{R}_{IN}\tilde{\mathbf{w}}_i}\frac{1}{\mathbf{a}_i^{\mathbf{H}}\mathbf{R}_{IN}^{-1}\mathbf{a}_i} \tag{3.16}$$

In [60], it is shown that $\hat{\eta}_i$ is Beta-distributed, i.e.,

$$\hat{\eta}_i \sim \beta(N - M + 2, M - 1) \tag{3.17}$$

where N is the number of samples used to estimate covariance matrix and M is the number of antennas. According to the Beta distribution,

$$\mathbf{E}\{\hat{\eta}_i\} = \frac{N - M + 2}{N + 1} \tag{3.18}$$

$$\mathbf{Var}(\hat{\eta}_i) = \frac{(N - M + 2)(N - 1)}{(N + 1)^2(N + 2)} \rightarrow \frac{1}{N^2}, \text{as } N \rightarrow \infty \tag{3.19}$$

For optimality, $\hat{\eta}_i = 1$ and as $N \rightarrow \infty$,

$$\mathbf{E}\{|\hat{\eta}_i - 1|\} = 1 - \mathbf{E}\{\hat{\eta}_i\} \rightarrow 0 \tag{3.20}$$

implying that $\hat{\eta}_i$ converges in the mean and in probability to the optimum **SINR**, which means that the proposed method's estimate of **SINR** is consistent. Also

$$\mathbf{E}\{|\hat{\eta}_i - 1|^2\} \rightarrow \mathbf{E}\{|\hat{\eta}_i - \mathbf{E}\{\hat{\eta}_i\}|^2\} = \mathbf{Var}(\hat{\eta}_i) \rightarrow 0 \tag{3.21}$$

implying that $\hat{\eta}_i$ converges in the mean-square sense to the optimum **SINR**.

Using results in [41, 60], we now show that $\mathbf{E}\{\hat{\eta}_i\} > \mathbf{E}\{\tilde{\eta}_i\}$. Let $\hat{\mathbf{R}}_{zz_i}, \hat{\mathbf{R}}_{yy_i}$ denote the maximum likelihood estimates of $\mathbf{R}_{zz_i}$ and $\mathbf{R}_{yy_i}$ respectively, where $\hat{\mathbf{R}}_{yy_i}$ is an estimate of the IN matrix. Using the well-known Matrix Inversion Lemma [66],

$$\begin{aligned}
\tilde{\mathbf{w}}_i &= \mathbf{R}_{na_i}^{-1}\mathbf{a}_i \\
&= [\hat{\mathbf{R}}_{zz_i} - LP_i\mathbf{a}_i\mathbf{a}_i^{\mathbf{H}}]^{-1}\mathbf{a}_i \\
&= \frac{1}{1 - LP_i\mathbf{a}_i^{\mathbf{H}}\hat{\mathbf{R}}_{zz_i}^{-1}\mathbf{a}_i}\hat{\mathbf{R}}_{zz_i}^{-1}\mathbf{a}_i \\
&= \phi\hat{\mathbf{R}}_{zz_i}^{-1}\mathbf{a}
\end{aligned} \tag{3.22}$$

where ϕ is a scalar which will not affect the **SINR**. We therefore define

$$\dot{\mathbf{w}}_i = \hat{\mathbf{R}}_{zz_i}^{-1}\mathbf{a}_i \tag{3.23}$$

and so Eq. (3.16)

$$\tilde{\eta}_i = \frac{|\dot{\mathbf{w}}_i^{\mathbf{H}}\mathbf{a}_i|^2}{\dot{\mathbf{w}}_i^{\mathbf{H}}\mathbf{R}_{IN}\dot{\mathbf{w}}_i}\frac{1}{\mathbf{a}_i^{\mathbf{H}}\mathbf{R}_{IN}^{-1}\mathbf{a}_i} \tag{3.24}$$

Letting $\mathbf{R}_{zz_i}$ denote the true value of $\hat{\mathbf{R}}_{zz_i}$, we form another random variable $\hat{\eta}_i^{'}$

$$\hat{\eta}_i^{'} = \frac{|\dot{\mathbf{w}}_i^{\mathbf{H}}\mathbf{a}_i|^2}{\dot{\mathbf{w}}_i^{\mathbf{H}}\mathbf{R}_{zz_i}\dot{\mathbf{w}}_i}\frac{1}{\mathbf{a}_i^{\mathbf{H}}\mathbf{R}_{zz_i}^{-1}\mathbf{a}_i} \tag{3.25}$$

and so the relationship between $\tilde{\eta}_i$ and $\hat{\eta}_i^{'}$ is

$$\tilde{\eta}_i = \frac{\hat{\eta}_i^{'}}{1+(1-\hat{\eta}_i^{'})\mathbf{SINR}_{imax}} \tag{3.26}$$

Since algebraically the random variable $\hat{\eta}_i^{'}$ is identical to $\hat{\eta}_i$ [41, 60], they have the same probability density function. Taking expectations,

$$\mathbf{E}\{\tilde{\eta}_i\} = \mathbf{E}\{\frac{\hat{\eta}_i^{'}}{1+(1-\hat{\eta}_i^{'})\mathbf{SINR}_{imax}}\} < \mathbf{E}\{\hat{\eta}_i^{'}\} = \mathbf{E}\{\hat{\eta}_i\} \tag{3.27}$$

The above inequality means that on the average, the output **SINR** achieved by Eq. (3.12) is greater than the output **SINR** achieved by Eq. (3.13), particularly if $\mathbf{SINR}_{imax}$ is greater than 1. However, if $\mathbf{SINR}_{imax} < 1$, the difference between the two methods becomes negligible.

3.5 Computational requirements comparison

In Table 3.1, we compare the computational requirements in terms of the number of floating point operations (flops) between our proposed signal cancellation algorithm and the code-filtering algorithm. Both of them apply the recursive least-squares algorithm (RLS) as described in [48]. The overall computational complexity of the code-filtering algorithm is $24M^2 + 16M$ plus the *power method* operations as shown [48] in Table 3.1. For our proposed signal cancellation algorithm, the overall computational complexity is $21M^2 + 13M$ plus the *power method* operations. In the step of estimating principal eigenvector $\mathbf{a}_i$, both algorithms employ the *power method* which

Step #	Code-filtering Method	Signal Cancellation Method
1. Initialization	$3M$	$3M$
2. Square root updating $\mathbf{R}_{xx_i}$	$4M^2 + 4M$	$4M^2 + 4M$
3. Square root updating $\mathbf{R}_{na_i}$	$7M^2 + 7M$	Not needed
4. Square root updating $\mathbf{R}_{yy_i}$	Not needed	$4M^2 + 4M$
5. Estimating principal eigenvector $\mathbf{a}_i$	$O(M^2)$	$O(M^2)$
6. Updating beamforming weights $\hat{\mathbf{w}}_i$	Not needed	M^2
7. Updating beamforming weights $\tilde{\mathbf{w}}_i$	M^2	Not needed
Total steps 1-7	$O(M^2)$	$O(M^2)$

Table 3.1: Computational requirements between the code-filtering method and the proposed signal cancellation method in terms of flops

requires $O(M^2)$ flops. Therefore, the proposed signal cancellation method requires the same order of computation as the code-filtering method, $O(M^2)$ as shown in Table 3.1.

3.6 Numerical and simulation results

To compare the algorithms described in Section 3.3, we perform a PN chip-level simulation [10], to determine the correlation matrices. Eq. (3.1) is used to calculate $\mathbf{x}_i(t)$, Eq. (3.4) is used to obtain $\mathbf{z}_i(n)$, and Eq. (3.10) is used to acquire $\mathbf{y}_i(n)$. With these data vectors, we can obtain their maximum likelihood finite-sample autocorrelation matrix estimates. In our simulation, we assume a 3-sector base station with a 5-element uniform linear array with half wavelength spacing in each sector. The cell radius is 500m, $1/T_b$ = 9600bps, **BPSK** modulation is used, and the spreading gain L=128. There are 25 mobiles randomly distributed in azimuth around the base station with uniform distribution in $[0°, 120°]$, and each mobile has three multipaths. The first path has **SNR** 7 dB, the second and third paths are 9.5 dB and 12 dB, respectively, less than the first path. The delay spread is assumed to be 7 chips over the three paths. We assume the fading channel is Rayleigh with a path loss exponent of four, perfect power control, random mobile speeds of less than 60km/hour and

weight vector updates occur every T_b seconds.

As shown in Figure 3.2, we observe DOA tracking of the first path (**SNR** 7dB) over 50 information bits, which is a clear improvement over the method in [51, 49]. We employ a 2D-RAKE receiver as in [51, 49], but with maximum-ratio combining to obtain a diversity gain [80]. In Figure 3.3, we observe the **SINR** gain of our method as compared to [51, 49], which shows that we would obtain increased cellular system capacity. We notice that for the first 10 bits, the performance gap is not clear. This is as expected because we need at least $2M$ (in our case, $M = 5$) samples to get an accurate estimate of the covariance matrices [60].

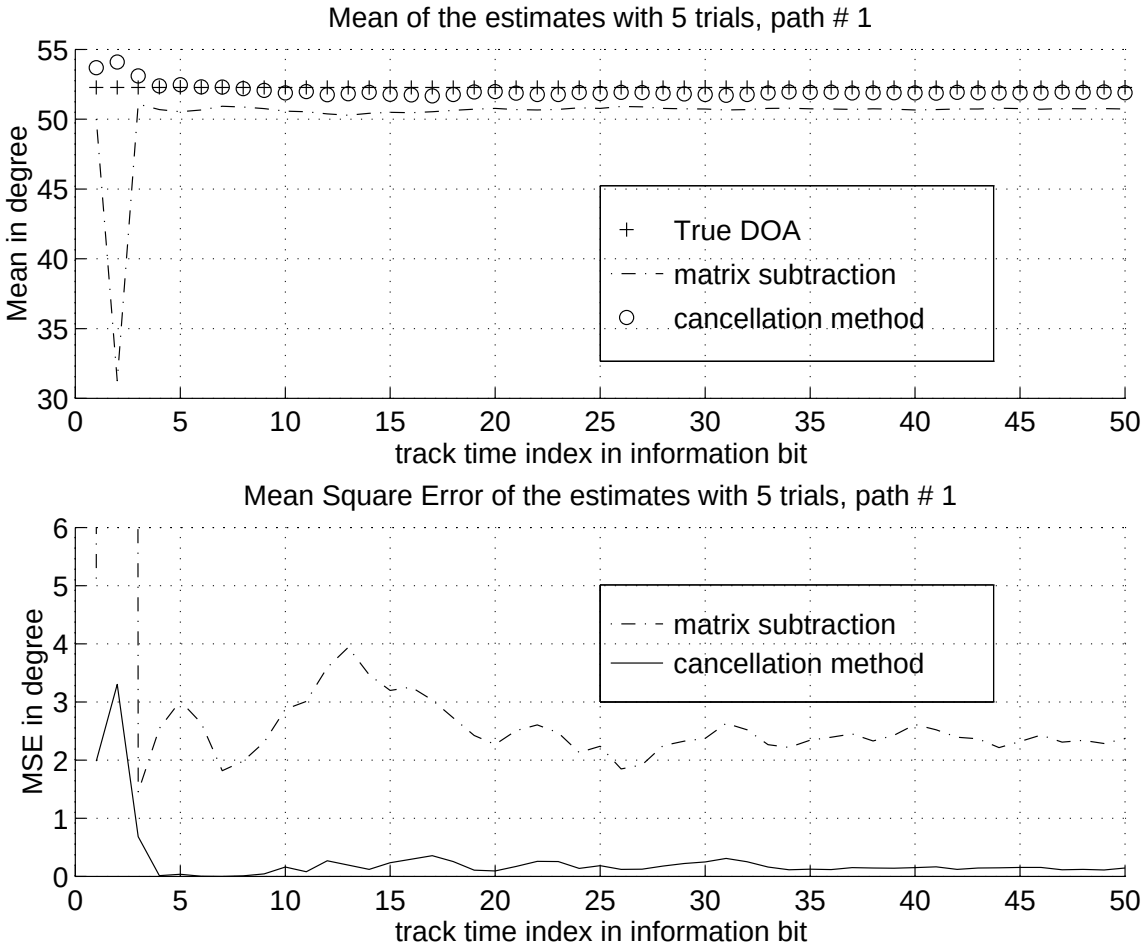

Figure 3.2: DOA of path 1 for 5 antenna elements and 25 mobiles each with 3 multipaths

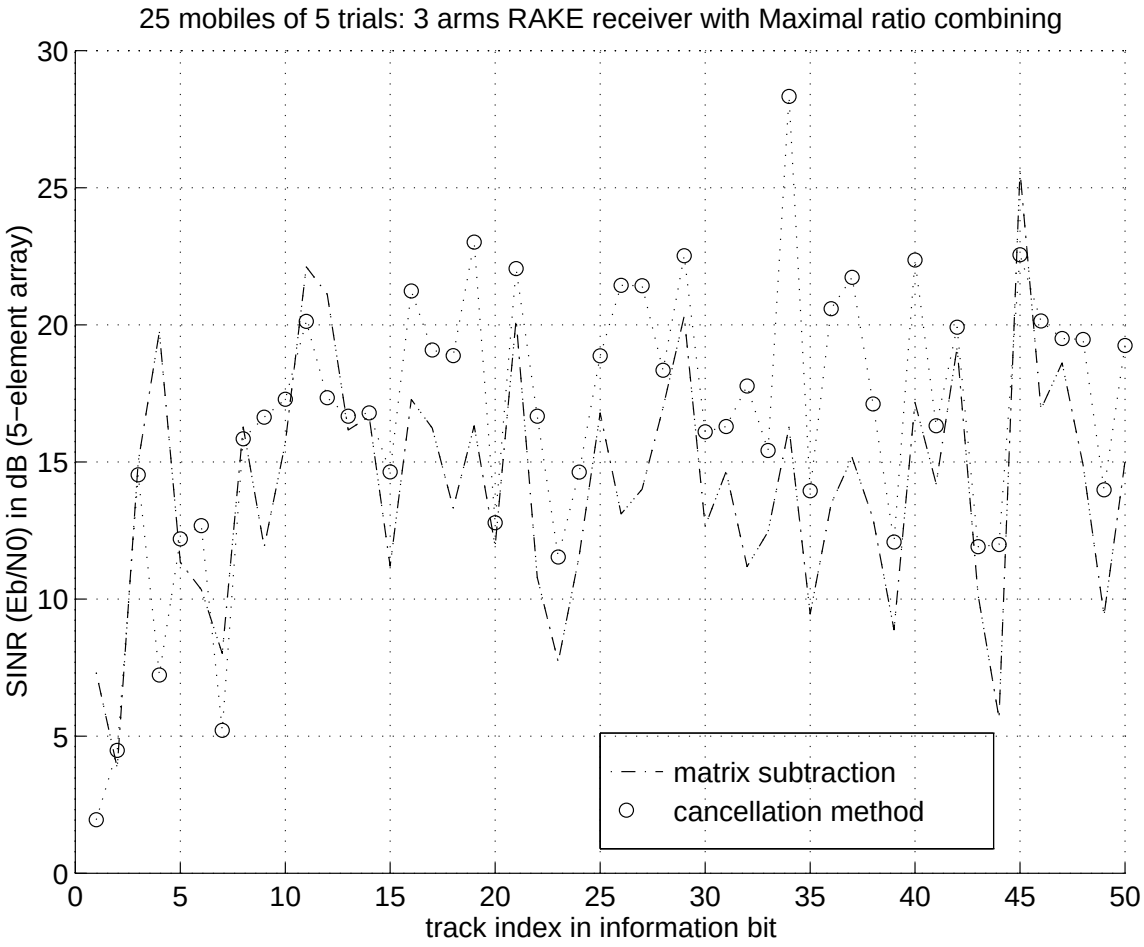

Figure 3.3: Output SINR for 5 antenna elements and 25 mobiles each with 3 multi-paths

3.7 Conclusions

In this chapter, we proposed a new algorithm to directly estimate the interference-noise covariance matrix using PN signal cancellation. We obtained improved DOA estimation and an average increase of 2.5dB in output SINR compared with [51, 49]. In addition, the computational complexity is less than that of [51, 49].

Chapter 4

The Effect of Antenna Array Beamforming Errors on DS-CDMA Communication Systems

4.1 Introduction

Digital beamforming can potentially increase system capacity several-fold by using an antenna array at the base station [49]. In optimum beamforming, we maximize the signal to interference plus noise ratio (SINR) to suppress interference. As discussed in Chapter 3, we must estimate the covariance matrix of the interference plus noise matrix as well as the array response vector from the sampled data of the array output to obtain weights which will be used to perform beamforming. There are several sources of errors in estimating these parameters, such as finite data sample-size, imperfect array response estimates, coloured noise, etc, which will reduce the performance of optimum beamforming algorithms.

The effects of random errors on the performance of optimum beamforming have been studied by several authors [23, 7, 6, 22, 53]. In [7, 6], Gidaram, Cox, Compton and Nitzberg considered the effect of mismatch which arises when there is imperfect knowledge of signal direction, such as when there is perturbation in the array response vector, as caused by random additive errors [6]. In [22], Godara considered random errors in phase shifters and Nitzberg considered the effect of the quantization of weights in [53]. In [23], Godara considered random errors in the array response

vector and random errors in weights separately.

In [23, 7, 6], Godara, Cox and Compton compared the different effects of random errors on two different methods to obtain the interference plus noise covariance: one is calculated on the condition that the desired signal is absent, another is calculated on the condition that the received signals are composed of the desired signal , the interference and thermal noise, and they showed that the first method is more robust to random errors. In a radar system, it may be easy to obtain a signal free received signal to estimate the interference plus noise covariance. In a cellular DS-CDMA system, however, it seems more difficult. In [76], Viberg and Swindlehurst analyzed the combined effects of finite samples and model errors on array processing performance on the condition that the number of the users is less than the number of antennas, a situation which is not suitable for CDMA systems.

However, there has not been an analysis of the effect of covariance matrix error only and the combined effect of errors in the covariance matrix and array response vector. In a generic DS-CDMA system, this is required since we must estimate both the covariance of the interference plus noise matrix as well as the array response vector from the sampled data of the array output to obtain optimum weights. In addition, the number of users is much larger than the number of antenna elements in the DS-CDMA system and the power levels of different users arriving at the base station are nearly the same because of power control at the mobiles.

In this chapter, the combined effect of estimation errors from finite-sample covariance data, interference and thermal noise is analytically determined. Simulation results show agreement with analytical results.

The organization of the chapter is as follows: Sections 4.2 $\sim$ 4.4 will derive the formula for the perturbed SINR, Section 4.5 will apply the result to the specific algorithm and simulation and numerical results will be presented in Section 4.6, finally, we state conclusions.

4.2 Error analysis formulation

In a CDMA beamforming system, the output **SINR** of the processor for a desired user is :

$$\mathbf{SINR} = \frac{||\mathbf{w^H a}||^2}{\mathbf{w^H Q w}} \tag{4.1}$$

where $||.||$ is the Euclidean norm and $\mathbf{a}$ is the desired user's array response vector, and $\mathbf{Q}$ represents the cochannel interference plus thermal noise covariance for this desired user. As discussed in Chapter 2, the weights

$$\mathbf{w} = \mathbf{Q}^{-1}\mathbf{a} \tag{4.2}$$

will maximize output **SINR**, and this maximum **SINR** is given by [41]:

$$\mathbf{SINR}_{max} = LP_i\mathbf{a^H Q}^{-1}\mathbf{a} \tag{4.3}$$

where P_i is the received power of the desired user, and L is the processing gain. By maximizing the desired user's **SINR** through suppressing the interferences from other users, we can greatly reduce the Bit Error Rate (**BER**) or, equivalently, we can reduce the transmitted power of the mobiles, although there is not a simple relationship between **BER** and **SINR**.

First, we consider an ideal array response vector $\mathbf{a}$ and we know the estimation error for $\mathbf{Q}$. Let $\hat{\mathbf{Q}}$ denote the estimated $\mathbf{Q}$ matrix. Ideally, in a DS-CDMA system, $\mathbf{Q}$ can be shown to be [49][72]:

$$\mathbf{Q} = \xi \sum_{j=1, j\neq i}^{N} P_j \mathbf{a}_j(n)\mathbf{a}_j(n)^{\mathbf{H}} + \frac{\sigma^2}{T_c}\mathbf{I} \tag{4.4}$$

where we have considered N users in the system and user i is the desired user, σ^2 is the thermal noise power and $\mathbf{a}_j$ is the array response vector for user j, P_j is the received power of user j, $\mathbf{I}$ is the identity matrix. We can see that $\mathbf{Q}$ is a Hermitian matrix. If we estimate $\mathbf{Q}$ using the maximum likelihood method, for example, at least we can ensure $\hat{\mathbf{Q}}$ is Hermitian as well. Therefore, the error or perturbation matrix, ε, in the following equation is a Hermitian matrix, i.e.,

$$\hat{\mathbf{Q}} = \mathbf{Q} + \varepsilon \tag{4.5}$$

$$\varepsilon = \varepsilon^{\mathbf{H}} \tag{4.6}$$

We make the following further reasonable assumptions: each element of ε has a zero mean, i.i.d complex Gaussian distribution:

$$\mathbf{E}\{\varepsilon\} = 0 \tag{4.7}$$

$$\mathbf{E}\{\varepsilon_{i,j}\varepsilon^*_{k,l}\} = {\sigma_w}^2\delta_{i,k}\delta_{j,l} \tag{4.8}$$

$$\mathbf{E}\{\varepsilon^2_{i,j}\} = 0 \; ; for \; i \neq j \tag{4.9}$$

where $\delta_{i,k}$ represents the Kronecker delta function. We note that the error in the diagonal of ε is real-valued, because ε is a difference of two Hermitian matrices.

Proposition 1

$$\mathbf{E}\{\varepsilon\varepsilon^{\mathbf{H}}\} = M{\sigma_w}^2\mathbf{I} \tag{4.10}$$

Where M is the number of the antenna array elements.

Proof: Let $\mathbf{\Delta}$ denote the matrix $\varepsilon\varepsilon^{\mathbf{H}}$. The (i,j)th element of $\mathbf{\Delta}$ can be obtained through matrix multiplication

$$\mathbf{\Delta}_{i,j} = \sum_{l=1}^{M} \varepsilon_{i,l}\varepsilon_{l,j} \tag{4.11}$$

If $i \neq j$, using (4.8) , we know that

$$\mathbf{\Delta}_{i,j} = 0 \tag{4.12}$$

otherwise, if $i = j$, then

$$\begin{aligned} \mathbf{\Delta}_{i,j} &= \sum_{l=1}^{M} \varepsilon_{i,l}\varepsilon_{l,i} \\ &= \sum_{l=1}^{M} \varepsilon_{i,l}\varepsilon^*_{i,l} \end{aligned} \tag{4.13}$$

Taking the expectation of both sides, we obtain

$$\mathbf{E}\{\mathbf{\Delta}_{i,j}\} = M{\sigma_w}^2 \tag{4.14}$$

QED

4.3 Analysis of covariance matrix errors

4.3.1 Expected noise plus interference power

Using first-order perturbations [69] we obtain

$$\hat{\mathbf{Q}}^{-1} \approx \mathbf{Q}^{-1} - \mathbf{Q}^{-1}\varepsilon\mathbf{Q}^{-1} \tag{4.15}$$

Let $\hat{\mathbf{w}}$ denote the estimated weight due to the perturbation of covariance matrix $\mathbf{Q}$, e.g.,

$$\hat{\mathbf{w}} = \hat{\mathbf{Q}}^{-1}\mathbf{a} \tag{4.16}$$

We obtain, using $\mathbf{Q} = \mathbf{Q}^{\mathbf{H}}$, that

$$\begin{aligned} \hat{\mathbf{w}}^{\mathbf{H}}\mathbf{Q}\hat{\mathbf{w}} &= \mathbf{a}^{\mathbf{H}}(\mathbf{Q}^{-1} - \mathbf{Q}^{-1}\varepsilon\mathbf{Q}^{-1})\mathbf{Q}(\mathbf{Q}^{-1} - \mathbf{Q}^{-1}\varepsilon\mathbf{Q}^{-1})\mathbf{a} \\ &= \mathbf{a}^{\mathbf{H}}\mathbf{Q}^{-1}\mathbf{a} - 2\mathbf{a}^{\mathbf{H}}\mathbf{Q}^{-1}\varepsilon\mathbf{Q}^{-1}\mathbf{a} + \mathbf{a}^{\mathbf{H}}\mathbf{Q}^{-1}\varepsilon\mathbf{Q}^{-1}\varepsilon\mathbf{Q}^{-1}\mathbf{a} \end{aligned} \tag{4.17}$$

It is easy to show that

$$\mathbf{E}\{\mathbf{a}^{\mathbf{H}}\mathbf{Q}^{-1}\varepsilon\mathbf{Q}^{-1}\mathbf{a}\} = 0 \tag{4.18}$$

Taking the expectation of both sides and using Eq. (4.18) result in

$$\mathbf{E}\{\hat{\mathbf{w}}^{\mathbf{H}}\mathbf{Q}\hat{\mathbf{w}}\} = \mathbf{a}^{\mathbf{H}}\mathbf{Q}^{-1}\mathbf{a} + \mathbf{E}\{\mathbf{a}^{\mathbf{H}}\mathbf{Q}^{-1}\varepsilon\mathbf{Q}^{-1}\varepsilon\mathbf{Q}^{-1}\mathbf{a}\} \tag{4.19}$$

where the right-hand term

$$\begin{aligned} \mathbf{E}\{\mathbf{a}^{\mathbf{H}}\mathbf{Q}^{-1}\varepsilon\mathbf{Q}^{-1}\varepsilon\mathbf{Q}^{-1}\mathbf{a}\} &= \mathbf{E}\{(\varepsilon\mathbf{Q}^{-1}\mathbf{a})^{\mathbf{H}}\mathbf{Q}^{-1}(\varepsilon\mathbf{Q}^{-1}\mathbf{a})\} \\ &= \mathbf{Tr}(\mathbf{E}\{(\varepsilon\mathbf{Q}^{-1}\mathbf{a})(\varepsilon\mathbf{Q}^{-1}\mathbf{a})^{\mathbf{H}}\mathbf{Q}^{-1}\}) \\ &= \mathbf{Tr}(\mathbf{E}\{(\varepsilon\mathbf{Q}^{-1}\mathbf{a})(\varepsilon\mathbf{Q}^{-1}\mathbf{a})^{\mathbf{H}}\}\mathbf{Q}^{-1}) \end{aligned} \tag{4.20}$$

where $\mathbf{Tr}(.)$ denotes trace.

Proposition 2

$$\mathbf{E}\{(\varepsilon\mathbf{Q}^{-1}\mathbf{a})(\varepsilon\mathbf{Q}^{-1}\mathbf{a})^{\mathbf{H}}\} = {\sigma_w}^2||\mathbf{Q}^{-1}\mathbf{a}||^2\mathbf{I} \tag{4.21}$$

where $||.||$ is the Euclidean norm.

Proof:

We define a vector $\mathbf{d}$ as

$$\begin{aligned} \mathbf{d} &= \mathbf{Q}^{-1}\mathbf{a} \\ &= [\mathbf{d}_1, \mathbf{d}_2, \ldots, \mathbf{d}_M]^{\mathbf{T}} \end{aligned} \tag{4.22}$$

Let $\mathbf{c}$ denote perturbation vector $\varepsilon\mathbf{d}$, i.e.,

$$\mathbf{c} = \varepsilon\mathbf{d} \tag{4.23}$$

Using matrix multiplication, we can obtain the ith element of vector $\mathbf{c}$ as

$$\mathbf{c}_i = \sum_{l=1}^{M} \varepsilon_{i,l}\mathbf{d}_l \tag{4.24}$$

Define

$$\begin{aligned} \mathbf{F} &= (\varepsilon\mathbf{d})(\varepsilon\mathbf{d})^{\mathbf{H}} \\ &= \mathbf{c}\mathbf{c}^{\mathbf{H}} \end{aligned} \tag{4.25}$$

Using matrix multiplication, we can show the (i,j)th element of matrix $\mathbf{F}$ is

$$\begin{aligned} \mathbf{F}_{i,j} &= \sum_{l=1}^{M} \varepsilon_{i,l}\mathbf{d}_l \left(\sum_{m=1}^{M} \varepsilon_{j,m}\mathbf{d}_m \right)^* \\ &= \sum_{l=1}^{M}\sum_{m=1}^{M} \varepsilon_{i,l}\varepsilon_{j,m}^*\mathbf{d}_l\mathbf{d}_m^* \end{aligned} \tag{4.26}$$

Taking the expectation of both sides and using Eq. (4.8), we know that only when

$$\begin{aligned} i &= j, \; and \\ l &= m \end{aligned}$$

is $\mathbf{E}\{\mathbf{F}_{i,j}\}$ nonzero, and they can expressed as

$$\begin{aligned} \mathbf{E}\{\mathbf{F}_{i,j}\} &= \sum_{l=1}^{M} \mathbf{E}\{\varepsilon_{i,l}\varepsilon_{i,l}^*\}\mathbf{d}_l\mathbf{d}_l^* \\ &= \sum_{l=1}^{M} {\sigma_w}^2 |\mathbf{d}_l|^2 \\ &= {\sigma_w}^2 ||\mathbf{d}||^2 \end{aligned} \tag{4.27}$$

and

$$\mathbf{E}\{\mathbf{F}_{i,j}\} = 0 \quad i \neq j \tag{4.28}$$

QED Using the above result, (4.20) can be reduced to

$$\begin{aligned} \mathbf{E}\{\mathbf{a}^{\mathbf{H}}\mathbf{Q}^{-1}\varepsilon^{-1}\mathbf{Q}^{-1}\varepsilon\mathbf{Q}^{-1}\mathbf{a}\} &= \mathbf{Tr}({\sigma_w}^2||\mathbf{Q}^{-1}\mathbf{a}||^2\mathbf{Q}^{-1}) \\ &= {\sigma_w}^2||\mathbf{Q}^{-1}\mathbf{a}||^2\mathbf{Tr}(\mathbf{Q}^{-1}) \end{aligned} \tag{4.29}$$

Substituting (4.29) in (4.19) gives

$$\mathbf{E}\{\hat{\mathbf{w}}^{\mathbf{H}}\mathbf{Q}\hat{\mathbf{w}}\} = \mathbf{a}^{\mathbf{H}}\mathbf{Q}^{-1}\mathbf{a} + {\sigma_w}^2||\mathbf{Q}^{-1}\mathbf{a}||^2\mathbf{Tr}(\mathbf{Q}^{-1}) \tag{4.30}$$

4.3.2 Expected signal power

In calculating the numerator of Eq. (4.1) for $\mathbf{w}$ replaced by $\hat{\mathbf{w}}$, i.e., $\mathbf{E}(||\hat{\mathbf{w}}^{\mathbf{H}}\mathbf{a}||^2)$, we notice that $\mathbf{a}^{\mathbf{H}}\hat{\mathbf{Q}}^{-1}\mathbf{a}$ is a real-valued scalar, so we have

$$\begin{aligned} ||\hat{\mathbf{w}}^{\mathbf{H}}\mathbf{a}||^2 &= ||\mathbf{a}^{\mathbf{H}}\hat{\mathbf{Q}}^{-1}\mathbf{a}||^2 \\ &= (\mathbf{a}^{\mathbf{H}}(\mathbf{Q}^{-1} - \mathbf{Q}^{-1}\varepsilon\mathbf{Q}^{-1})\mathbf{a})^2 \\ &= (\mathbf{a}^{\mathbf{H}}\mathbf{Q}^{-1}\mathbf{a})^2 - 2\mathbf{a}^{\mathbf{H}}\mathbf{Q}^{-1}\mathbf{a}\mathbf{a}^{\mathbf{H}}\mathbf{Q}^{-1}\varepsilon\mathbf{Q}^{-1}\mathbf{a} + (\mathbf{a}^{\mathbf{H}}\mathbf{Q}^{-1}\varepsilon\mathbf{Q}^{-1}\mathbf{a})^2 \end{aligned} \tag{4.31}$$

Taking the expectation of both sides, we obtain

$$\begin{aligned} \mathbf{E}\{||\hat{\mathbf{w}}^{\mathbf{H}}\mathbf{a}||^2\} &= (\mathbf{a}^{\mathbf{H}}\mathbf{Q}^{-1}\mathbf{a})^2 + \mathbf{E}\{(\mathbf{a}^{\mathbf{H}}\mathbf{Q}^{-1}\varepsilon\mathbf{Q}^{-1}\mathbf{a})^2\} \\ &= (\mathbf{a}^{\mathbf{H}}\mathbf{Q}^{-1}\mathbf{a})^2 + {\sigma_w}^2||\mathbf{Q}^{-1}\mathbf{a}||^2\mathbf{Tr}(\mathbf{Q}^{-1}\mathbf{a}\mathbf{a}^{\mathbf{H}}\mathbf{Q}^{-1}) \\ &= (\mathbf{a}^{\mathbf{H}}\mathbf{Q}^{-1}\mathbf{a})^2 + {\sigma_w}^2||\mathbf{Q}^{-1}\mathbf{a}||^4 \end{aligned} \tag{4.32}$$

4.3.3 Perturbed $SINR$

When there is error in estimating $\mathbf{Q}$, but we have a perfect array response vector $\mathbf{a}$, substituting Eq. (4.32) and Eq. (4.30) into Eq. (4.1), the perturbed output $\widehat{\mathbf{SINR}}$ is

$$\widehat{\mathbf{SINR}} = \frac{(\mathbf{a}^{\mathbf{H}}\mathbf{Q}^{-1}\mathbf{a})^2 + {\sigma_w}^2||\mathbf{Q}^{-1}\mathbf{a}||^4}{\mathbf{a}^{\mathbf{H}}\mathbf{Q}^{-1}\mathbf{a} + {\sigma_w}^2||\mathbf{Q}^{-1}\mathbf{a}||^2\mathbf{Tr}(\mathbf{Q}^{-1})} \tag{4.33}$$

We can easily show that

$$\frac{\partial\widehat{\mathbf{SINR}}}{\partial{\sigma_w}^2} < 0 \tag{4.34}$$

which means $\widehat{\mathbf{SINR}}$ decreases as the perturbation in $\mathbf{Q}$ increases. Also we can show that

$$\widehat{\mathbf{SINR}} < \mathbf{SINR}_{max} = LP_i\mathbf{a}^{\mathbf{H}}\mathbf{Q}^{-1}\mathbf{a} \tag{4.35}$$

We now consider the special case

$$\mathbf{Q} = K\mathbf{I} \tag{4.36}$$

It can be shown, after some algebra, that

$$\widehat{\mathbf{SINR}} = \mathbf{SINR}_{max}\frac{1+\frac{{\sigma_w}^2}{K^2}}{1+\frac{M}{K^2}{\sigma_w}^2} \tag{4.37}$$

From (4.37), as the number of antennas increases, the $\widehat{\mathbf{SINR}}$ decreases due to the estimation error in $\mathbf{Q}$.

4.4 Analysis of combined covariance and array response errors

Next we will consider the combined effect when there are estimation errors in both $\mathbf{Q}$ and the array response vector $\mathbf{a}$. Let $\hat{\mathbf{a}}$ denote the perturbed array response vector, i.e.,

$$\hat{\mathbf{a}} = \mathbf{a} + \eta \tag{4.38}$$

where we assume that η is a zero mean, complex Gaussian vector, such that

$$\mathbf{E}\{\eta\} = 0 \tag{4.39}$$

$$\mathbf{E}\{\eta_i\eta_i^*\} = {\sigma_a}^2 \tag{4.40}$$

so we have

$$\mathbf{E}\{\eta\eta^{\mathbf{H}}\} = {\sigma_a}^2\mathbf{I} \tag{4.41}$$

In addition, we suppose the error in $\mathbf{a}$ is independent of the error in $\mathbf{Q}$. Usually, the error in $\mathbf{a}$ is not independent of the error in $\mathbf{Q}$ because we may use the same sampled data to estimate $\mathbf{Q}$ and $\mathbf{a}$ [49]. However, in our proposed algorithm [38], we can prove

that they are independent. Details are given in Section 4.5. The perturbed weight is defined as

$$\hat{\mathbf{w}} = \hat{\mathbf{Q}}^{-1}\hat{\mathbf{a}} \tag{4.42}$$

4.4.1 Expected signal power

First we determine $\mathbf{E}(||\hat{\mathbf{w}}^{\mathbf{H}}\mathbf{a}||^2)$ which is the numerator of the perturbed **SINR**, where

$$\begin{aligned} \hat{\mathbf{w}}^{\mathbf{H}}\mathbf{a} &= \hat{\mathbf{a}}^{\mathbf{H}}\hat{\mathbf{Q}}^{-1}\mathbf{a} \\ &= \hat{\mathbf{a}}^{\mathbf{H}}\mathbf{Q}^{-1}\mathbf{a} - \hat{\mathbf{a}}^{\mathbf{H}}\mathbf{Q}^{-1}\varepsilon\mathbf{Q}\mathbf{a} \end{aligned} \tag{4.43}$$

Also we have

$$(\hat{\mathbf{w}}^{\mathbf{H}}\mathbf{a})^{\mathbf{H}} = \mathbf{a}^{\mathbf{H}}\mathbf{Q}^{-1}\hat{\mathbf{a}} - \mathbf{a}^{\mathbf{H}}\mathbf{Q}^{-1}\varepsilon\mathbf{Q}^{-1}\hat{\mathbf{a}} \tag{4.44}$$

Therefore

$$\begin{aligned} ||\hat{\mathbf{w}}^{\mathbf{H}}\mathbf{a}||^2 &= \mathbf{a}^{\mathbf{H}}\mathbf{Q}^{-1}\hat{\mathbf{a}}\hat{\mathbf{a}}^{\mathbf{H}}\mathbf{Q}^{-1}\mathbf{a} - \mathbf{a}^{\mathbf{H}}\mathbf{Q}^{-1}\varepsilon\mathbf{Q}^{-1}\hat{\mathbf{a}}\hat{\mathbf{a}}^{\mathbf{H}}\mathbf{Q}^{-1}\mathbf{a} \\ &\quad -\mathbf{a}^{\mathbf{H}}\mathbf{Q}^{-1}\hat{\mathbf{a}}\hat{\mathbf{a}}^{\mathbf{H}}\mathbf{Q}^{-1}\varepsilon\mathbf{Q}^{-1}\mathbf{a} + \mathbf{a}^{\mathbf{H}}\mathbf{Q}^{-1}\varepsilon\mathbf{Q}^{-1}\hat{\mathbf{a}}\hat{\mathbf{a}}^{\mathbf{H}}\mathbf{Q}^{-1}\varepsilon\mathbf{Q}^{-1}\mathbf{a} \end{aligned} \tag{4.45}$$

Using similar reasoning, it is easy to show that

$$\mathbf{E}\{\hat{\mathbf{a}}\hat{\mathbf{a}}^{\mathbf{H}}\} = \mathbf{a}\mathbf{a}^{\mathbf{H}} + {\sigma_a}^2\mathbf{I} \tag{4.46}$$

Taking the the expectation of both sides of (4.45), we obtain

$$\begin{aligned} \mathbf{E}\{||\hat{\mathbf{w}}^{\mathbf{H}}\mathbf{a}||^2\} &= \mathbf{a}^{\mathbf{H}}\mathbf{Q}^{-1}(\mathbf{a}\mathbf{a}^{\mathbf{H}} + {\sigma_a}^2\mathbf{I})\mathbf{Q}^{-1}\mathbf{a} \\ &\quad +\mathbf{E}\{\mathbf{a}^{\mathbf{H}}\mathbf{Q}^{-1}\varepsilon\mathbf{Q}^{-1}(\mathbf{a}\mathbf{a}^{\mathbf{H}} + {\sigma_a}^2\mathbf{I})\mathbf{Q}^{-1}\varepsilon\mathbf{Q}^{-1}\mathbf{a}\} \end{aligned} \tag{4.47}$$

Splitting the right hand side expectation, we can show that

$$\begin{aligned} \mathbf{E}\{(\varepsilon\mathbf{Q}^{-1}\mathbf{a})^{\mathbf{H}}\mathbf{Q}^{-1}\mathbf{a}\mathbf{a}^{\mathbf{H}}\mathbf{Q}(\varepsilon\mathbf{Q}^{-1}\mathbf{a})\} &= {\sigma_w}^2||\mathbf{Q}^{-1}\mathbf{a}||^2\mathbf{Tr}(\mathbf{Q}^{-1}\mathbf{a}\mathbf{a}^{\mathbf{H}}\mathbf{Q}^{-1}) \\ &= {\sigma_w}^2||\mathbf{Q}^{-1}\mathbf{a}||^4 \end{aligned} \tag{4.48}$$

and

$$\mathbf{E}\{(\varepsilon\mathbf{Q}^{-1}\mathbf{a})^{\mathbf{H}}\mathbf{Q}^{-1}\mathbf{Q}^{-1}(\varepsilon\mathbf{Q}^{-1}\mathbf{a})\} = {\sigma_w}^2||\mathbf{Q}^{-1}\mathbf{a}||^2\mathbf{Tr}(\mathbf{Q}^{-1}\mathbf{Q}^{-1}) \tag{4.49}$$

Finally, we obtain

$$\begin{aligned}\mathbf{E}\{||\hat{\mathbf{w}}^{\mathbf{H}}\mathbf{a}||^2\} &= (\mathbf{a}^{\mathbf{H}}\mathbf{Q}^{-1}\mathbf{a})^2 + {\sigma_a}^2\mathbf{a}^{\mathbf{H}}\mathbf{Q}^{-1}\mathbf{Q}^{-1}\mathbf{a} + {\sigma_w}^2||\mathbf{Q}^{-1}\mathbf{a}||^4 \\ &\quad +{\sigma_a}^2{\sigma_w}^2||\mathbf{Q}^{-1}\mathbf{a}||^2\mathbf{Tr}(\mathbf{Q}^{-1}\mathbf{Q}^{-1}) \\ &\approx (\mathbf{a}^{\mathbf{H}}\mathbf{Q}^{-1}\mathbf{a})^2 + {\sigma_a}^2\mathbf{a}^{\mathbf{H}}\mathbf{Q}^{-1}\mathbf{Q}^{-1}\mathbf{a} + {\sigma_w}^2||\mathbf{Q}^{-1}\mathbf{a}||^4 \\ &= (\mathbf{a}^{\mathbf{H}}\mathbf{Q}^{-1}\mathbf{a})^2 + {\sigma_a}^2||\mathbf{Q}^{-1}\mathbf{a}||^2 + {\sigma_w}^2||\mathbf{Q}^{-1}\mathbf{a}||^4 \qquad (4.50)\end{aligned}$$

where we have omitted the second-order term.

4.4.2 Expected noise plus interference power

Next we take $\mathbf{E}(\hat{\mathbf{w}}^{\mathbf{H}}\mathbf{Q}\hat{\mathbf{w}})$, the expectation of the denominator of the perturbed **SINR**. First of all

$$\begin{aligned}\hat{\mathbf{w}}^{\mathbf{H}}\mathbf{Q}\hat{\mathbf{w}} &= \hat{\mathbf{a}}^{\mathbf{H}}\hat{\mathbf{Q}}^{-1}\mathbf{Q}\hat{\mathbf{Q}}^{-1}\hat{\mathbf{a}} \\ &= \hat{\mathbf{a}}^{\mathbf{H}}(\mathbf{Q}^{-1} - \mathbf{Q}^{-1}\varepsilon\mathbf{Q}^{-1})\mathbf{Q}(\mathbf{Q}^{-1} - \mathbf{Q}^{-1}\varepsilon\mathbf{Q}^{-1})\hat{\mathbf{a}} \\ &= \hat{\mathbf{a}}^{\mathbf{H}}\mathbf{Q}^{-1}\hat{\mathbf{a}} - 2\hat{\mathbf{a}}^{\mathbf{H}}\mathbf{Q}^{-1}\varepsilon\mathbf{Q}^{-1}\hat{\mathbf{a}} + \hat{\mathbf{a}}^{\mathbf{H}}\mathbf{Q}^{-1}\varepsilon\mathbf{Q}^{-1}\varepsilon\mathbf{Q}^{-1}\hat{\mathbf{a}} \qquad (4.51)\end{aligned}$$

Taking the expectation of both sides, we obtain

$$\begin{aligned}\mathbf{E}\{\hat{\mathbf{w}}^{\mathbf{H}}\mathbf{Q}\hat{\mathbf{w}}\} &= \mathbf{Tr}(\mathbf{E}\{\hat{\mathbf{a}}\hat{\mathbf{a}}^{\mathbf{H}}\}\mathbf{Q}^{-1}) + \mathbf{E}\{\hat{\mathbf{a}}^{\mathbf{H}}(\mathbf{Q}^{-1}\varepsilon\mathbf{Q}^{-1})(\mathbf{Q}^{-1}\varepsilon\mathbf{Q}^{-1})\hat{\mathbf{a}}\} \\ &= \mathbf{Tr}((\mathbf{a}\mathbf{a}^{\mathbf{H}} + {\sigma_a}^2\mathbf{I})\mathbf{Q}^{-1}) \\ &\quad +\mathbf{Tr}((\mathbf{a}\mathbf{a}^{\mathbf{H}} + {\sigma_a}^2\mathbf{I})\mathbf{E}\{\mathbf{Q}^{-1}\varepsilon\mathbf{Q}^{-1}\varepsilon\mathbf{Q}^{-1}\}) \qquad (4.52)\end{aligned}$$

We note that

$$\mathbf{Tr}(\mathbf{a}\mathbf{a}^{\mathbf{H}}\mathbf{Q}^{-1}) = \mathbf{Tr}(\mathbf{Q}^{-1}\mathbf{a}\mathbf{a}^{\mathbf{H}}) = \mathbf{a}^{\mathbf{H}}\mathbf{Q}^{-1}\mathbf{a} \qquad (4.53)$$

We can show that

$$\mathbf{Tr}(\mathbf{a}\mathbf{a}^{\mathbf{H}}\mathbf{E}\{\mathbf{Q}^{-1}\varepsilon\mathbf{Q}^{-1}\varepsilon\mathbf{Q}^{-1}\}) = {\sigma_w}^2||\mathbf{Q}^{-1}\mathbf{a}||^2\mathbf{Tr}(\mathbf{Q}^{-1}) \qquad (4.54)$$

Finally, we obtain

$$\begin{aligned}\mathbf{E}\{\hat{\mathbf{w}}^{\mathbf{H}}\mathbf{Q}\hat{\mathbf{w}}\} &= {\sigma_a}^2\mathbf{Tr}(\mathbf{Q}^{-1}) + \mathbf{a}^{\mathbf{H}}\mathbf{Q}^{-1}\mathbf{a} + {\sigma_w}^2||\mathbf{Q}^{\mathbf{H}}\mathbf{a}||^2\mathbf{Tr}(\mathbf{Q}^{-1}) \\ &\quad +{\sigma_a}^2\mathbf{Tr}(\mathbf{E}\{\mathbf{Q}^{-1}\varepsilon\mathbf{Q}^{-1}\mathbf{Q}^{-1}\varepsilon\mathbf{Q}^{-1}\}) \\ &\approx \mathbf{a}^{\mathbf{H}}\mathbf{Q}^{-1}\mathbf{a} + {\sigma_a}^2\mathbf{Tr}(\mathbf{Q}^{-1}) + {\sigma_w}^2||\mathbf{Q}^{-1}\mathbf{a}||^2\mathbf{Tr}(\mathbf{Q}^{-1}) \qquad (4.55)\end{aligned}$$

In the above equation, we have assumed that the second order term is negligible.

4.4.3 Perturbed output $SINR$

The perturbed output $\widetilde{\mathbf{SINR}}$ is found by taking the ratio of Eq. (4.50) and Eq. (4.55):

$$\widetilde{\mathbf{SINR}} = \frac{(\mathbf{a^H Q^{-1} a})^2 + {\sigma_a}^2 ||\mathbf{Q^{-1} a}||^2 + {\sigma_w}^2 ||\mathbf{Q^{-1} a}||^4}{\mathbf{a^H Q^{-1} a} + {\sigma_a}^2 \mathbf{Tr}(\mathbf{Q^{-1}}) + {\sigma_w}^2 ||\mathbf{Q^{-1} a}||^2 \mathbf{Tr}(\mathbf{Q^{-1}})} \tag{4.56}$$

Again, let us consider the special case, where

$$\mathbf{Q} = K\mathbf{I} \tag{4.57}$$

where K is a constant scalar. We can show that

$$\widetilde{\mathbf{SINR}} = \mathbf{SINR}_{max} \frac{1 + \frac{1}{M}{\sigma_a}^2 + \frac{1}{K^2}{\sigma_w}^2}{1 + {\sigma_a}^2 + \frac{M}{K^2}{\sigma_w}^2} \tag{4.58}$$

which is a generalization of (4.37). If we assume that ${\sigma_w}^2$ is zero, then we obtain the perturbed $\overline{\mathbf{SINR}}$ due to the error in array response vector only

$$\overline{\mathbf{SINR}} = \mathbf{SINR}_{max} \frac{1 + \frac{1}{M}{\sigma_a}^2}{1 + {\sigma_a}^2} \tag{4.59}$$

We will examine the sensitivity of $\mathbf{SINR}$ with respect to covariance error and array response error. These sensitivities are defined as [32]

$$\mathbf{sen_{array}} = \frac{\frac{\partial \widetilde{\mathbf{SINR}}}{\widetilde{\mathbf{SINR}}}}{\frac{\partial {\sigma_a}^2}{{\sigma_a}^2}} \tag{4.60}$$

and

$$\mathbf{sen_{matrix}} = \frac{\frac{\partial \widetilde{\mathbf{SINR}}}{\widetilde{\mathbf{SINR}}}}{\frac{\partial {\sigma_w}^2}{{\sigma_w}^2}} \tag{4.61}$$

We can show that (omitting the minus sign)

$$\mathbf{sen_{array}} = \frac{\frac{M-1}{M}{\sigma_a}^2}{(1 + {\sigma_a}^2 + M{\sigma_w}^2)^2} \tag{4.62}$$

and

$$\mathbf{sen_{matrix}} = \frac{(M-1){\sigma_w}^2}{(1 + {\sigma_a}^2 + \frac{M}{K^2}{\sigma_w}^2)^2} \tag{4.63}$$

Recall that ${\sigma_a}^2$ and ${\sigma_w}^2$ represent the estimation error variance for the array response and MAI, respectively, K^2 represents the variance of the actual MAI, and M is the

number of antennas. As a way of interpreting Eqs. (4.62) and (4.63), in the context of the signal cancellation algorithm, consider the case where the estimation errors, ${\sigma_a}^2$ and ${\sigma_w}^2$ are small. It is clear that

$$\mathbf{sen_{array}} \longrightarrow {\sigma_a}^2 \frac{(M-1)}{M} \tag{4.64}$$

while

$$\mathbf{sen_{matrix}} \longrightarrow {\sigma_w}^2 (M-1) \tag{4.65}$$

As we increase the number of antennas to increase the $SINR$, the sensitivity to array response errors does not change while the sensitivity to MAI matrix estimates increases proportionally.

4.5 Application to maximum $SINR$ beamforming

In Chapter 3.3 we proposed a new algorithm to estimate the MAI directly through signal cancellation using PN chip properties. We estimate $\mathbf{a}$ from post-correlation $\mathbf{z}_i(n)$ as the principle eigenvector of the autocorrelation of $\mathbf{z}_i(n)$ accurately if the processing gain is high and we estimate $\mathbf{Q}$ directly from $\mathbf{y}_i(n)$. We have the following result:

Proposition 3 *The error in* $\mathbf{a}$ *is uncorrelated with the error in* $\mathbf{Q}$ *in our proposed algorithm. Further, if we make the assumption that the sampled data is an i.i.d Gaussian process, the error in* $\mathbf{a}$ *is independent of the error in* $\mathbf{Q}$ *in our proposed algorithm.*

Proof:

To prove this, we only need to show that the outputs of two correlators are uncorrelated. Define vectors

$$\begin{aligned}
\mathbf{a}_z &= \sqrt{T_b}\sqrt{P_i} b_i(n) \mathbf{a}_i(n) \\
\mathbf{b}_z &= \frac{1}{\sqrt{T_b}} \int_0^{T_b} \mathbf{n}(t) c c_i(t) dt \\
\mathbf{c}_z &= \sum_{j=1, j\neq i}^{N} \frac{1}{\sqrt{T_b}} \int_0^{T_b} \sqrt{P_j} b_j(t-\tau_{i,j}) c_j(t-\tau_{i,j}) c_i(t) \mathbf{a}_j(n) dt
\end{aligned}$$

and

$$\begin{aligned}\mathbf{b}_y &= \frac{1}{\sqrt{T_b}}\int_0^{T_b}\mathbf{n}(t)c_i(t)dt \\ \mathbf{c}_y &= \sum_{j=1,j\neq i}^{N}\frac{1}{\sqrt{T_b}}\int_0^{T_b}\sqrt{P_j}b_j(t-\tau_{i,j})c_j(t-\tau_{i,j})cc_i(t)\mathbf{a}_j(n)dt\end{aligned}$$

in terms of the quantities defined in Chapter 3. In DS-CDMA systems, recall that we have made the following assumptions:

(a) Signal is uncorrelated with thermal noise;

(b) Different users have uncorrelated zero mean random information bits, taking value ± 1; and

(c) Noises in different correlators are independent zero-mean Gaussian processes.

Using assumption (a), we obtain

$$\mathbf{E}\{\mathbf{a}_z\mathbf{b}_y^{\mathbf{H}}\} = \mathbf{0}$$

$$\mathbf{E}\{\mathbf{b}_z\mathbf{c}_y^{\mathbf{H}}\} = \mathbf{0}$$

$$\mathbf{E}\{\mathbf{c}_z\mathbf{b}_y^{\mathbf{H}}\} = \mathbf{0}$$

Using assumption (b), we obtain

$$\mathbf{E}\{\mathbf{a}_z\mathbf{c}_y^{\mathbf{H}}\} = \mathbf{0}$$

Using assumption (c), we obtain

$$\mathbf{E}\{\mathbf{b}_z\mathbf{b}_y^{\mathbf{H}}\} = \mathbf{0}$$

Next we show that

$$\mathbf{E}\{\mathbf{c}_z\mathbf{c}_y^{\mathbf{H}}\} = \mathbf{0}$$

Thus,

$$\mathbf{E}\{\mathbf{c}_z\mathbf{c}_y^{\mathbf{H}}\} = \mathbf{E}\{\sum_{j=1,j\neq i}^{N}\frac{1}{\sqrt{T_b}}\int_0^{T_b}\sqrt{P_j}b_j(t-\tau_{i,j})c_j(t-\tau_{i,j})c_i(t)\mathbf{a}_j(n)dt$$

$$\times \sum_{l=1,l\neq i}^{N} \frac{1}{\sqrt{T_b}} \int_0^{T_b} \sqrt{P_l} b_l(t-\tau_{i,l}) c_l(t-\tau_{i,l}) cc_i(t) \mathbf{a}_l(n)^{\mathbf{H}} dt)\}$$

$$= \mathbf{E}\{ \sum_{j=1,j\neq i}^{N} \sum_{l=1,l\neq i}^{N} \frac{1}{\sqrt{T_b}} \int_0^{T_b} \int_0^{T_b} \sqrt{P_j}\sqrt{P_l} b_j(t-\tau_{i,j}) b_l(u-\tau_{i,l})$$

$$\times c_j(t-\tau_{i,j}) c_l(u-\tau_{i,l}) c_i(t) cc_i(u) \mathbf{a}_j(n) \mathbf{a}_l(n)^{\mathbf{H}} dt du\}$$

Using assumption (b), we know that

$$\mathbf{E}\{b_j(t-\tau_{i,j}) b_l(u-\tau_{i,l})\} = \delta_{j,l}$$

So

$$\mathbf{E}\{\mathbf{c}_z \mathbf{c}_y^{\mathbf{H}}\} = \sum_{j=1,j\neq i}^{N} \frac{1}{\sqrt{T_b}} \int_0^{T_b} P_j \mathbf{E}\{c_i(t) cc_i(t)\} \mathbf{a}_j(n) \mathbf{a}_j(n)^{\mathbf{H}} dt$$

$$= \mathbf{0}$$

We have used the property that over one information bit

$$c_i(t) cc_i(t) = 0$$

Actually, we have used this PN chip property to cancel the signal in our proposed algorithm. Finally, we can conclude that

$$\mathbf{E}\{\mathbf{y}_i(n) \mathbf{z}_i(n)^{\mathbf{H}}\} = \mathbf{0}$$

QED

So Eq. (4.56) can be applied to the proposed signal cancellation algorithm of Section 3.3. That is, errors in array response are decoupled from errors in the MAI matrix, and the previous sensitivity analysis applies. However, in the case of code-filtering, it is not true that the errors ${\sigma_a}^2$ and ${\sigma_w}^2$ are independent. In fact, the array response errors are a function of the MAI matrix errors in the code-filtering algorithm due to the matrix subtraction. This further limits the performance of the code-filtering algorithm since as the number of antennas are increased, both $\mathbf{sen_{array}}$ and $\mathbf{sen_{matrix}}$ must increase.

4.6 Numerical results and simulations

In our simulations we assume a 3-sector base station with uniform linear array with half wavelength spacing in each sector. We will consider, 3, 5 and 7 element antenna

arrays. There are 25 mobiles randomly distributed in azimuth around the base station with uniform distribution in $[-60°, 60°]$. We suppose that we have perfect power control and input $\mathbf{E}_b/\mathbf{N}_0$ is 7 dB. The desired signal comes from 30°. Also, the error in $\mathbf{Q}$ is relative to its diagonal elements which are much larger than the off-diagonal elements. The error in $\mathbf{a}$ can be relative to any element of $\mathbf{a}$ because they have the same amplitude for a uniform linear array. For each simulation, 10000 runs were used. In Figure 4.1, we assume we have the perfect array response vector and we show the effect of errors in $\mathbf{Q}$. In Figure 4.2, we assume we have perfect $\mathbf{Q}$ and show the effect of errors in the array response vector. In Figures 4.3-4.6, we assume we have errors both in $\mathbf{Q}$ and the array response vector, and we hold the errors in the array response vector constant. We can see that the simulation results agree closely with the theoretical results . As expected, the degradation of the output **SINR** increases as the number of antennas increases. We notice that for the same error variance in $\mathbf{a}$ and $\mathbf{Q}$, there is more **SINR** decrease due to errors in $\mathbf{Q}$ which are shown in Figure 4.1 and Figure 4.2.

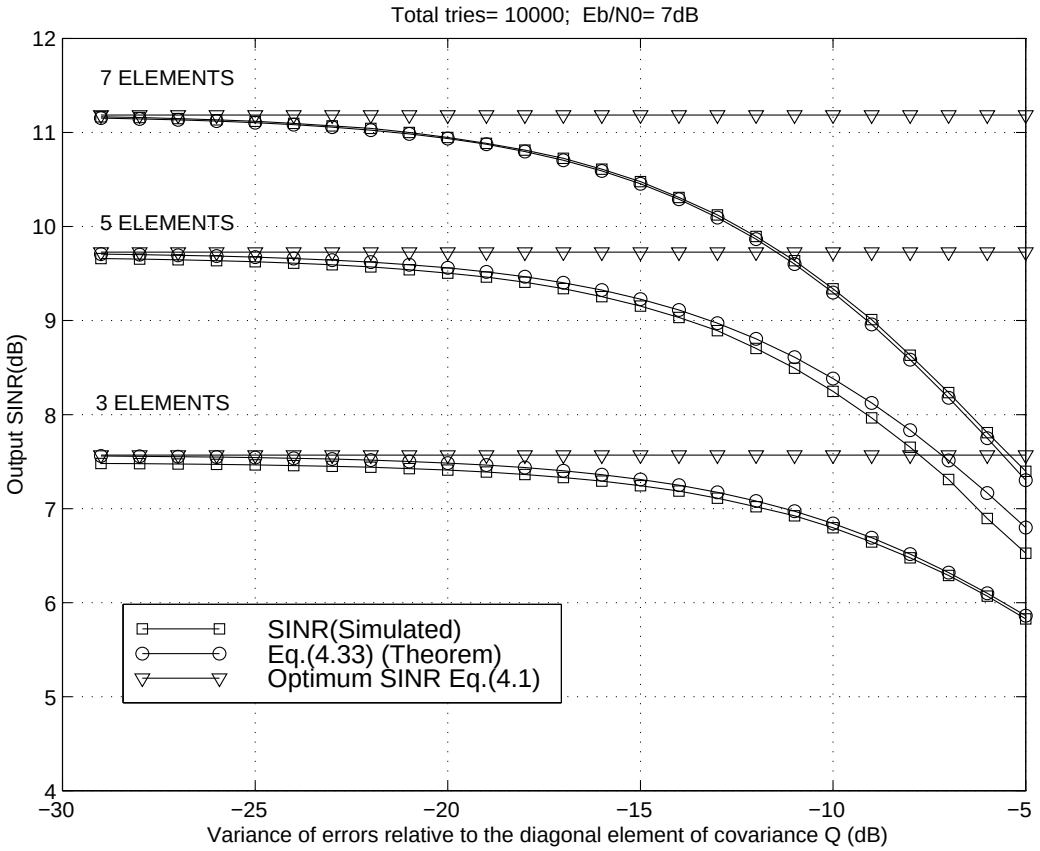

Figure 4.1: Output SINR with respect to errors in the MAI matrix

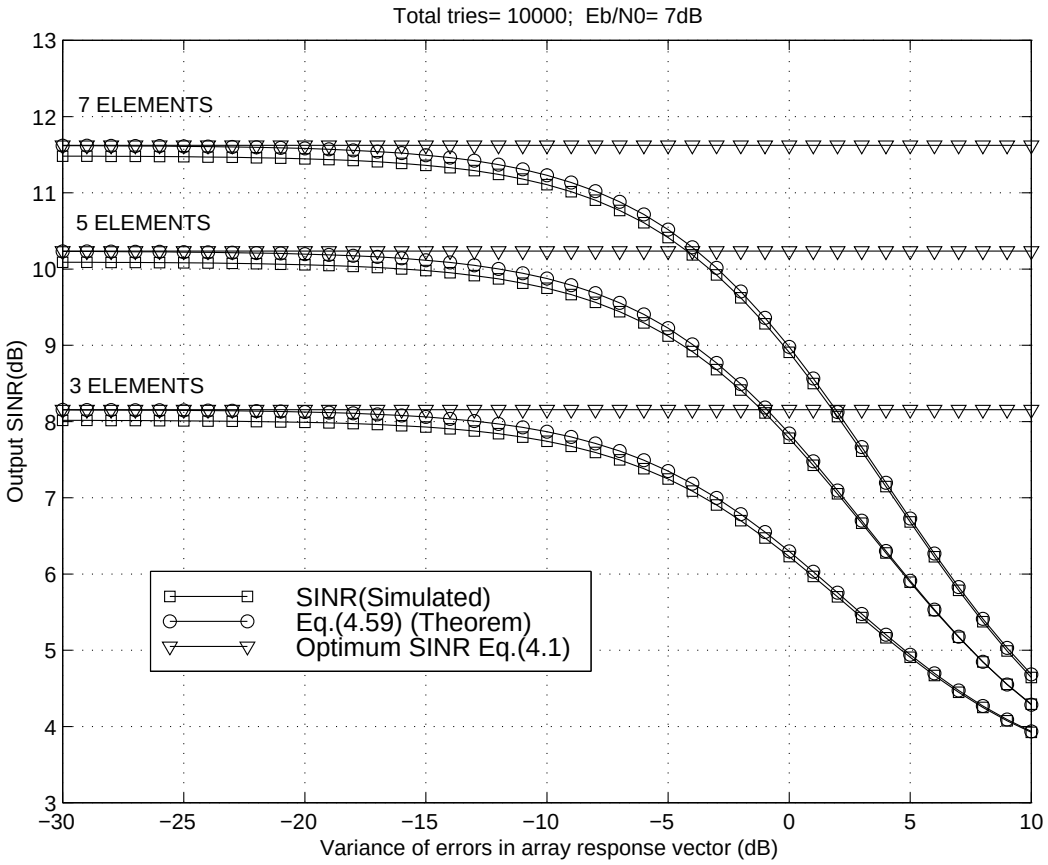

Figure 4.2: Output SINR with respect to errors in the array response vector

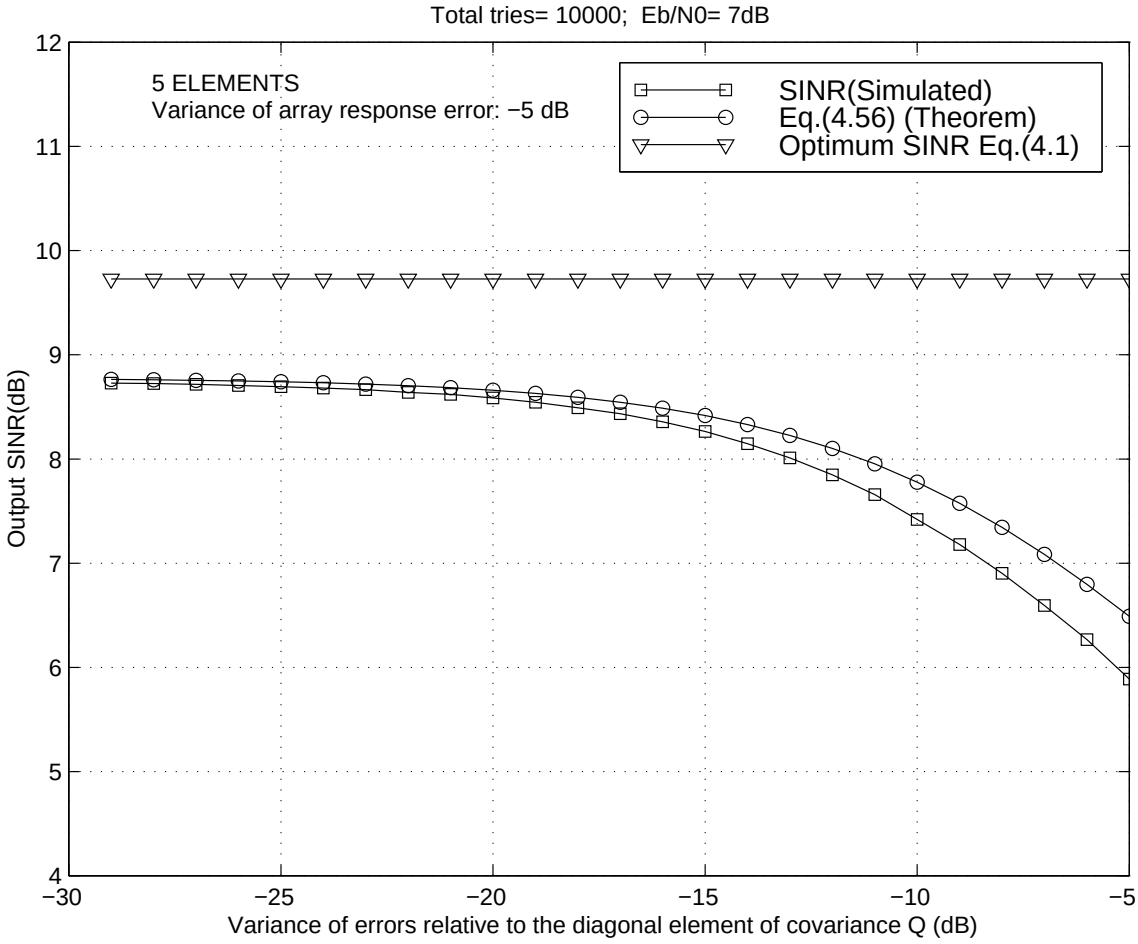

Figure 4.3: Output SINR with respect to errors in the MAI matrix and the array response vector: array response error $-5dB$

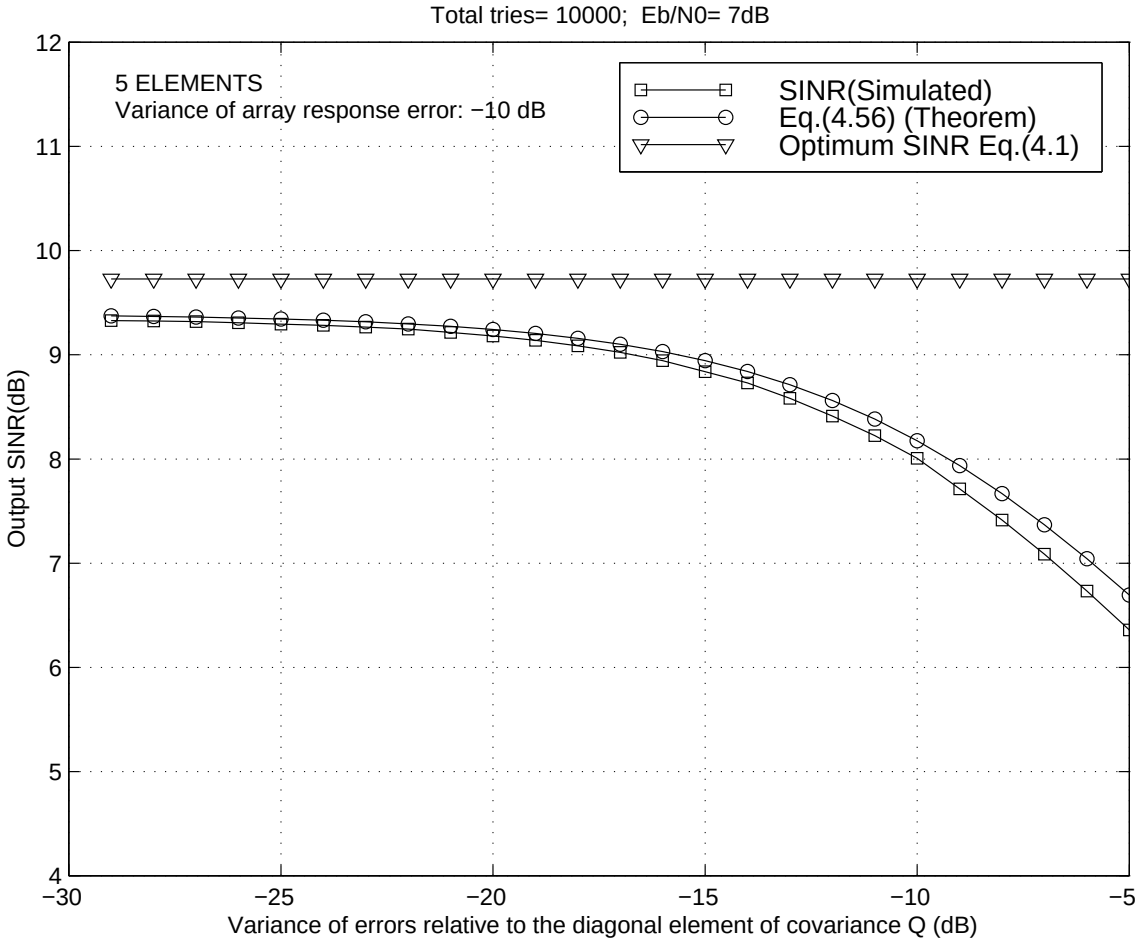

Figure 4.4: Output SINR with respect to errors in the MAI matrix and the array response vector: array response error $-10dB$

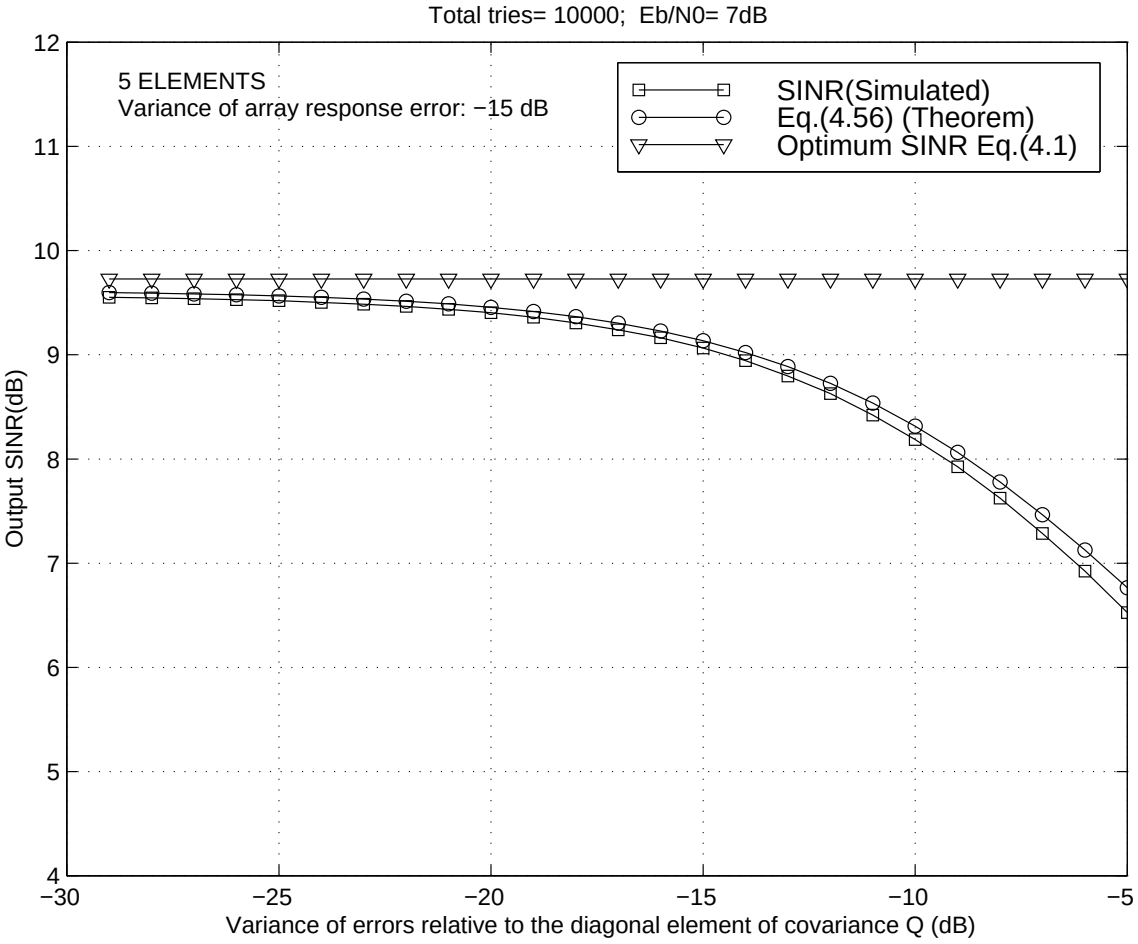

Figure 4.5: Output SINR with respect to errors in the MAI matrix and the array response vector: array response error $-15dB$

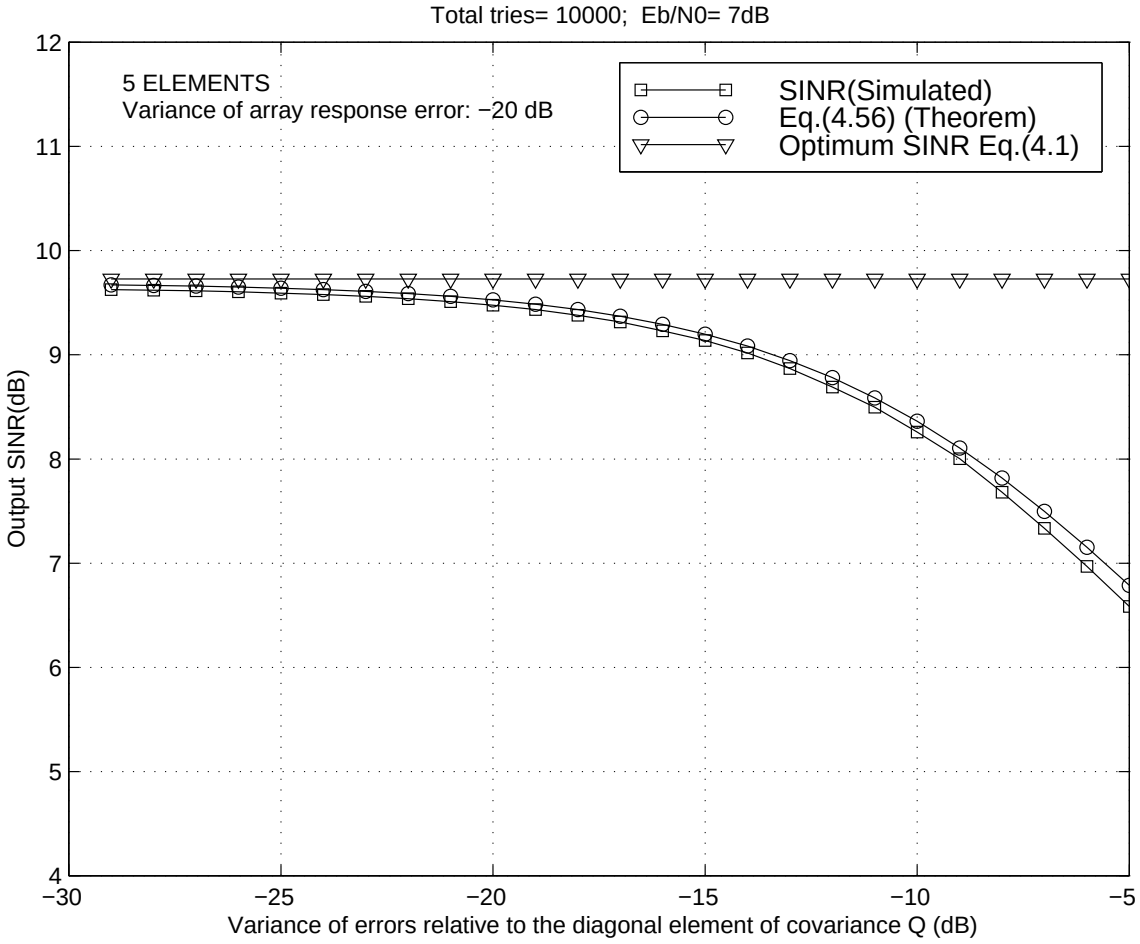

Figure 4.6: Output SINR with respect to errors in the MAI matrix and the array response vector

4.7 Conclusion

In this chapter, we presented the effect of antenna array beamforming errors on DS-CDMA communication systems. We have considered the situation where the errors in estimating the array response are independent from the errors in estimating the MAI. We have shown that the degradation of the output **SINR** increases as the number of antennas increases. When the variance of the errors in both the array response and the MAI matrix are the same, such as -15dB, there is nearly no degradation in the output **SINR** due to array errors but there is a 0.5dB **SINR** degradation due to MAI matrix errors in the case of a 7-element array. We have also shown that as we increase the number of antennas to increase the **SINR**, the sensitivity to array response error does not change while the sensitivity to MAI matrix estimates increases proportionally. This analysis has been applied to the signal cancellation algorithm presented in Chapter 3, where Monte-Carlo simulation results and analytical calculation agreed quite closely.

Chapter 5

A Feedforward Approach to Downlink Beamforming

5.1 Introduction

In a cellular CDMA communication system, there are two links in the system; the uplink (mobile-to-base-station) and the downlink(base-station-to-mobile). As the capacity is only partially determined by the uplink, we also address downlink capacity. In [71, 52, 51], researchers have shown that the capacity may be improved with a transmitting antenna array at the base station. In this thesis, we also consider a transmitting antenna array at the base station. As the mobile should be kept as small as possible, an antenna array at the mobile may be impractical. One advantage of an antenna array at the mobile is that the antennas may be implemented in a compact manner. However, the cost and complexity of implementing an antenna array at the mobile is much greater overall than that of implementing only one array at each base station [75]. Here we consider a single antenna at the mobile and a single cell. Generalization to a multi-cell situation is left as future work.

In order to perform downlink beamforming, we need to know the downlink channel vectors for all the users in the same cell. For the uplink, the base station may estimate the channel vector for the mobiles. However, there is no such inherent feedback for the downlink. Therefore, the key problem in the downlink is how to estimate the downlink channel vector.

This chapter presents downlink beamforming in a cellular CDMA system. The relationship between the uplink and the downlink channel is described in Section 5.3. A thorough analysis of downlink beamforming and then the criteria for downlink beamforming are conducted in Section 5.4. In Section 5.5, we present a new approach for downlink channel estimation through the feedforward method. A perturbation RLS algorithm is proposed in Section 5.6. In Section 5.7, we compare our proposed method with a previous probing and feedback method. The conclusions are presented in Section 5.8.

5.2 Related research

The uplink beamforming in a CDMA system has been well studied [42, 9, 50, 43, 45, 44, 70, 47, 46, 49, 51, 11, 84]. There are some studies for downlink beamforming for a FDMA or TDMA system [19, 20, 17, 83, 63, 21, 24, 18, 13, 14, 40, 81, 54, 5]. In a TDMA system, the base station can use the estimated uplink channel vector for downlink beamforming as long as the time difference is small. For a FDMA system, the base station may use the estimated uplink channel vector for the downlink beamforming as long as the frequency difference is small. In [21], Raleigh proposes to use channel subspace invariance to estimate downlink channel spatial covariance from the uplink channel spatial covariance on the condition that the carrier frequency difference between the uplink and downlink is small. Channel subspace invariance is described in Section 5.3.1. This beamforming method degrades with an increase in frequency difference. In [84], Zetterberg proposes to form a transmitting beam towards the mobile based on array response and directional information estimated from the uplink data in a TDMA system. The result in [84] is that capacity is largely dependent on the spread angle of the locally scattered rays in vicinity of the mobile. In [19, 20, 17], Gerlach proposes to use probing and feedback to estimate downlink channel vectors in a TDMA/FDMA system. However, for CDMA systems, to the best knowledge of the author, there are few results. We may not use the estimated uplink channel vector information for a CDMA system as we will explain in Sections 5.3 and 5.4.1. Therefore, the key problem in downlink beamforming in a CDMA system is

to estimate the downlink channel vector of the mobiles and make this information available to the base station where the downlink weights are formed. The viable methods seem to involve feedback as in [19, 20, 17]. The feedback idea originates from [79], where Widrow presents a method of maximizing the delivered power by a satellite antenna array to a ground station using feedback from the ground station back to the satellite. Akaiwa proposes a feedback scheme for diversity transmission in a TDMA system in [1]. The mobile feeds back the information about which antenna has the strongest signal arriving at the mobile. In [36], Liang proposes to perturb the transmitter weight vector with orthogonal variations and feedback the perturbation responses at the mobile to the base station. The base station uses a Kalman filter to track the variations of the channel vector for an indoor FDD communication system.

5.3 Relationship between uplink and downlink channels

5.3.1 Channel subspace invariance between the uplink and downlink

First, we review the channel model for the uplink and then we use reciprocity to obtain the downlink channel model. Here, for brevity we omit the white noise in the base station receiver as it does not affect the channel propagation model. For simplicity, we use complex baseband signals to represent the output signals of the antenna array due to the kth mobile:

$$\mathbf{r}_{up}(m) = \sum_{l=1}^{L} \mathbf{a}_k(\theta_{k,l}, \omega_{up}) \beta_{up,k,l}(mT_b, \omega_{up}) b_k(mT_b - \tau_{k,l}) \tag{5.1}$$

where we suppose there are L different paths for the kth mobile and each path has an associated DOA, $\theta_{k,l}$, a corresponding array response vector $\mathbf{a}_k(\theta_{k,l}, \omega_{up})$, a complex channel gain $\beta_{up,k,l}(mT_b, \omega_{up})$ and a relative delay $\tau_{k,l}$. In Eq. (5.1), T_b is the symbol period and $b_k(mT_b - \tau_{k,l})$ is the transmitted symbol sequence of the kth mobile, and ω_{up} is the uplink carrier frequency. There are three factors that affect the channel gain $\beta_{up,k,l}(mT_b, \omega_{up})$: fast fading resulting from the local scatterers surrounding the

kth mobile, shadowing and path loss. Therefore, we may write $\beta_{up,k,l}(mT_b, \omega_{up})$ as

$$\beta_{up,k,l}(mT_b, \omega_{up}) = \frac{\alpha_{k,l}(mT_b, \omega_{up})\sqrt{\Gamma_{k,l}(mT_b)}}{d_k^{\frac{\hat{n}}{2}}} \tag{5.2}$$

where $\alpha_{k,l}(mT_b, \omega_{up})$ represents the fast fading effect, $\Gamma_{k,l}(mT_b)$ represents shadowing, usually modelled as having a log-normal distribution, and $\hat{n}$ is the order of the path loss with a typical value of 4. The local scatterers around the kth mobile cause the fast fading. The motion of the kth mobile causes Doppler shifts. The large buildings or trees cause shadowing or slow fading. Supposing there are a total of $S_{k,l}$ scatterers affecting the lth path of the kth mobile, then we may write [64]

$$\alpha_{k,l}(mT_b, \omega_{up}) = K \sum_{i=1}^{S_{k,l}} C_i e^{j\omega_{up}\frac{v}{c}cos(\Omega_i)mT_b} \tag{5.3}$$

where Ω_i is the angle of local scatterer i with respect to the direction of the mobile velocity vector, C_i is the complex reflection coefficient of the ith local scatterer, c is the speed of light, and K is a gain constant. Defining $\sigma^2_{up,\beta_{k,l}}$ as the variance of $\beta_{up,k,l}(mT_b, \omega_{up})$, it is easy to show that

$$\sigma^2_{up,\beta_{k,l}} = \frac{\Gamma_{k,l}(mT_b)K^2\sum_{i=1}^{S_{k,l}}|C_i|^2}{d_k^{\hat{n}}} \tag{5.4}$$

From Eq. (5.4), we see that the long term average of the variance is independent of the carrier frequency ω_{up}. However, for this to be true, the scatterers around the kth mobile must not change abruptly. For a weak path, we should not expect this invariance. Using reciprocity, we may write the downlink response due to the lth path at the kth mobile as

$$r_{down,k,l} = \mathbf{w}_{k,l}^{\mathbf{H}}\mathbf{a}_k(\theta_{k,l}, \omega_{down})\beta_{down,k,l}(mT_b, \omega_{down})b_k(mT_b - \tau_{k,l}) \tag{5.5}$$

where $\mathbf{w}_{k,l}$ is the weight we apply to the lth path. We will present the criterion later in this chapter to describe how to select the $\mathbf{w}_{k,l}$. We use $\mathbf{a}_k(\theta_{k,l}, \omega_{down})$ to represent the downlink array response vector for the lth path of the kth mobile. Similar to Eq. (5.2),

$$\beta_{down,k,l}(mT_b, \omega_{down}) = \frac{\alpha_{k,l}(mT_b, \omega_{down})\sqrt{\Gamma_{k,l}(mT_b)}}{d_k^{\frac{\hat{n}}{2}}} \tag{5.6}$$

We also see that $\sigma^2_{up,\beta_{k,l}}$ is independent of frequency, and if the scatterers around the kth mobile do not change abruptly in a short time for a strong path, we obtain

$$\begin{aligned}\sigma^2_{down,\beta_{k,l}} &= \sigma^2_{up,\beta_{k,l}} \\ &= \frac{\Gamma_{k,l}(mT_b)K^2\sum_{i=1}^{S_{k,l}}|C_i|^2}{d_k^{\frac{\hat{n}}{2}}}\end{aligned} \tag{5.7}$$

5.3.2 Instantaneous relationship between the uplink and downlink channel gain

In this section we examine the instantaneous relationship between the uplink channel vector and the downlink channel vector. Generally, for a CDMA system, for example IS-95, the uplink and the downlink use different carrier frequencies and the difference is more than 45MHz. We can show that when the frequency difference is more than 200kHz, the instantaneous correlation between the uplink channel gain and the downlink channel gain is very small. Assuming that the relative delays between different mobiles are uniformly distributed over $[-\tau_{max}, \tau_{max}]$, by using the model in Section 5.3.1, it is straightforward to show that:

$$E\{\beta_{down,k,l}(mT_b,\omega_{down})\beta_{up,k,l}(mT_b,\omega_{up})^*\} = \sigma^2_{up,\beta_{k,l}} sinc(\tau_{max}(\omega_{up}-\omega_{down})) \tag{5.8}$$

where $\sigma^2_{up,\beta_{k,l}}$ is independent of carrier frequency. A typical value for τ_{max} is 10μsec, if $|\omega_{up}-\omega_{down}|$ is more than 200KHz. From Figure 5.1, we obtain

$$E\{\beta_{down,k,l}(mT_b,\omega_{down})\beta_{up,k,l}(mT_b,\omega_{up})^*\} \approx 0 \tag{5.9}$$

The above expression is in contrast to Eq. (5.7), where the long term average of the channel gain is the same for the uplink and the downlink.

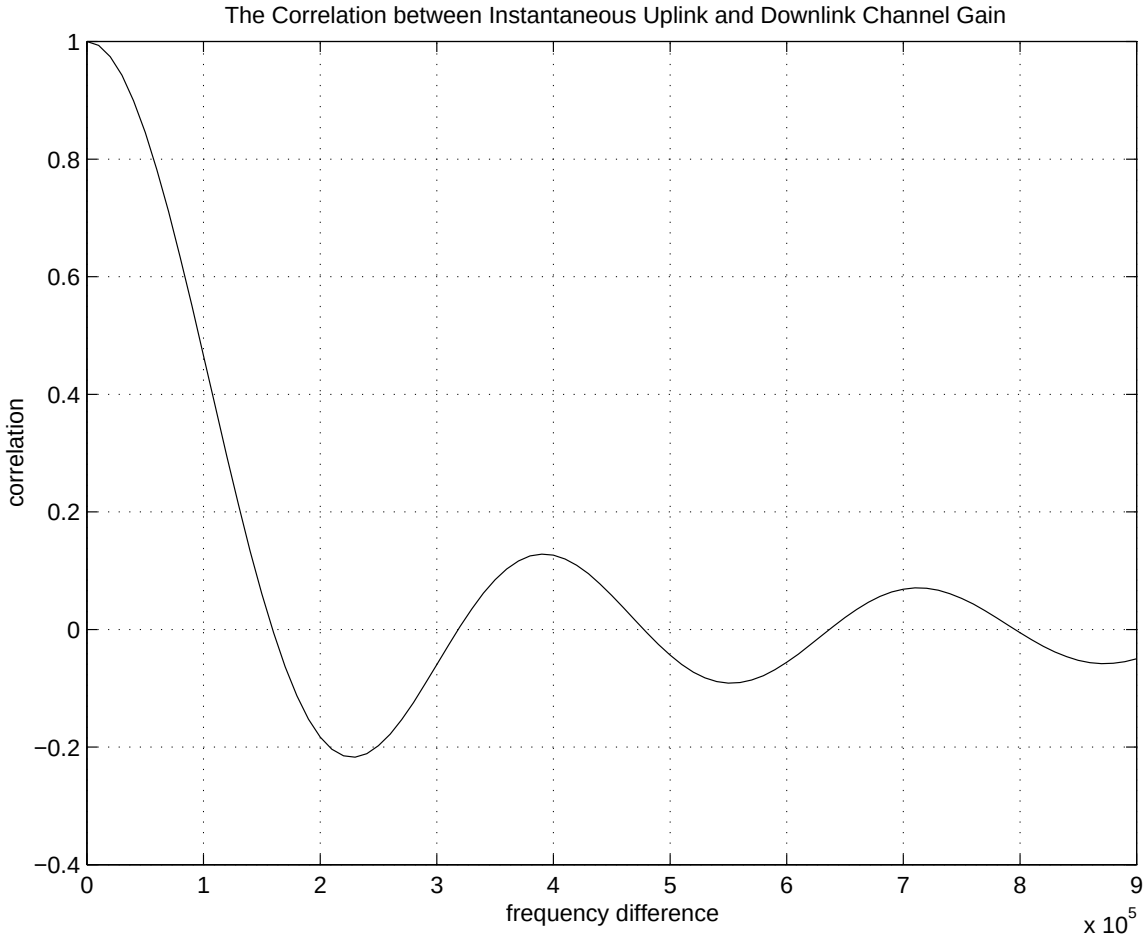

Figure 5.1: The correlation between instantaneous uplink and downlink channel gain

5.4 Downlink beamforming problem formulation

Here we consider downlink beamforming in a cellular CDMA system. The downlink differs greatly from the uplink in terms of interference, existing information, etc. In the uplink, the signals arrive at a base station from different mobiles and typically have different angles of arrival (DOA), thus they experience different channels. As a result of this fact, the signals from different mobiles have different fading channel gains. For a desired mobile signal, the interferences will fluctuate in magnitude because of the different fading channel gains for the interferences. In contrast, in the downlink, the interferences for a desired mobile go through the same fading channel as the desired mobile, and therefore, its signal model will change accordingly.

First, we consider the simplest case and omit the interferences from the other cell base stations. Suppose there are N users in a cell and the base station forms a different weight vector for each user. The criteria of selecting the weights will be addressed later in this chapter. Without loss in generality, we consider the kth user and its corresponding array response vector, $\mathbf{a}_k$. For notational simplicity, we drop the time index t when it's not required. After de-spreading, the received signal at kth mobile is

$$r_k = \sum_{j=1, j\neq k}^{N} \mathbf{w}_j^{\mathbf{H}} \mathbf{a}_k b_k + \mathbf{w}_k^{\mathbf{H}} \mathbf{a}_k b_k + n_k \tag{5.10}$$

where n_k is white noise and is independent of the interferences and the desired signal. Here, $\mathbf{a}_k$ includes both the array response vector and the channel gain. For convenience, we may rewrite Eq. (5.10) as:

$$r_k = \mathbf{w}^{\mathbf{H}} \mathbf{a}_k b_k + n_k \tag{5.11}$$

where

$$\mathbf{w} = \sum_{j=1}^{N} \mathbf{w}_j \tag{5.12}$$

Now we will find a demodulation method to decode b_k given r_k. As we use a **BPSK** signal, there are only two choices for estimate $\hat{b}_k$: +1 or -1. If we know the true value of $\mathbf{w}$ and b_k or $\mathbf{w}^{\mathbf{H}} \mathbf{a}_k$, we propose to use an MMSE estimator to decode b_k. We choose

an estimate $\hat{b}_k$ to minimize

$$||r_k - \mathbf{w^H a}_k \hat{b}_k||^2 \tag{5.13}$$

Expanding Eq. (5.13) we obtain

$$||r_k||^2 - (\mathbf{w^H a}_k)^* r_k \hat{b}_k - \mathbf{w^H a}_k r_k^* \hat{b}_k + ||\mathbf{w^H a}_k||^2 \tag{5.14}$$

Obviously, $||r_k||^2$ and $||\mathbf{w^H a}_k||^2$ do not affect the selection of $\hat{b}_k$. It can be shown that [61]

$$\hat{b}_k = \zeta Re\{(\mathbf{w^H a}_k)^* r_k\} \tag{5.15}$$

minimizes Eq. (5.13), where ζ is a positive constant. This is simply a decorrelator if we know $\mathbf{w^H a}_k$. Now we examine the output of this correlator. Letting y_k denote the output, we obtain

$$y_k = (\mathbf{w^H a}_K b_k + n_k)(\mathbf{w^H a}_k)^* \tag{5.16}$$

The average SNR of the kth mobile is given by

$$\begin{aligned} \mathbf{SNR}_k &= \frac{\mathbf{E}\{||\mathbf{w^H a}_k||^4\}}{\mathbf{E}\{||(\mathbf{w^H a}_k)^* n_k||^2\}} \\ &= \frac{\mathbf{E}\{||\mathbf{w^H a}_k||^2\}}{\sigma^2} \end{aligned} \tag{5.17}$$

The signal-to-noise ratio (SNR) affects the quality of decoding. We should maintain the average SNR above a threshold so that the bit error rate (**BER**) is below some preset value. Since we can not transmit arbitrary power at the base station, therefore, we constrain the transmission power according to

$$||\mathbf{w}||^2 = P \tag{5.18}$$

where P is a constant. Rather than maximize the SNR for the kth mobile in isolation, we need to maximize the SNR jointly for all the users in the same cell. That is, we

$$Maximize \quad \mathbf{SNR}_k \quad for \quad k = 1, 2, \ldots, N. \tag{5.19}$$

To simplify Eq. (5.19), we instead propose to maximize the sum of all users' average SNR. That is, we maximize

$$\sum_{k=1}^{N} \mathbf{E}\{||\mathbf{w^H a}_k||^2\} \tag{5.20}$$

subject to

$$||\mathbf{w}||^2 = P \tag{5.21}$$

It can be shown that $\mathbf{w}$ is the eigenvector corresponding to the largest eigenvalue of the matrix $\mathbf{E}\{\sum_{j=1}^{N} \mathbf{a}_k \mathbf{a}_k^{\mathbf{H}}\}$ [41].

5.4.1 Effect of uncorrelated noise

To maximize the SNR of the kth mobile, we need to set our weights to the eigenvector corresponding to the maximum eigenvalue of the matrix $\mathbf{E}\{\sum_{j=1}^{N} \mathbf{a}_k \mathbf{a}_k^{\mathbf{H}}\}$. Here we define

$$\mathbf{P}_{ideal} = \mathbf{E}\{\sum_{k=1}^{N} \mathbf{a}_k \mathbf{a}_k^{\mathbf{H}}\} \tag{5.22}$$

when the base station knows the exact value of all downlink channel vectors. Let $\mathbf{w}_{ideal}$ denote the eigenvector corresponding to the largest eigenvalue of matrix $\mathbf{P}_{ideal}$. In addition, we define

$$\mathbf{P}_{estimate} = \mathbf{E}\{\sum_{k=1}^{N} \hat{\mathbf{a}}_k \hat{\mathbf{a}}_k^{\mathbf{H}}\} \tag{5.23}$$

when the base station may only estimate the value of downlink channel vectors. In Eq. (5.23), $\hat{\mathbf{a}}_k$ denotes the estimated downlink channel vector. Let $\mathbf{w}_{estimate}$ denote the eigenvector corresponding to the largest eigenvalue of matrix $\mathbf{P}_{estimate}$. The SNR of the kth mobile is

$$\mathbf{SNR}_k = \frac{\mathbf{E}\{||\mathbf{w}^{\mathbf{H}} \mathbf{a}_k||^2\}}{\sigma^2} \tag{5.24}$$

We normalize the SNR calculated by using weights $\mathbf{w}_{estimate}$ by the SNR calculated by using weights $\mathbf{w}_{ideal}$ so we may obtain the relative SNR by using estimated channel vectors. We define the relative SNR as

$$\rho_{SNR} = \frac{\mathbf{E}\{||\mathbf{w}_{estimate}^{\mathbf{H}} \mathbf{a}_k||^2\}}{\mathbf{E}\{||\mathbf{w}_{ideal}{}^{\mathbf{H}} \mathbf{a}_k||^2\}} \tag{5.25}$$

To maximize Eq. (5.25), we should choose $\mathbf{w}_{estimate}$ as close as possible to $\mathbf{w}_{ideal}$. From Eq. (5.25), we need to know the downlink array response vector for each user in the cell. In a rural area, there are few scatterers around the mobiles, and we may treat the downlink array response vector the same as the uplink channel vector. We may use the algorithm in Chapter 3 to perform downlink beamforming. However, due to

estimation errors in the uplink, the uplink array response vector is corrupted by noise.

Proposition 1 *If the errors are Gaussian white noise, $\rho_{SNR} = 1$, and so there is no degradation in the SNR at the mobiles.*

Proof:
Assume that

$$\hat{\mathbf{a}}_k = \mathbf{a}_k + n_k \tag{5.26}$$

where n_k is white noise vector with variance ψ_k and is uncorrelated with the $\mathbf{a}_k$. We remark that for each mobile the white noise variance does not have to be the same. Therefore,

$$\begin{aligned} \mathbf{P}_{estimate} &= \mathbf{E}\{\sum_{k=1}^{N} \hat{\mathbf{a}}_k \hat{\mathbf{a}}_k^{\mathbf{H}}\} \\ &= \mathbf{E}\{\sum_{k=1}^{N} \mathbf{a}_k \mathbf{a}_k^{\mathbf{H}}\} + \sum_{k=1}^{N} \psi_k \mathbf{I} \\ &= \mathbf{P}_{ideal} + \sum_{k=1}^{N} \psi_k \mathbf{I} \end{aligned} \tag{5.27}$$

where $\mathbf{I}$ is the identity matrix. As long as the second term in Eq. (5.27) is a diagonal matrix, the principal eigenvector of $\mathbf{P}_{estimate}$ and $\mathbf{P}_{ideal}$ will be the same, so $\rho_{SNR} = 1$, i.e, $\mathbf{w}_{estimate} = \mathbf{w}_{ideal}$ and there is no degradation in performance in terms of average SNR.
QED
In an urban area, however, due to the fading and the Doppler effects, the instantaneous complex channel gain of the uplink and the downlink are uncorrelated. For a strong path, we may expect that the scattering environment around the mobile does not change abruptly in a short time, but for a weak path, this is not true. Forming a beam by using the estimated uplink channel vector may generate more multi-path interference instead of making a beneficial contribution to the received signal at the mobile. In urban areas, therefore, we need to estimate the downlink channel vector without the help of the uplink channel vector. Furthermore, it has been shown in

[51] that with perfect downlink channel vectors, we may increase system capacity several-fold.

5.5 A feedforward approach for downlink channel estimation

Gerlach has proposed to use probing and feedback to estimate the downlink channel vectors in the TDMA or FDMA access scheme [19, 20, 17].

In [4, 3, 2], the European **CODIT** system is proposed and analyzed. Every mobile transmits data and a control signal to the base station. The control channel is used to adapt the configuration of the data channel to a service or demand of the radio network.

Here we suppose that the feedback channel from the mobile to the base station is available. We propose a feedforward approach to estimate the channel vector at the mobiles and feed it back to the base station in a CDMA system. Without loss in generality, suppose we need to estimate the channel vector for the kth mobile. We notice that in Eq. (5.10), $\mathbf{w} = \sum_{j=1}^{N} \mathbf{w}_j$ is common to all the users in the same cell. We propose to feedforward this information to all users in the same cell through the pilot or other dedicated channel to ensure reliable reception. Here, we propose to use the pilot channel or other dedicated channel to transmit weight information. We may use any other channel which ensures reliable transmission. This is different from Gerlach's methods in [19, 20, 17], where required probing signals must lie in or near the frequency band of the information signals. In [19, 20, 17], the information signals may not be transmitted in the probing stage while in our proposed method simultaneous probing and information transmission is possible.

5.5.1 Using MMSE to estimate the initial channel vector

Currently, we suppose we may obtain a noise-free $\mathbf{w}$ at the mobile through the pilot channel. Further, due to the pilot channel, at the mobile stations, we may estimate the scalar channel gain from the base station, i.e., $\mathbf{w}^{\mathbf{H}}\mathbf{a}_k$, for the kth user which we

denote by

$$g_k = \mathbf{w}^{\mathbf{H}}\mathbf{a}_k \tag{5.28}$$

$\mathbf{a}_k$ is the channel vector we desire to estimate. We remark that g_k will be contaminated by the thermal noise at the mobile. The estimation of g_k from the pilot channel will not be addressed in this thesis. The reader may refer to [4]. For g_k and the $\mathbf{w}$, we propose to use the minimum mean square error criteria to estimate $\mathbf{a}_k$, i.e.,

$$\hat{\mathbf{a}}_k = arg \max_{\hat{\mathbf{a}}_k} ||g_k - \mathbf{w}^{\mathbf{H}}\hat{\mathbf{a}}_k||^2 \tag{5.29}$$

Define

$$y_{mmse} = ||g_k - \mathbf{w}^{\mathbf{H}}\hat{\mathbf{a}}_k||^2 \tag{5.30}$$

Expanding (5.30),

$$\begin{aligned} y_{mmse} &= (g_k - \mathbf{w}^{\mathbf{H}}\hat{\mathbf{a}}_k)^{\mathbf{H}}(g_k - \mathbf{w}^{\mathbf{H}}\hat{\mathbf{a}}_k) \\ &= ||g_k||^2 - g_k^{\mathbf{H}}\mathbf{w}^{\mathbf{H}}\hat{\mathbf{a}}_k - \hat{\mathbf{a}}_k^{\mathbf{H}}\mathbf{w}g_k + \hat{\mathbf{a}}_k^{\mathbf{H}}\mathbf{w}\mathbf{w}^{\mathbf{H}}\hat{\mathbf{a}}_k \end{aligned} \tag{5.31}$$

Differentiating y_{mmse} with respect to $\hat{\mathbf{a}}_k$, we obtain

$$\frac{\partial y_{mmse}}{\partial \hat{\mathbf{a}}_k} = -(g_k^{\mathbf{H}}\mathbf{w}^{\mathbf{H}})^{\mathbf{T}} + (\mathbf{w}\mathbf{w}^{\mathbf{H}}\hat{\mathbf{a}}_k)^* \tag{5.32}$$

Setting Eq. (5.32) to zero,

$$\mathbf{w}\mathbf{w}^{\mathbf{H}}\hat{\mathbf{a}}_k = \mathbf{w}g_k \tag{5.33}$$

We notice that $\mathbf{w}\mathbf{w}^{\mathbf{H}}$ is a rank-one matrix and therefore the solution of Eq. (5.33) is not unique. One possible solution is

$$\hat{\mathbf{a}}_k = (\mathbf{w}\mathbf{w}^{\mathbf{H}})^{\dagger}\mathbf{w}g_k \tag{5.34}$$

where $\dagger$ denotes the Moore-Penrose pseudo-inverse [66]. We will use this solution later to obtain an initial estimate of $\hat{\mathbf{a}}_k$.

5.5.2 Recursive updating channel vector estimates

Here we propose to use the recursive least-squares (RLS) algorithm to estimate downlink channel vectors [26]. Without loss in generality, we estimate the kth mobile's channel vector. At time i, we have the following equation:

$$g_k(i) = \mathbf{w}^{\mathbf{H}}(i)\mathbf{a}_k + n_k(i) \tag{5.35}$$

As before, $g_k(i)$ is the estimated scalar channel gain for the kth mobile at time instant i. If we obtain $\hat{L}$ snapshots of the scalar gain $g_k(i)$, we have:

$$\begin{aligned} g_k(1) &= \mathbf{w^H}(1)\mathbf{a}_k + n_k(1) && (5.36)\\ g_k(2) &= \mathbf{w^H}(2)\mathbf{a}_k + n_k(2) && (5.37)\\ &\vdots \\ g_k(\hat{L}) &= \mathbf{w^H}(\hat{L})\mathbf{a}_k + n_k(\hat{L}) && (5.38) \end{aligned}$$

Define the error term

$$e(i) = g_k(i) - \mathbf{w^H}(i)\mathbf{a}_k \tag{5.39}$$

Our fading memory cost function is defined as

$$\vartheta(\hat{L}) = \sum_{i=1}^{\hat{L}} \alpha^{\hat{L}-i}|e(i)|^2 \tag{5.40}$$

where α is the forgetting factor and is usually chosen in the range

$$0 < \alpha \leq 1 \tag{5.41}$$

To minimize $\vartheta(\hat{L})$, we express Eq. (5.35) to Eq. (5.40) as the system of equations

$$\mathbf{W}(\hat{L})\mathbf{a}_k = \mathbf{F}(\hat{L}) \tag{5.42}$$

where the $\hat{L} \times M$ matrix

$$\mathbf{W}(\hat{L}) = \sum_{i=1}^{\hat{L}} \alpha^{\hat{L}-i}\mathbf{w}(i)\mathbf{w^H}(i) \tag{5.43}$$

where M is the number of transmitting antennas at the base station, and we have the $\hat{L} \times 1$ vector

$$\mathbf{F}(\hat{L}) = \sum_{i=1}^{\hat{L}} \alpha^{\hat{L}-i}\mathbf{w}(i)g_k^*(i) \tag{5.44}$$

We notice that $\mathbf{W}(\hat{L})$ may also be written recursively as

$$\begin{aligned} \mathbf{W}(\hat{L}) &= \sum_{i=1}^{\hat{L}-1} \alpha^{\hat{L}-i-1}\mathbf{w}(i)\mathbf{w^H}(i) + \mathbf{w}(\hat{L})\mathbf{w^H}(\hat{L}) \\ &= \alpha\mathbf{W}(\hat{L}-1) + \mathbf{w}(\hat{L})\mathbf{w^H}(\hat{L}) && (5.45) \end{aligned}$$

and $\mathbf{F}(\hat{L})$ may be written as

$$\mathbf{F}(\hat{L}) = \alpha \mathbf{F}(\hat{L}-1) + \mathbf{w}(\hat{L}) g_k^*(\hat{L}) \tag{5.46}$$

Applying the well-known matrix inversion lemma [66] to Eq. (5.45), we obtain a recursive equation for the inverse of the weight matrix $\mathbf{W}(\hat{L})$:

$$\mathbf{W}^{-1}(\hat{L}) = \alpha^{-1}\mathbf{W}^{-1}(\hat{L}-1) - \frac{\alpha^{-2}\mathbf{W}^{-1}(\hat{L}-1)\mathbf{w}(\hat{L})\mathbf{w}^{\mathbf{H}}(\hat{L})\mathbf{W}^{-1}(\hat{L}-1)}{1+\alpha^{-1}\mathbf{w}^{\mathbf{H}}(\hat{L})\mathbf{W}^{-1}(\hat{L}-1)\mathbf{w}(\hat{L})} \tag{5.47}$$

Define the terms in Eq. (5.47)

$$\mathbf{S}(\hat{L}) = \mathbf{W}^{-1}(\hat{L}) \tag{5.48}$$

and

$$\mathbf{u}(\hat{L}) = \frac{\alpha^{-1}\mathbf{S}(\hat{L}-1)\mathbf{w}(\hat{L})}{1+\alpha^{-1}\mathbf{w}^{\mathbf{H}}(\hat{L})\mathbf{S}(\hat{L}-1)\mathbf{w}(\hat{L})} \tag{5.49}$$

We obtain the weight inverse update as

$$\mathbf{S}(\hat{L}) = \alpha^{-1}\mathbf{S}(\hat{L}-1) - \alpha^{-1}\mathbf{u}(\hat{L})\mathbf{w}^{\mathbf{H}}(\hat{L})\mathbf{S}(\hat{L}-1) \tag{5.50}$$

Similarly we obtain the array response update as

$$\mathbf{a}_k(\hat{L}) = \mathbf{a}_k(\hat{L}-1) + \mathbf{u}(\hat{L})\chi(\hat{L}) \tag{5.51}$$

where the innovation sequence is

$$\chi(\hat{L}) = g_k(\hat{L}) - \mathbf{w}^{\mathbf{H}}(\hat{L}-1)\mathbf{a}_k(\hat{L}) \tag{5.52}$$

From Eqs. (5.49) and (5.52), we may update the channel estimates recursively. To initialize of the above RLS algorithm, we set $\mathbf{a}_k(0)$ according to Section 5.5.1. Usually, we initialize $\mathbf{W}(0)$ (and therefore $\mathbf{S}(0)$) by

$$\mathbf{W}(0) = \zeta \mathbf{I} \tag{5.53}$$

where ζ is a small positive constant. In Figure 5.2, we summarize the RLS algorithm to estimate the kth mobile's channel vector.

Initialize the RLS algorithm:

set $\hat{L} = 0$;

$\mathbf{W}(0) = \zeta \mathbf{I} \quad (\mathbf{S}(0) = \zeta^{-1}\mathbf{I})$ and

$\mathbf{a}_k(0) = (\mathbf{w}(0)\mathbf{w}^{\mathbf{H}}(0))^{\dagger}\mathbf{w}(0)g_k(0)$

For each instant of time, $\hat{L} = 1, 2, \ldots$, compute

{

1. Updating $\mathbf{u}(\hat{L})$

$$\mathbf{u}(\hat{L}) = \frac{\alpha^{-1}\mathbf{S}(\hat{L}-1)\mathbf{w}(\hat{L})}{1+\alpha^{-1}\mathbf{w}^{\mathbf{H}}(\hat{L})\mathbf{S}(\hat{L}-1)\mathbf{w}(\hat{L})}$$

2. Updating $\chi(\hat{L})$

$$\chi(\hat{L}) = g_k(\hat{L}) - \mathbf{w}^{\mathbf{H}}(\hat{L})\mathbf{a}_k(\hat{L}-1)$$

3. Updating $\mathbf{a}_k(\hat{L})$

$$\mathbf{a}_k(\hat{L}) = \mathbf{a}_k(\hat{L}-1) + \mathbf{u}(\hat{L})\chi^*(\hat{L})$$

4. Updating $\mathbf{S}(\hat{L})$

$$\mathbf{S}(\hat{L}) = \alpha^{-1}\mathbf{S}(\hat{L}-1) - \alpha^{-1}\mathbf{u}(\hat{L})\mathbf{w}^{\mathbf{H}}(\hat{L})\mathbf{S}(\hat{L}-1)$$

}

Figure 5.2: Summary of the RLS algorithm for estimating the kth mobile's downlink channel vector

5.5.3 Implementation issues in the RLS algorithm

We note that Eq. (5.47) involves finding inverse of matrix $\mathbf{W}$, which requires $\mathbf{W}$ to be full rank. To lessen this requirement, we may express $\mathbf{W}$ as

$$\mathbf{W}(\hat{L}) = \mathbf{G}\mathbf{T}\mathbf{G}^{\mathbf{H}} \tag{5.54}$$

where $M \times \hat{L}$ matrix $\mathbf{G}$ is a function of the chosen weights

$$\mathbf{G} = \left[\mathbf{w}(1)\ \ \mathbf{w}(2) \ldots \mathbf{w}(\hat{L})\right] \tag{5.55}$$

and full rank $\hat{L} \times \hat{L}$ matrix $\mathbf{T}$ is defined as:

$$\mathbf{T} = \begin{bmatrix} \alpha^{\hat{L}-1} & 0 & \ldots & 0 \\ 0 & \alpha^{\hat{L}-2} & \ldots & 0 \\ \vdots & \vdots & \ddots & \vdots \\ 0 & 0 & \ldots & \alpha^{0} \end{bmatrix} \tag{5.56}$$

where $\alpha > 0$. Next, we show the necessary condition of making matrix $\mathbf{W}$ full rank.

Proposition 2 *The rank of $M \times \hat{L}$ matrix $\mathbf{U}$ is equal to the rank of $M \times M$ matrix $\mathbf{U}\mathbf{U}^{\mathbf{H}}$, i.e.,*

$$rank(\mathbf{U}) = rank(\mathbf{U}\mathbf{U}^{\mathbf{H}}) \tag{5.57}$$

where $\mathbf{U} \in \mathbf{C}^{M \times \hat{L}}$, where $\mathbf{C}$ denotes complex field.

Proof:

The range space of $\mathbf{U}$ is defined as

$$Range(\mathbf{U}) = \{\mathbf{U}\underline{\mathbf{x}}, \forall \underline{\mathbf{x}} \in \mathbf{C}^{\hat{L}}\} \tag{5.58}$$

Similarly,

$$Range(\mathbf{U}^{\mathbf{H}}) = \{\mathbf{U}^{\mathbf{H}}\underline{\mathbf{x}}, \forall \underline{\mathbf{x}} \in \mathbf{C}^{M}\} \tag{5.59}$$

$Range(\mathbf{U}^{\mathbf{H}})$ is a subspace of $\mathbf{C}^{\hat{L}}$. The null space of $\mathbf{U}$, $\Upsilon(\mathbf{U})$, is defined as

$$\Upsilon(\mathbf{U}) \stackrel{\triangle}{=} \{\underline{\mathbf{x}} \in \mathbf{C}^{\hat{L}} \ \ such\ \ that\ \ \mathbf{U}\underline{\mathbf{x}} = \mathbf{0}\} \tag{5.60}$$

$\Upsilon(\mathbf{U})$ is a subspace of $\mathbf{C}^{\hat{L}}$ as well. It is well known [66] that

$$\mathbf{C}^{\hat{L}} = Range(\mathbf{U}^{\mathbf{H}}) + \Upsilon(\mathbf{U}) \tag{5.61}$$

where the sum refers to direct summation of subspaces. As $\underline{\mathbf{x}} \in \mathbf{C}^{\hat{L}}$, we obtain

$$\underline{\mathbf{x}} = \mathbf{U}^{\mathbf{H}}\underline{\theta} + \underline{\mathbf{w}} \tag{5.62}$$

where $\underline{\theta} \in \mathbf{C}^{M}$ and $\mathbf{U}\underline{\mathbf{w}} = \mathbf{0}$. Therefore, we obtain

$$\begin{aligned} Range(\mathbf{U}) &= \{\mathbf{U}(\mathbf{U}^{\mathbf{H}}\underline{\theta} + \underline{\mathbf{w}}), \forall \underline{\theta} \in \mathbf{C}^{M}, \underline{\mathbf{w}} \in \Upsilon(\mathbf{U})\} \\ &= \{\mathbf{U}\mathbf{U}^{\mathbf{H}}\underline{\theta}, \forall \underline{\theta} \in \mathbf{C}^{M}\} \\ &= Range(\mathbf{U}\mathbf{U}^{\mathbf{H}}) \end{aligned} \tag{5.63}$$

Therefore

$$rank(\mathbf{U}) = rank(\mathbf{U}\mathbf{U}^{\mathbf{H}}) \tag{5.64}$$

QED

Proposition 3 *To make* $\mathbf{W}(\hat{L})$ *full rank, we must have*

$$rank(\mathbf{G}) = M \tag{5.65}$$

Proof:
Since the dimension of matrix $\mathbf{G}$ is $M \times \hat{L}$ where $M \leq \hat{L}$,

$$rank(\mathbf{G}) \leq M \tag{5.66}$$

Therefore, we need only show that

$$rank(\mathbf{G}) < M \tag{5.67}$$

leads to a contradiction. Now suppose

$$rank(\mathbf{G}) < M \tag{5.68}$$

As α is a positive constant, the matrix $\mathbf{T}$ may be factored as

$$\mathbf{T} = \mathbf{E}\mathbf{E} \tag{5.69}$$

where the matrix $\mathbf{E}$ is defined as

$$\mathbf{E} = \begin{bmatrix} \alpha^{\frac{\hat{L}-1}{2}} & 0 & \dots & 0 \\ 0 & \alpha^{\frac{\hat{L}-2}{2}} & \dots & 0 \\ \vdots & \vdots & \ddots & \vdots \\ 0 & 0 & \dots & \alpha^{0} \end{bmatrix} \tag{5.70}$$

Define matrix $\mathbf{U}$ as

$$\begin{aligned} \mathbf{U} &= \mathbf{GE} \\ &= \begin{bmatrix} \alpha^{\frac{\hat{L}-1}{2}}\mathbf{w}(1) & \alpha^{\frac{\hat{L}-2}{2}}\mathbf{w}(2) & \dots & \alpha^{\frac{\hat{L}-\hat{L}}{2}}\mathbf{w}(\hat{L}) \end{bmatrix} \end{aligned} \tag{5.71}$$

In the following, we will show that

$$rank(\mathbf{U}) = rank(\mathbf{G}) \tag{5.72}$$

First, suppose that

$$rank(\mathbf{U}) < rank(\mathbf{G}) \tag{5.73}$$

then there exist a set of complex scalars e_i $(i = 1, 2, \dots, \hat{L})$ so that

$$\sum_{i=1}^{\hat{L}} e_i \alpha^{\frac{\hat{L}-i}{2}} \mathbf{w}(i) = 0 \tag{5.74}$$

where there are exactly $rank(\mathbf{U}) + 1$ nonzero e_i. Therefore we can find $rank(\mathbf{U}) + 1$ nonzero scalars $\dot{e}_i$, so that

$$\sum_{i=1}^{\hat{L}} \dot{e}_i \mathbf{w}(i) = 0 \tag{5.75}$$

where

$$\dot{e}_i = e_i \alpha^{\frac{\hat{L}-i}{2}} \tag{5.76}$$

Therefore

$$rank(\mathbf{G}) < rank(\mathbf{U}) + 1 \leq rank(\mathbf{G}) \tag{5.77}$$

Using a similar argument, we can show that $rank(\mathbf{U}) > rank(\mathbf{G})$ is impossible. Since

$$\mathbf{W}(\hat{L}) = \mathbf{GTG^H} = \mathbf{GE}(\mathbf{GE})^{\mathbf{H}} = \mathbf{UU^H} \tag{5.78}$$

and we have shown in *Proposition* 2

$$rank(\mathbf{UU^H}) = rank(\mathbf{U}) < M \tag{5.79}$$

we may obtain

$$rank(\mathbf{W}) < M \tag{5.80}$$

This is a contradiction to $rank(\mathbf{W}) = M$. Therefore, we conclude that $rank(\mathbf{W}) < M$ is impossible.

QED

The matrix $\mathbf{W}(\hat{L})$ is dependent on the channel vector of all the users in the cell. The fading and mobility of the mobiles affect $\mathbf{W}(\hat{L})$. It is desired that if the transmitted weights change over time, $\mathbf{W}(\hat{L})$ should remain full rank. At the same time, these weights should not change abruptly so that the feedforward update rate can be minimized.

5.5.4 Numerical and simulation results

5.5.4.1 The relative change of the downlink beamforming weights

Here we observe the behaviour of weight changes through simulation. We assume there are N users uniformly distributed in azimuth in the cell. A circular antenna array with M elements is installed at the base station for downlink beamforming. We use the third-order Butterworth filter fading model [37, 28] shown in Figure 5.3.

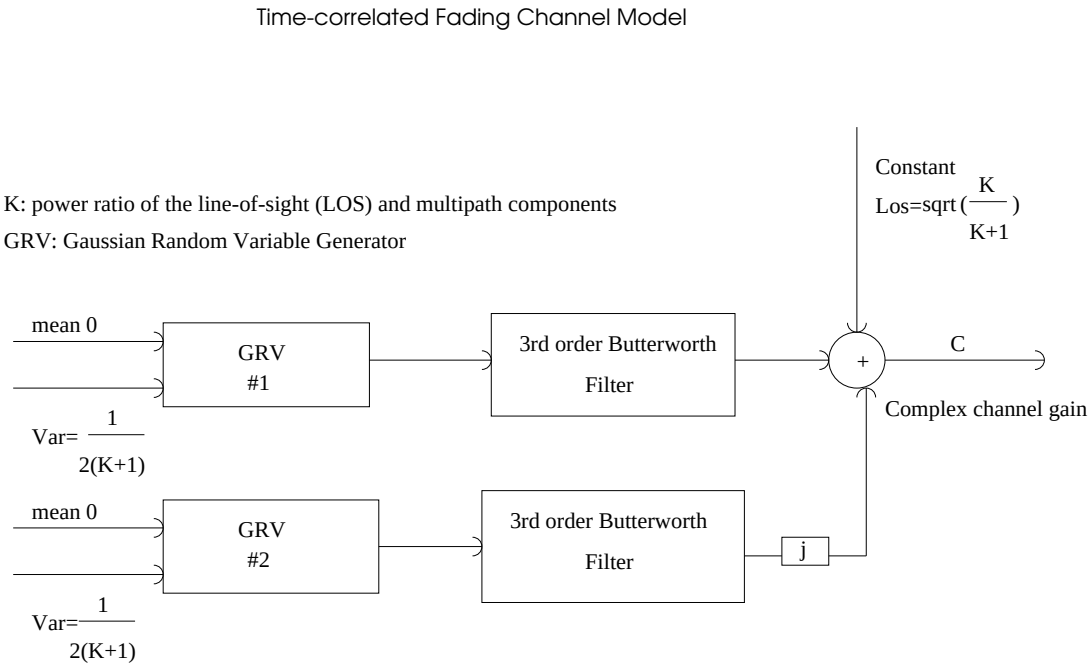

Figure 5.3: Third-order fading channel model

Each user experiences a fading channel which depends on the velocity of the mobiles. We define a maximum speed v_{max} and a minimum speed v_{min} respectively. The velocities of the mobiles are assumed uniformly distributed between $[v_{min}, v_{max}]$. Here we assume that the data rate is $9600 bits/sec$. For each symbol, we collect all channel vectors and calculate the principal eigenvector of the scatter matrix $\mathbf{S} = \sum_{k=1}^{N} \mathbf{a}_k \mathbf{a}_k^{\mathbf{H}}$. Then we put a time window on these vectors of length $\hat{L}$ to form a matrix with dimension $M \times \hat{L}$ and continuously check whether its rank is M (full rank). In addition, we define the measure of similarity

$$\rho_{weight,i} = \frac{||\mathbf{w}_1||||\mathbf{w}_i||}{||\mathbf{w}_1^{\mathbf{H}} \mathbf{w}_i||} \tag{5.81}$$

where $||.||$ is the Euclidean norm. We use $\rho_{weight,i}$ to measure the relative change between the weight vector $\mathbf{w}_1$ and weight vectors $\mathbf{w}_i$.

In a simulation run, we fix the number of users ($N = 30$) and vary the speed ranges: one is $[0,\ 50] Km/h$, the other is $[0,\ 100] Km/h$. We generate the speeds of the mobiles through a uniform distribution generator. Two hundred independent Monte Carlo simulations are conducted to calculate $\rho_{weight,i}$. The results are compared in Figure 5.4. We repeat the above but instead fix the speed range of the mobiles to $[0,\ 50] Km/h$ and vary the number of users in the cell: one is 30 users, the other is 50 users. The results are compared in Figure 5.5. We notice that in Figure 5.4, the absolute value of $\rho_{weight,i}$ increases with the speed as the channel vector of a higher speed mobile changes more quickly; in Figure 5.5, the absolute value of $\rho_{weight,i}$ decreases with the increased number of the mobiles as the sum of more users' channel vectors are less random. The simulations indicate that the matrix $\mathbf{W}$ always maintains full rank and the weights $\mathbf{w}_i$ change gradually rather than abruptly which is desirable to reduce downlink transmission bandwidth.

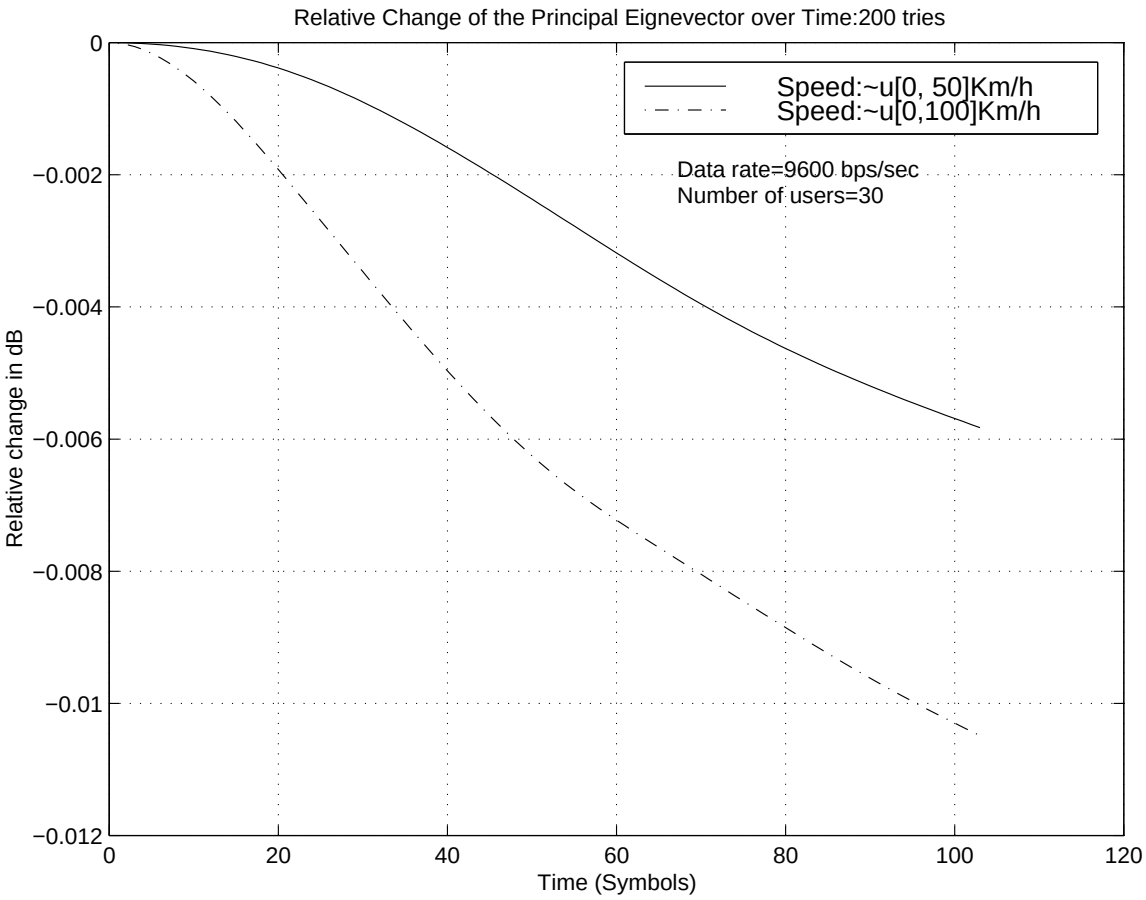

Figure 5.4: Relative change of the principal eigenvector for different speed ranges. The vertical axis plots $\rho_{weight,i}$ in dB.

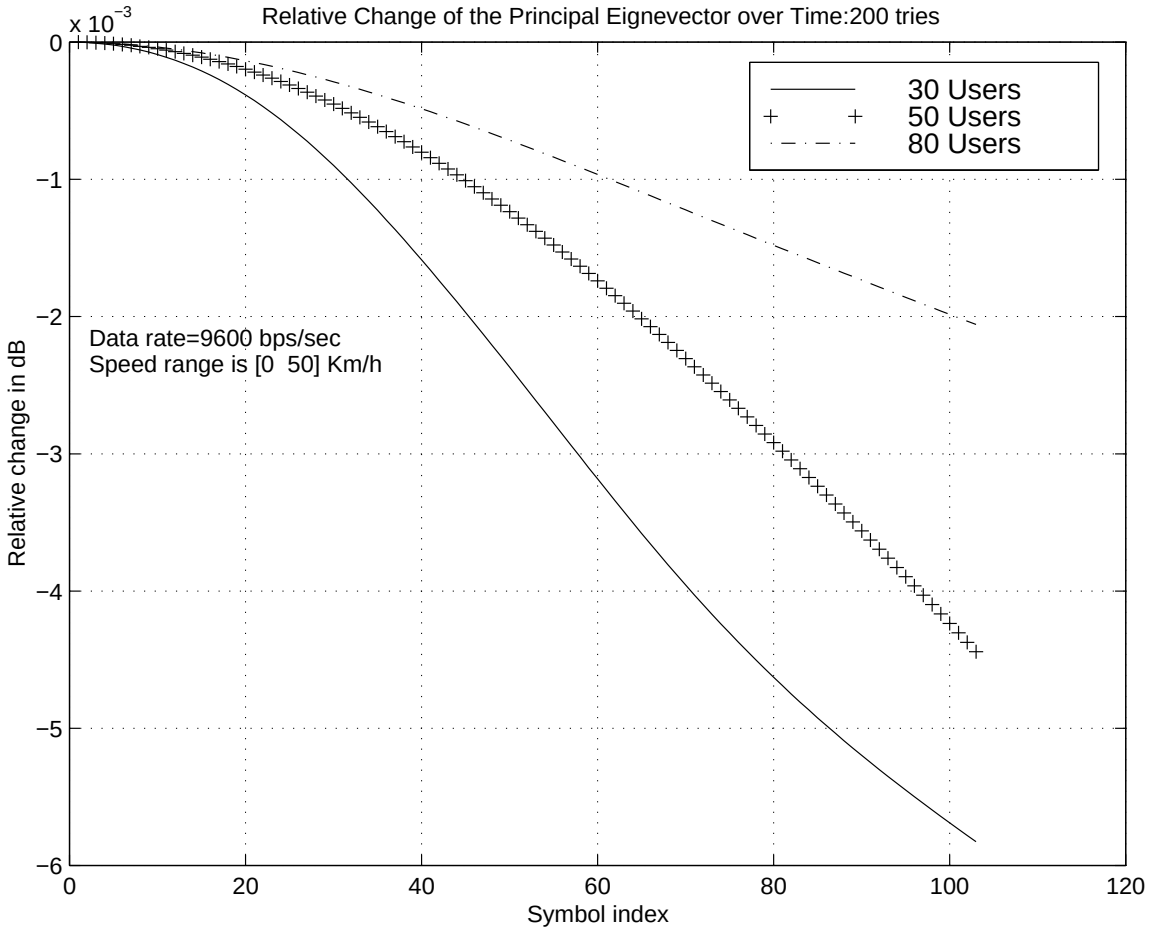

Figure 5.5: Relative change of the principal eigenvector for different number of users. The vertical axis plots $\rho_{weight,i}$ in dB.

5.5.4.2 Ill-conditioning due to slow change in the weight sequence

Now we use the RLS algorithm to estimate channel vectors of the mobiles. First, we assume that the channel vector of user i remains constant. We use the weights $\mathbf{w}_i$ obtained through the simulation in Section 5.5.4.1. The ideal scalar response g_i is obtained through Eq. (5.28) (assuming a perfect pilot channel). We compare the mean square error (MSE) for different forgetting factors α. The mean square error at time i is defined in [26] and we normalize it by the norm square of the true channel vector, i.e.,

$$\mathbf{MSE}_i = \frac{||\hat{\mathbf{a}}_i - \mathbf{a}_i||^2}{||\mathbf{a}_i||^2} \tag{5.82}$$

where $||.||$ is the Euclidean norm, $\hat{\mathbf{a}}_i$ is the estimated channel vector of user i and $\mathbf{a}_i$ is the corresponding true channel vector. We apply the RLS algorithm and the results are compared in Figure 5.6 for different forgetting factors. Apparently, there are large errors in estimating the channel vector. The reason is the slow change of the weight sequence $\mathbf{w}_i$ over the time window. This may be demonstrated by the following simulation. We replace the weight sequence $\mathbf{w}_i$ by a sequence of complex Gaussian random vectors with unity variance, and use Eq. (5.28) to obtain the corresponding ideal scalar response. We then use the RLS algorithm to estimate the channel vector and calculate the MSE. The results are shown in Figure 5.7.

Now we examine the non-stationary case. The channel vector of user i changes with the time. Unlike the stationary case, if we use the weights $\mathbf{w}_i$ obtained in Section 5.5.4.1 to track the the channel vector, the RLS algorithm completely fails to track the channel vector. The reason is the small change of the weights $\mathbf{w}_i$.

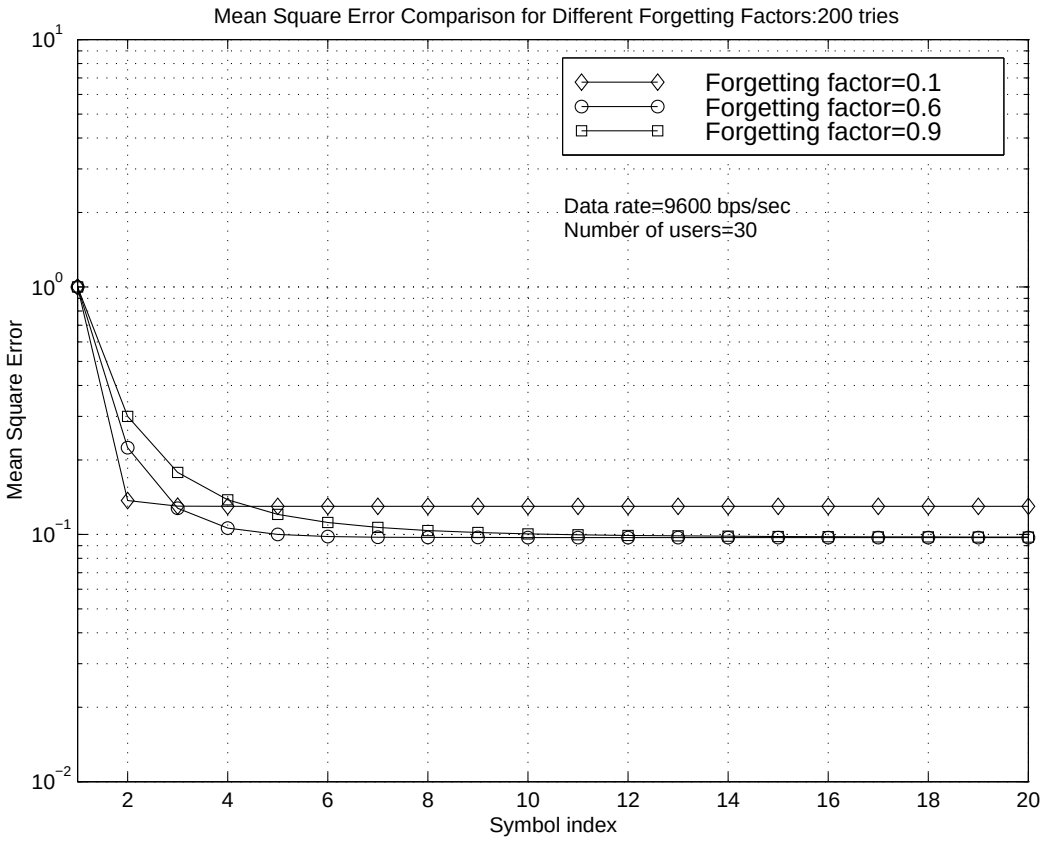

Figure 5.6: Using RLS algorithm to estimate the channel vector: stationary case

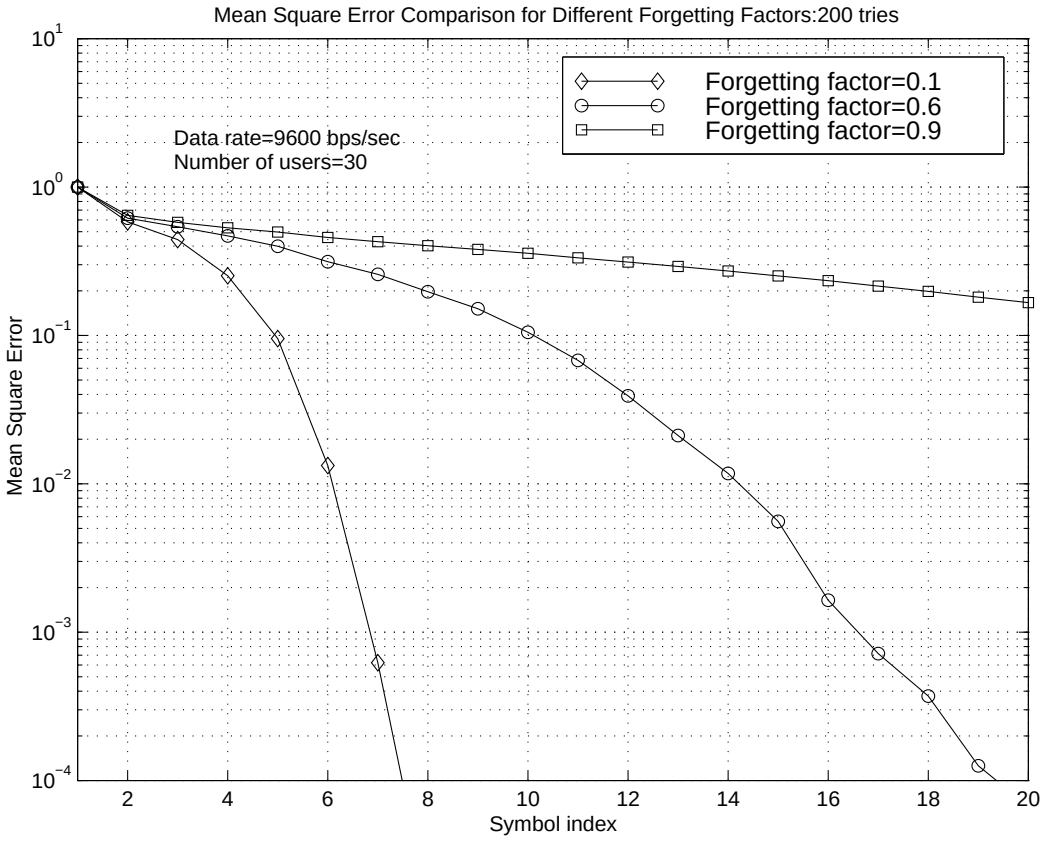

Figure 5.7: Using RLS algorithm to estimate the channel vector: the weights replaced by a sequence of Gaussian random vectors

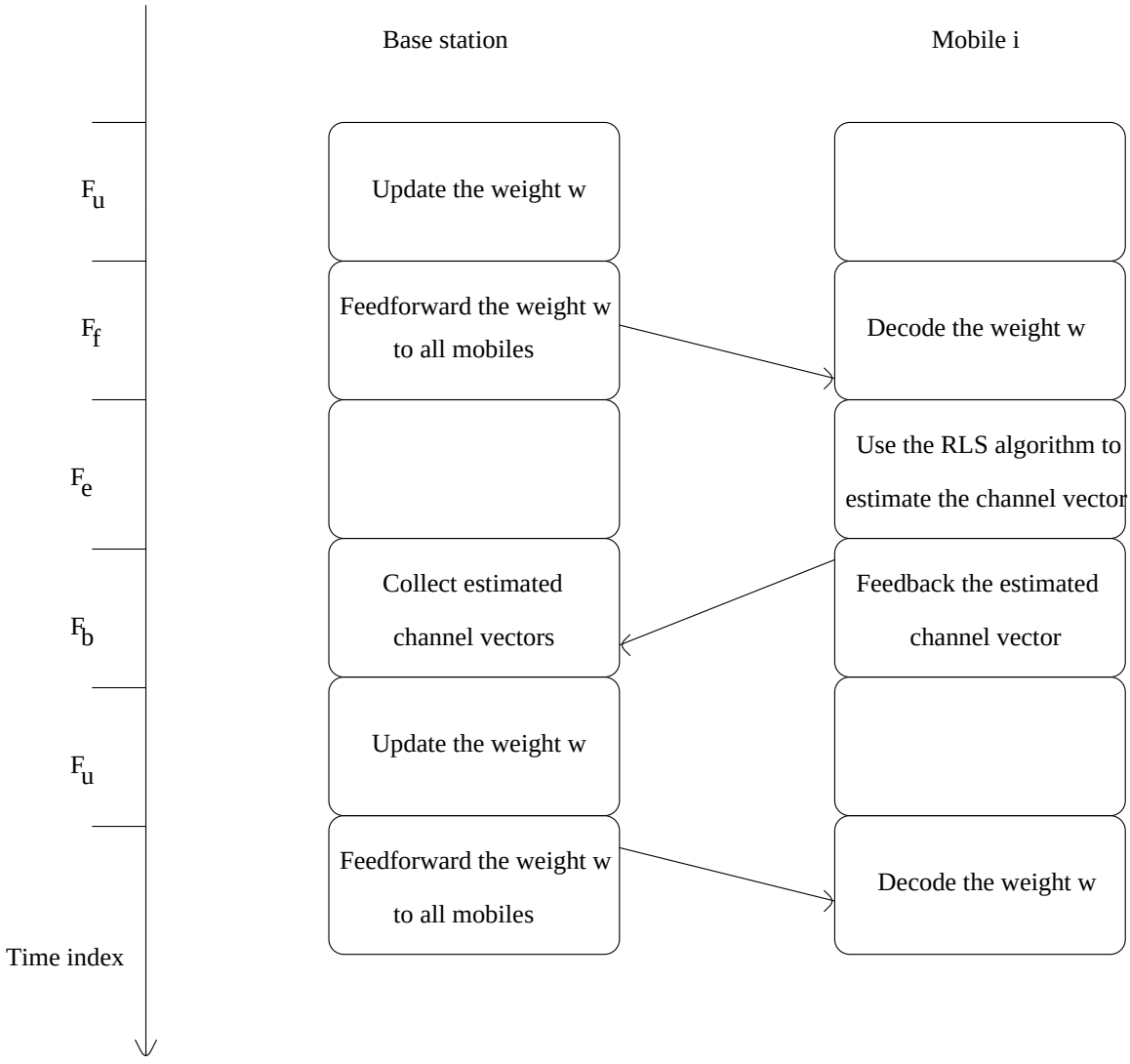

Figure 5.8: Interaction between the base station and mobiles

5.6 A perturbation RLS algorithm (PRLS)

5.6.1 PRLS algorithm

Feedforwarding $\mathbf{w}_i$ at each symbol to the mobiles may cause a large number of extra transmissions although we may transmit the differences of the weights. In addition, the feedforward channel should have a higher data rate than normal information transmission channels to provide the RLS algorithm a weight vector $\mathbf{w}_i$ at each update. In Section 5.5.4.1, we have shown that the weight sequence $\mathbf{w}_i$ changes slowly. In Section 5.5.4.2, we have demonstrated through simulation that a random weight sequence improves the RLS algorithm performance. It has been shown in [33] that good parameter identification requires the application of a frequency-rich input. A random sequence is the ideal candidate for such application. In the following, we propose a perturbation RLS algorithm (PRLS) to estimate downlink channel vectors. We divide the downlink transmission time into equal time intervals. Each time interval is equivalent to F_{Total} symbols (each lasting T_b seconds). The weight vector $\mathbf{w}_i$ remains constant during an interval and is updated at the end of each interval. Each interval is further divided into four consecutive stages as in Figure 5.8:

Stage-I Feedforward a weight vector to all mobiles. This lasts F_f symbols.

Stage-II Use the RLS algorithm to estimate channel vectors at mobiles. This lasts F_e symbols.

Stage-III The mobiles feedback the estimated channel vector to the base station. This lasts F_b symbols.

Stage-IV The base station updates the weight vector $\mathbf{w}_i$. This lasts F_u symbols.

Therefore we obtain

$$F_{Total} = F_f + F_e + F_b + F_u \tag{5.83}$$

F_f and F_b may be minimized by appropriate quantization and coding. F_e is determined by the RLS algorithm and should be minimized. We use simulation to determine F_u. F_u depends on the efficiency of the algorithm to calculate the principal eigenvector of the matrix $\sum_{k=1}^{N} \mathbf{a}_k \mathbf{a}_k^{\mathbf{H}}$ and may be omitted and is not considered here.

As we fix the weight vector $\mathbf{w}_i$ during one interval, the full rank condition in Eq. (5.65) is not valid. Here we propose to perturb the weight $\mathbf{w}_i$ in the channel estimation stage by a sequence of independent and identically distributed (i.i.d) Gaussian random vectors as in Figure 5.9. Therefore, the new weight vector is

$$\hat{\mathbf{w}}_i = \mathbf{w}_i + \varpi ||\mathbf{w}_i|| \delta_{\mathbf{w}_i} \tag{5.84}$$

where $||.||$ is the Euclidean norm, ϖ is a real positive scalar and $\delta_{\mathbf{w}_i}$ is a unit variance Gaussian random vector, i.e.,

$$\mathbf{E}\{\delta_{\mathbf{w}_i} \delta_{\mathbf{w}_i}^{\mathbf{H}}\} = \mathbf{I} \tag{5.85}$$

where $\mathbf{I}$ is the identity matrix. As perturbations in Gaussian random vectors may be made the same at both the base station and mobiles, we need not transmit these Gaussian vectors to the mobiles. In addition, the base station knows the weight $\mathbf{w}_i$ at the beginning of the perturbation stage, the variance of the perturbation Gaussian random vectors may be chosen as a scalar multiple of the norm of the weight $\mathbf{w}_i$, i.e., $\varpi ||\mathbf{w}_i||$. The scalar channel gain due to the perturbed weights $\hat{\mathbf{w}}_i$ is

$$\hat{g}_i = \hat{\mathbf{w}}_i^{\mathbf{H}} \mathbf{a}_i \tag{5.86}$$

where $\mathbf{a}_i$ is the true channel vector. Then we may apply the RLS algorithm to estimate downlink channel vectors.

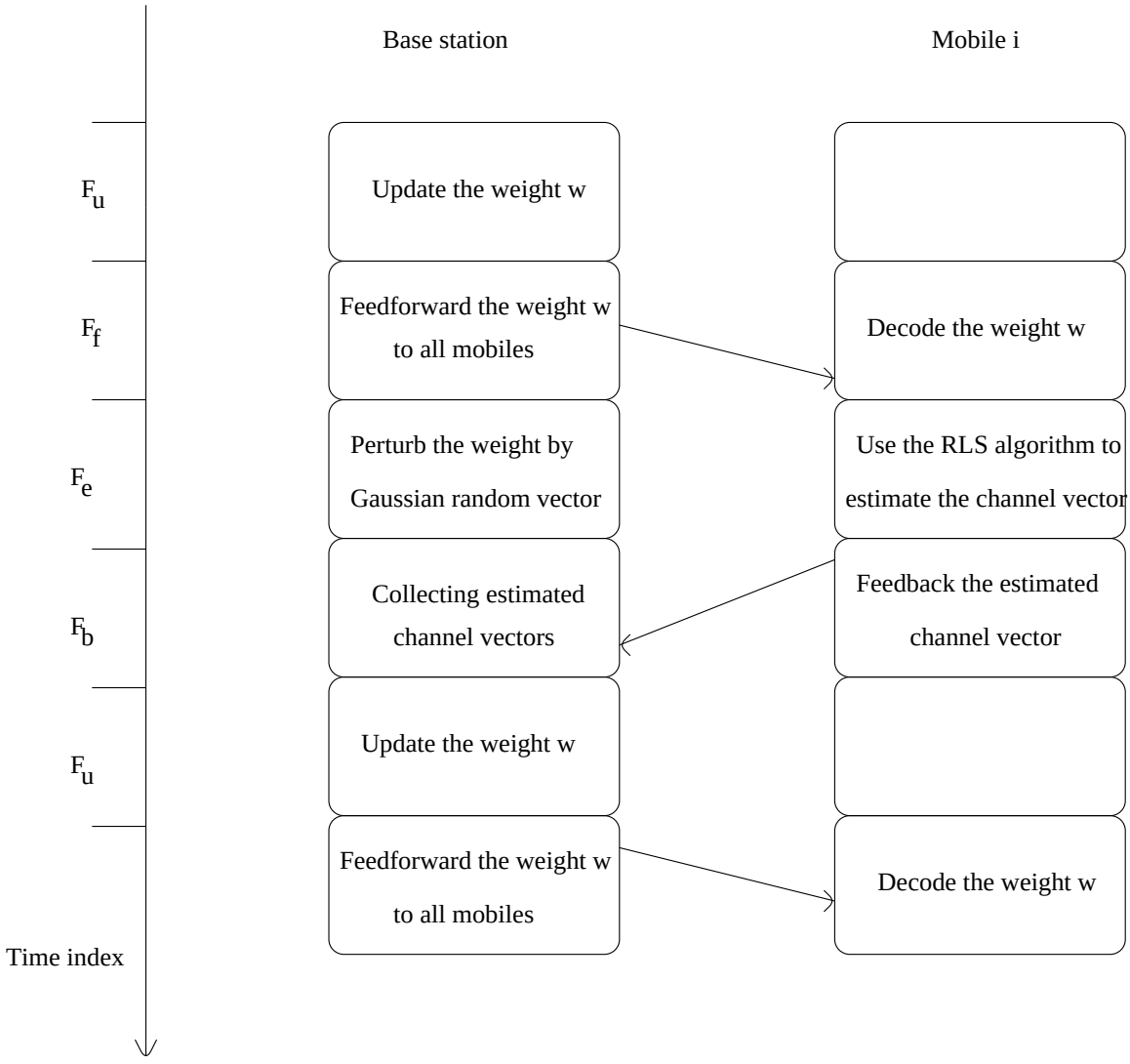

Figure 5.9: Interaction between the base station and mobile for PRLS algorithm

5.6.2 Effects of the perturbation

Now we examine the average **SNR** of the kth mobile due to the perturbation. Let $\mathbf{SNR}_{k,p}$ denote the average **SNR** of the kth mobile due to the perturbation. Analogous to Eq. (5.16), the output of the correlator at the perturbation stage is

$$y_{k,p} = (\hat{\mathbf{w}}^{\mathbf{H}}\mathbf{a}_k b_k + n_k)(\hat{\mathbf{w}}^{\mathbf{H}}\mathbf{a}_k)^* \tag{5.87}$$

where $\hat{\mathbf{w}}$ comes from Eq. (5.84) and we have dropped the time index i as the weight vector $\mathbf{w}_i$ is constant over one interval. Therefore, similarly to Eq. (5.17), we obtain

$$\begin{aligned}
\mathbf{SNR}_{k,p} &= \frac{\mathbf{E}\{||\hat{\mathbf{w}}^{\mathbf{H}}\mathbf{a}_k||^2\}}{\sigma^2} \\
&= \frac{\mathbf{E}\{||(\mathbf{w} + \varpi||\mathbf{w}||\delta_{\mathbf{w}_i})^{\mathbf{H}}\mathbf{a}_k||^2\}}{\sigma^2} \\
&= \frac{\mathbf{E}\{||\mathbf{w}^{\mathbf{H}}\mathbf{a}_k||^2 + ||\mathbf{w}||^2||(\varpi\delta_{\mathbf{w}_i})^{\mathbf{H}}\mathbf{a}_k||^2\}}{\sigma^2} \\
&= \frac{\mathbf{E}\{||\mathbf{w}^{\mathbf{H}}\mathbf{a}_k||^2 + ||\mathbf{w}||^2\varpi^2||\mathbf{a}_k^{\mathbf{H}}\mathbf{a}_k||\}}{\sigma^2}
\end{aligned} \tag{5.88}$$

where we have used Eq. (5.85) to simplify $\mathbf{SNR}_{k,p}$. Compared with Eq. (5.17), we obtain extra power as we perturb the weight vector $\mathbf{w}$ to estimate channel vectors

$$P_{extra} = ||\mathbf{w}||^2\varpi^2\mathbf{E}\{||\mathbf{a}_k^{\mathbf{H}}\mathbf{a}_k||\} \tag{5.89}$$

The relative extra power is defined as

$$\begin{aligned}
\rho_{extra} &= \frac{P_{extra}}{\mathbf{E}\{||\mathbf{w}^{\mathbf{H}}\mathbf{a}_k||^2\}} \\
&= \frac{||\mathbf{w}||^2\varpi^2\mathbf{E}\{||\mathbf{a}_k^{\mathbf{H}}\mathbf{a}_k||\}}{\mathbf{E}\{||\mathbf{w}^{\mathbf{H}}\mathbf{a}_k||^2\}}
\end{aligned} \tag{5.90}$$

Proposition 4 *ρ_{extra} has a lower bound of ϖ^2.*

Proof:
Using the well-known *$Cauchy - Schwarz$ inequality*, we obtain

$$||\mathbf{w}^{\mathbf{H}}\mathbf{a}_k||^2 \leq ||\mathbf{w}||^2||\mathbf{a}_k||^2 \tag{5.91}$$

Therefore

$$\rho_{extra} \geq \frac{||\mathbf{w}||^2 \varpi^2 \mathbf{E}\{||\mathbf{a}_k^{\mathbf{H}} \mathbf{a}_k||\}}{\mathbf{E}\{||\mathbf{w}||^2 ||\mathbf{a}_k||^2\}} \tag{5.92}$$

As we fix the weight vector during updates, $||\mathbf{w}||^2$ may be pulled out from the expectation in the denominator, we obtain

$$\rho_{extra} \geq \frac{||\mathbf{w}||^2 \varpi^2 \mathbf{E}\{||\mathbf{a}_k^{\mathbf{H}} \mathbf{a}_k||\}}{||\mathbf{w}||^2 \mathbf{E}\{||\mathbf{a}_k||^2\}} = \varpi^2 \tag{5.93}$$

The equality holds if and only if

$$\mathbf{w} = \kappa \mathbf{a}_k \tag{5.94}$$

where κ is a constant.

QED

We implement the *PRLS* algorithm at the cost of extra power consumption. However, as shown in Section 5.6.4, the perturbation stage is very short ($15 \sim 20$ symbols for three antenna elements) because of the fast convergence of the PRLS algorithm. In addition, we may select a small ϖ, such as 0.1, so that we get improved performance with trivial extra power consumption.

5.6.3 *SNR* loss due to the PRLS algorithm

Here we examine the loss in average *SNR* due to fixing the weight vector during an interval. We compare with the case of updating the weight $\mathbf{w}$ at each symbol. In the latter case, the average output *SNR* during one interval according to Eq. (5.17) is

$$\begin{aligned} \mathbf{SNR}_{opt} &= \frac{\mathbf{E}\{||\mathbf{w}_i^{\mathbf{H}} \mathbf{a}_i||^2\}}{\sigma^2} \\ &= \frac{\sum_{i=1}^{F_{Total}} ||\mathbf{w}_i^{\mathbf{H}} \mathbf{a}_i||^2}{\sigma^2 F_{Total}} \end{aligned} \tag{5.95}$$

In the case of the PRLS algorithm, the average output *SNR* during one interval according to Eq. (5.90) is

$$\begin{aligned} \mathbf{SNR}_{PRLS} &= \frac{\mathbf{E}\{||\mathbf{w}^{\mathbf{H}} \mathbf{a}_i||^2\} + P_{extra}}{\sigma^2} \\ &= \frac{\sum_{i=1}^{F_{Total}} ||\mathbf{w}^{\mathbf{H}} \mathbf{a}_i||^2 + \frac{F_{Total} ||\mathbf{w}||^2 \varpi^2 \sum_{k=F_f+1}^{F_f+F_e+1} ||\mathbf{a}_k^{\mathbf{H}} \mathbf{a}_k||^2}{F_e}}{\sigma^2 F_{Total}} \end{aligned} \tag{5.96}$$

As the perturbation increases $\mathbf{SNR}_{PRLS}$, we may examine the worst case where we omit the extra power due to the perturbation, therefore

$$\widehat{\mathbf{SNR}}_{PRLS} = \frac{\sum_{i=1}^{F_{Total}} ||\mathbf{w}^{\mathbf{H}}\mathbf{a}_i||^2}{\sigma^2 F_{Total}} \tag{5.97}$$

Define

$$\rho_{PRLS} = \frac{|\widehat{\mathbf{SNR}}_{PRLS} - \mathbf{SNR}_{opt}|}{\mathbf{SNR}_{opt}} \tag{5.98}$$

Therefore we obtain

$$\rho_{PRLS} = \frac{|\sum_{i=1}^{F_{Total}} ||\mathbf{w}^{\mathbf{H}}\mathbf{a}_i||^2 - \sum_{i=1}^{F_{Total}} ||\mathbf{w}_i^{\mathbf{H}}\mathbf{a}_i||^2|}{\sum_{i=1}^{F_{Total}} ||\mathbf{w}_i^{\mathbf{H}}\mathbf{a}_i||^2} \tag{5.99}$$

5.6.4 Numerical and simulation results

Here we conduct simulations to compare the performance of the PRLS algorithm under different conditions. We track three typical mobiles: the mobile with the maximum speed, the mobile with the median speed, the mobile with the minimum speed. We vary the number of the users in the cell and vary the speed ranges of the mobiles and compare the **MSE** calculated by Eq. (5.82). In addition, we may estimate the DOA from the estimated channel vector. The DOA is estimated by

$$\hat{\theta} = arg \min_{\hat{\theta}} ||\mathbf{a}(\theta) - \hat{\mathbf{a}}(\hat{\theta})||^2 \tag{5.100}$$

where $||.||$ is the Euclidean norm, θ is the true DOA and $\hat{\theta}$ is the estimated DOA. The mean square error for the DOA estimation is defined as

$$\mathbf{MSE}_{\hat{\theta}} = (\hat{\theta} - \theta)^2 \tag{5.101}$$

The forgetting factor α is 0.6 in the simulation. In Figures 5.10 to 5.19, we show mean square errors of channel vector estimates in terms of the relative Euclidean norm defined in Eq. (5.82) and DOA defined in Eq. (5.101). In the case of speed range $0 \sim 50Km/h$, the $PRLS$ algorithm converges very fast, e.g., $15 \sim 20$ symbols for a 3-element array; for the case of speed range $0 \sim 80Km/h$, the $PRLS$ algorithm converges slower, taking about 40 symbols to converge. Also the convergence rate increases as the number of users increases. At the same symbol index, e.g., 15, MSE is 10^{-2} for 50 users but nearly 10^{-3} for 80 users as shown in Figures 5.12 and 5.14.

To get an accurate DOA estimate, the Euclidean norm of channel estimation errors should be around 10^{-3}. The results also show that F_e is around $15 \sim 20$ or $5M \sim 7M$, respectively, where M is the number of antennas. Such a small value of F_e makes Eq. (5.90) nearly zero which means that very little extra transmitted power is needed in implementing the PRLS algorithm. In addition, we calculate the relative SNR change through Eq. (5.99) and results are compared in Figures 5.20 to 5.24. The results show that there is only a very small performance penalty by fixing the beamforming weights over 40 symbols.

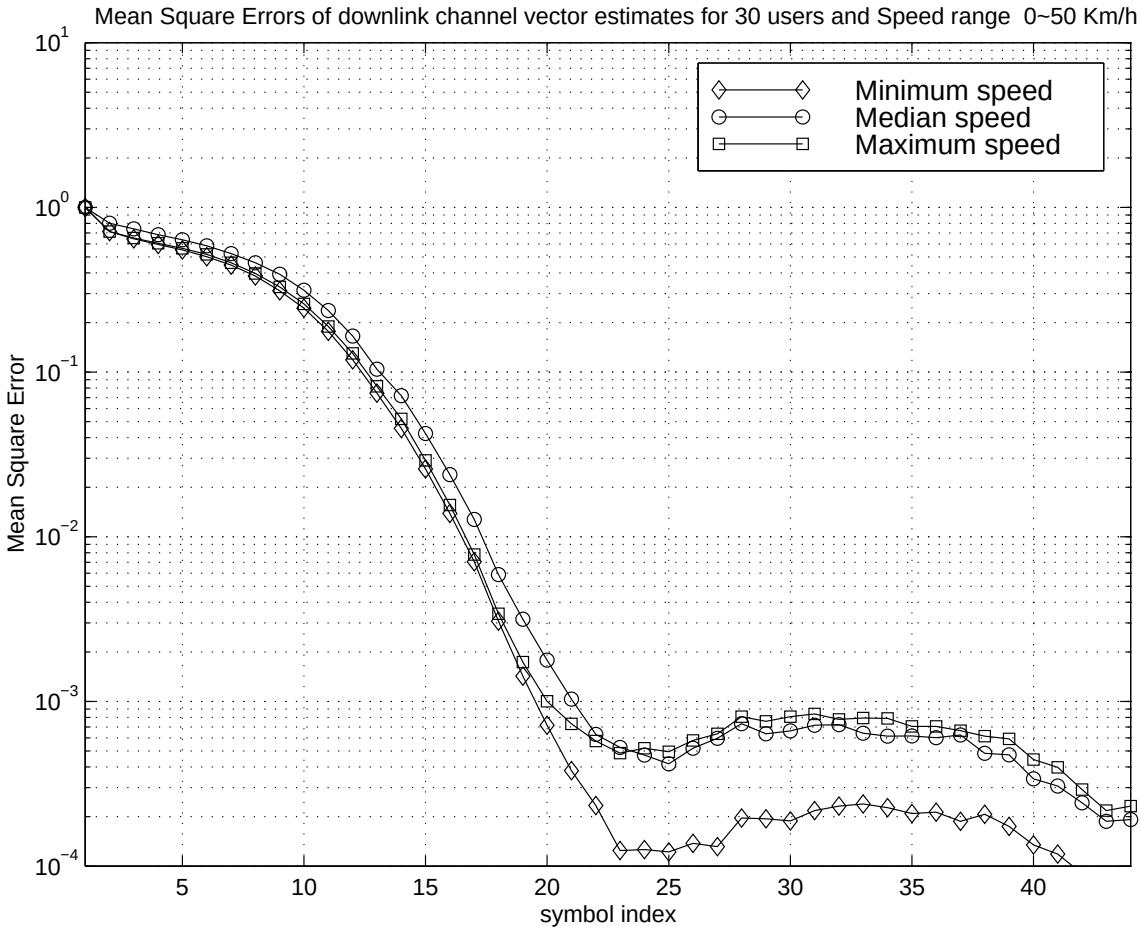

Figure 5.10: Using the PRLS algorithm to estimate the channel vector for 30 users and the speed range $0 \sim 50$ Km/h

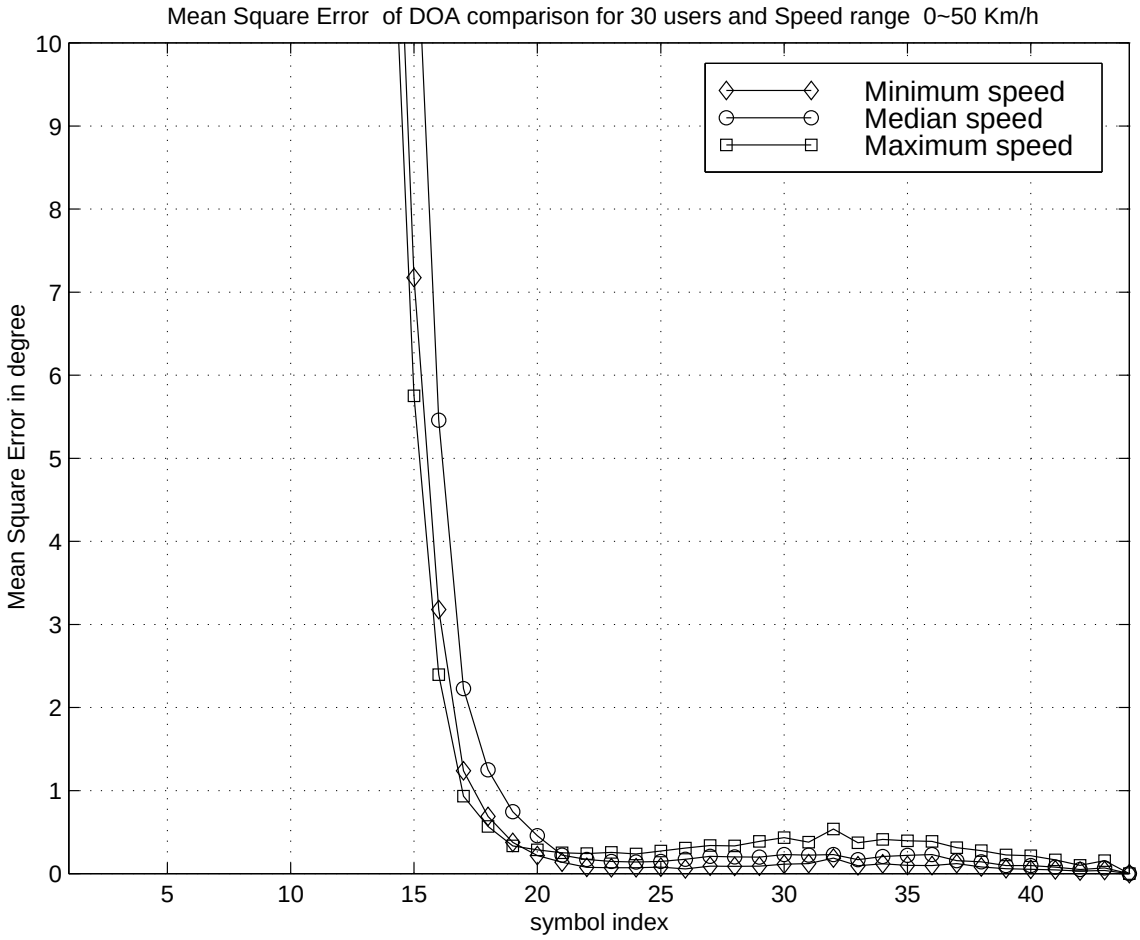

Figure 5.11: Using the PRLS algorithm to estimate DOA for 30 users and the speed range $0 \sim 50$ Km/h

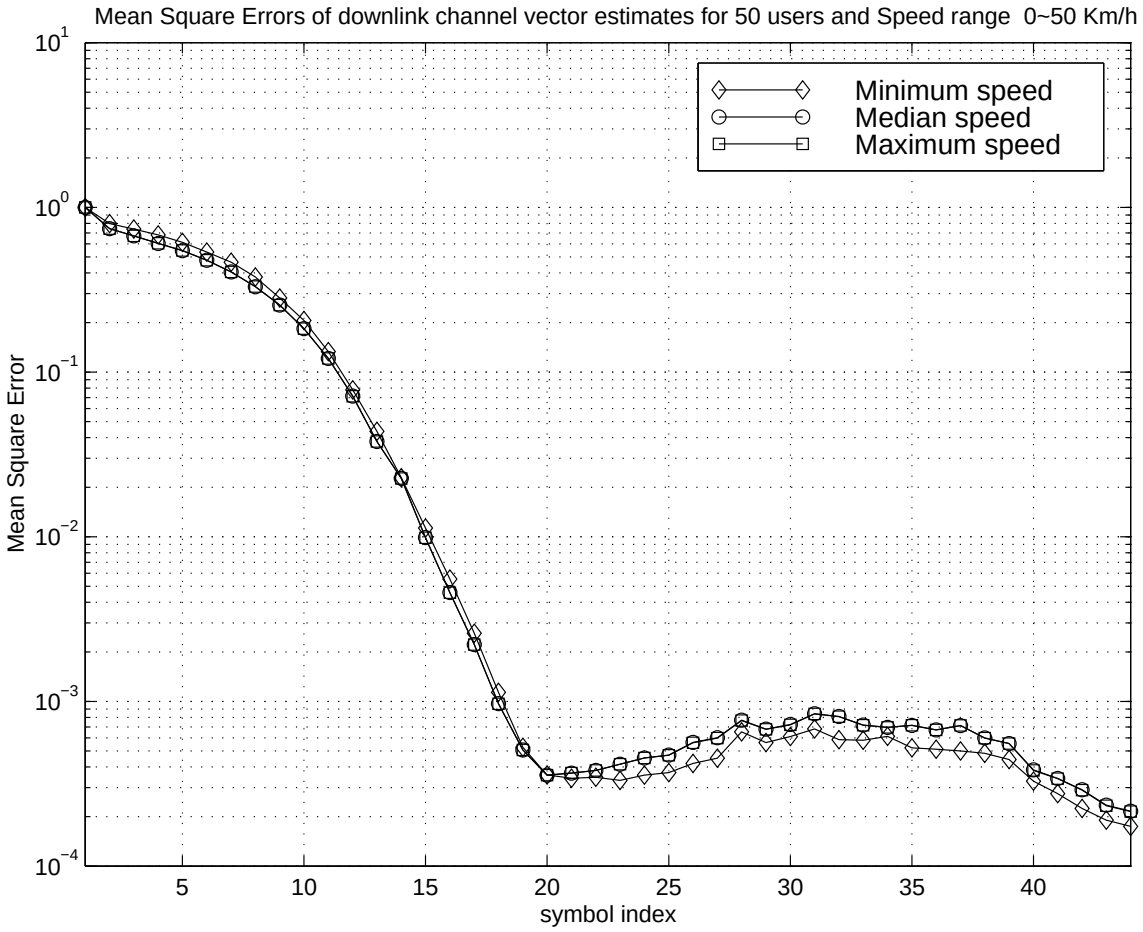

Figure 5.12: Using the PRLS algorithm to estimate the channel vector for 50 users and the speed range $0 \sim 50$ Km/h

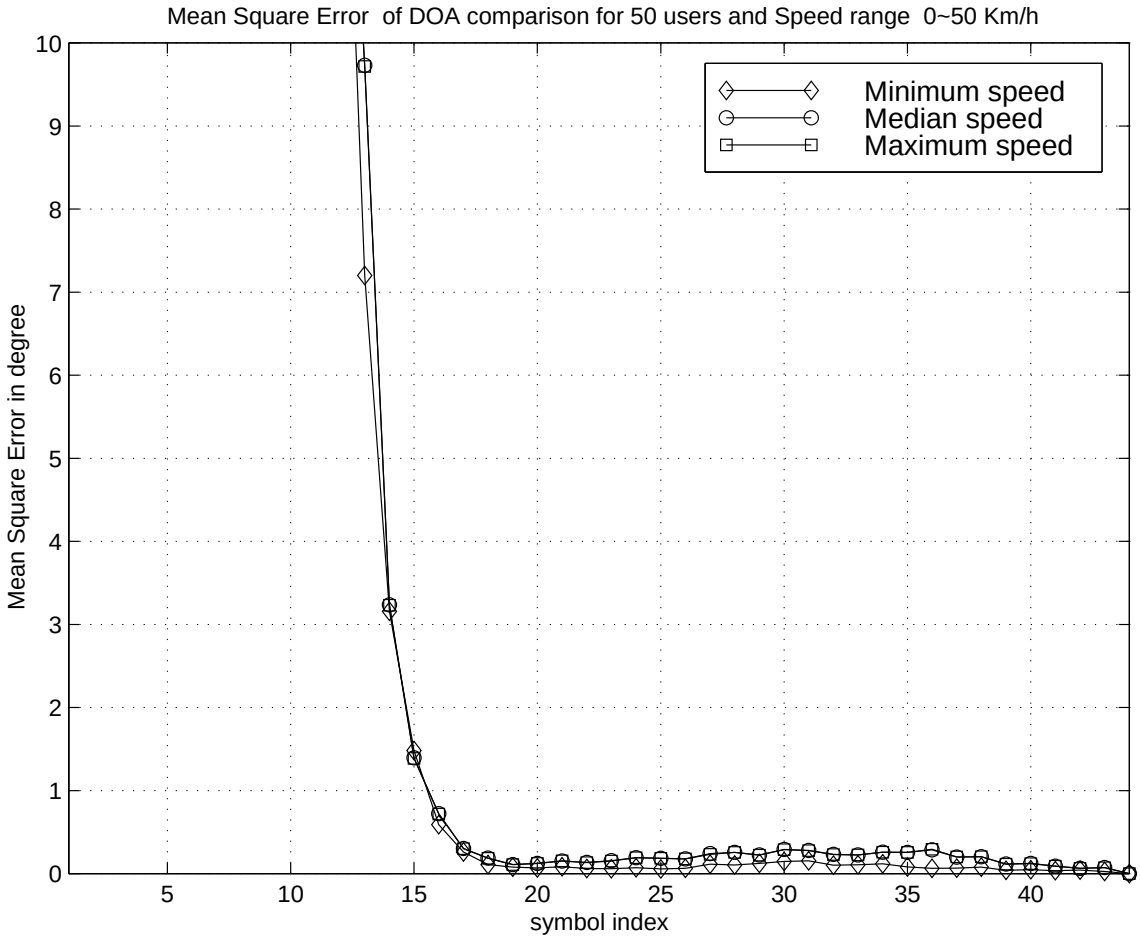

Figure 5.13: Using the PRLS algorithm to estimate DOA for 50 users and the speed range $0 \sim 50$ Km/h

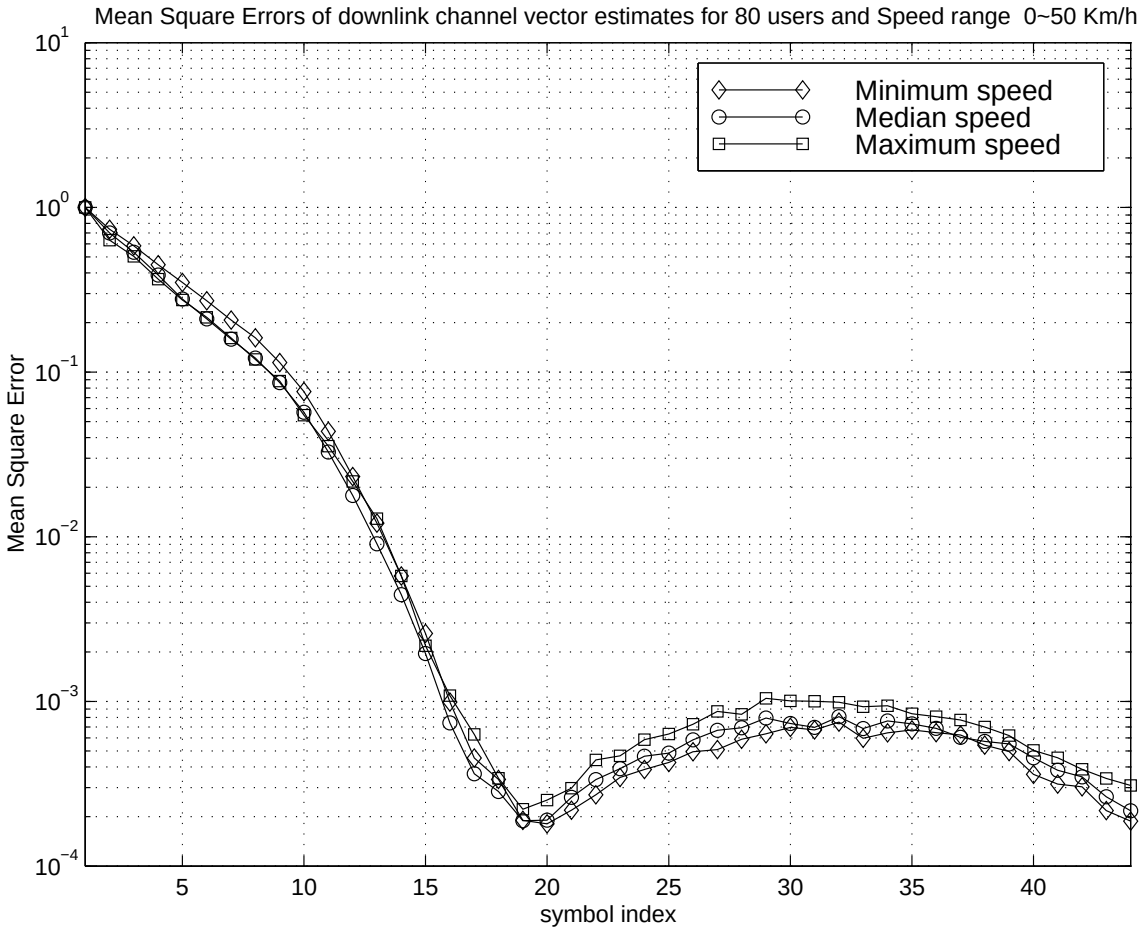

Figure 5.14: Using the PRLS algorithm to estimate the channel vector for 80 users and the speed range $0 \sim 50$ Km/h

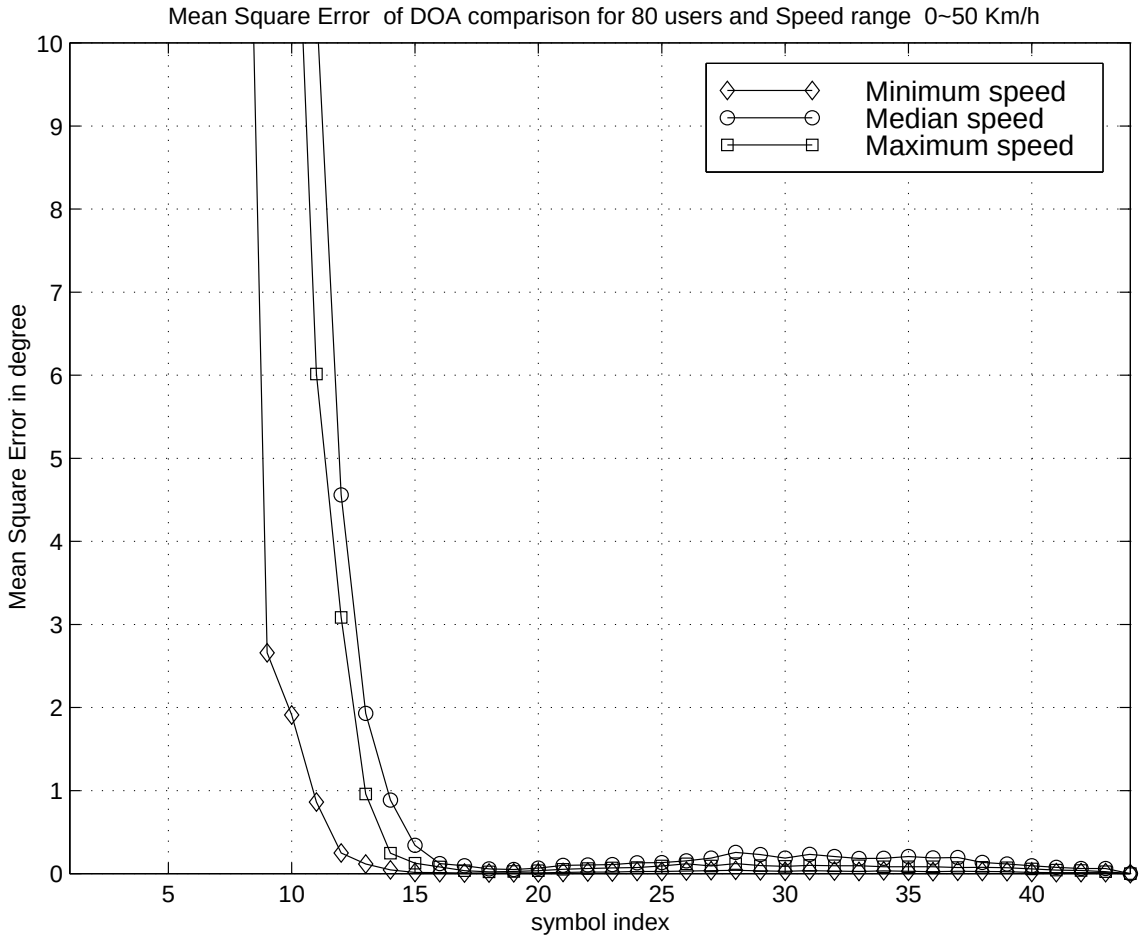

Figure 5.15: Using the PRLS algorithm to estimate DOA for 80 users and the speed range $0 \sim 50$ Km/h

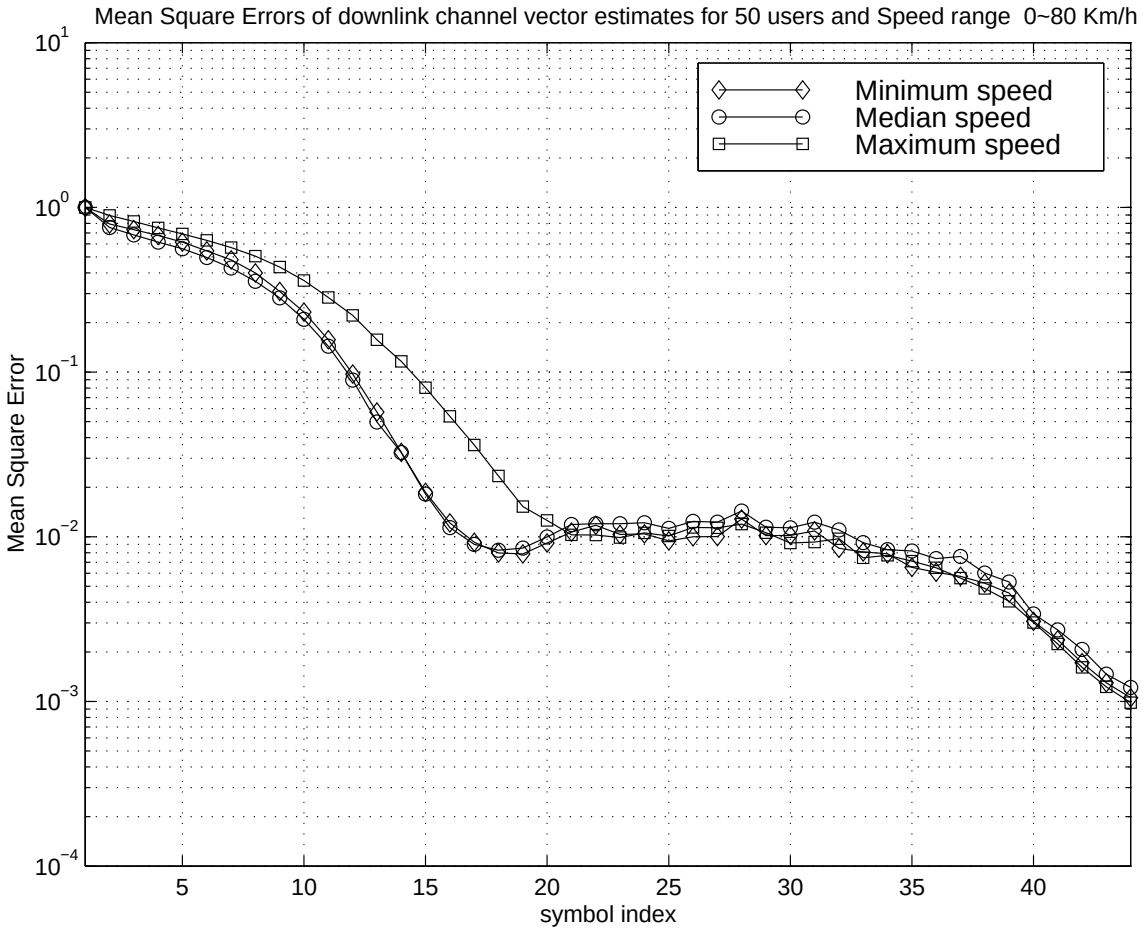

Figure 5.16: Using the PRLS algorithm to estimate the channel vector for 50 users and the speed range $0 \sim 80$ Km/h

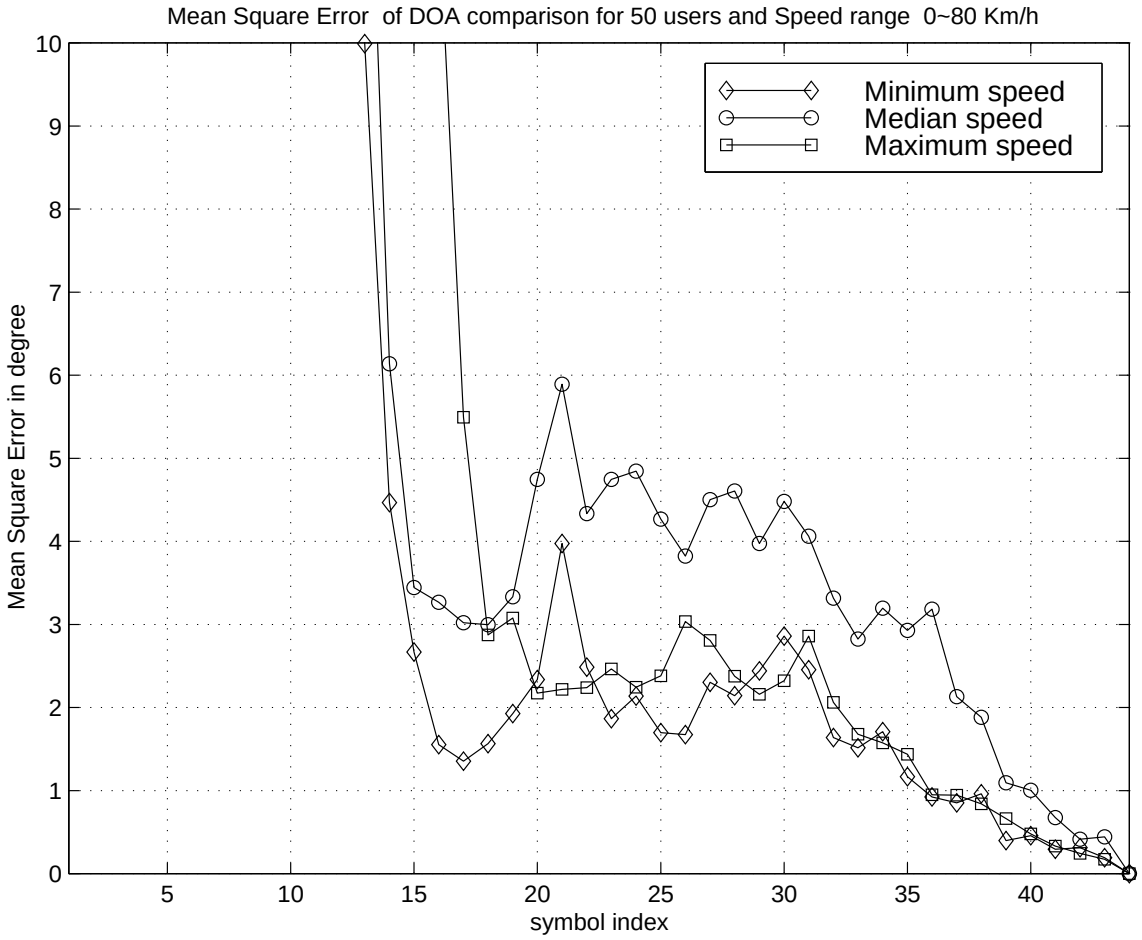

Figure 5.17: Using the PRLS algorithm to DOA for 50 users and the speed range $0 \sim 80$ Km/h

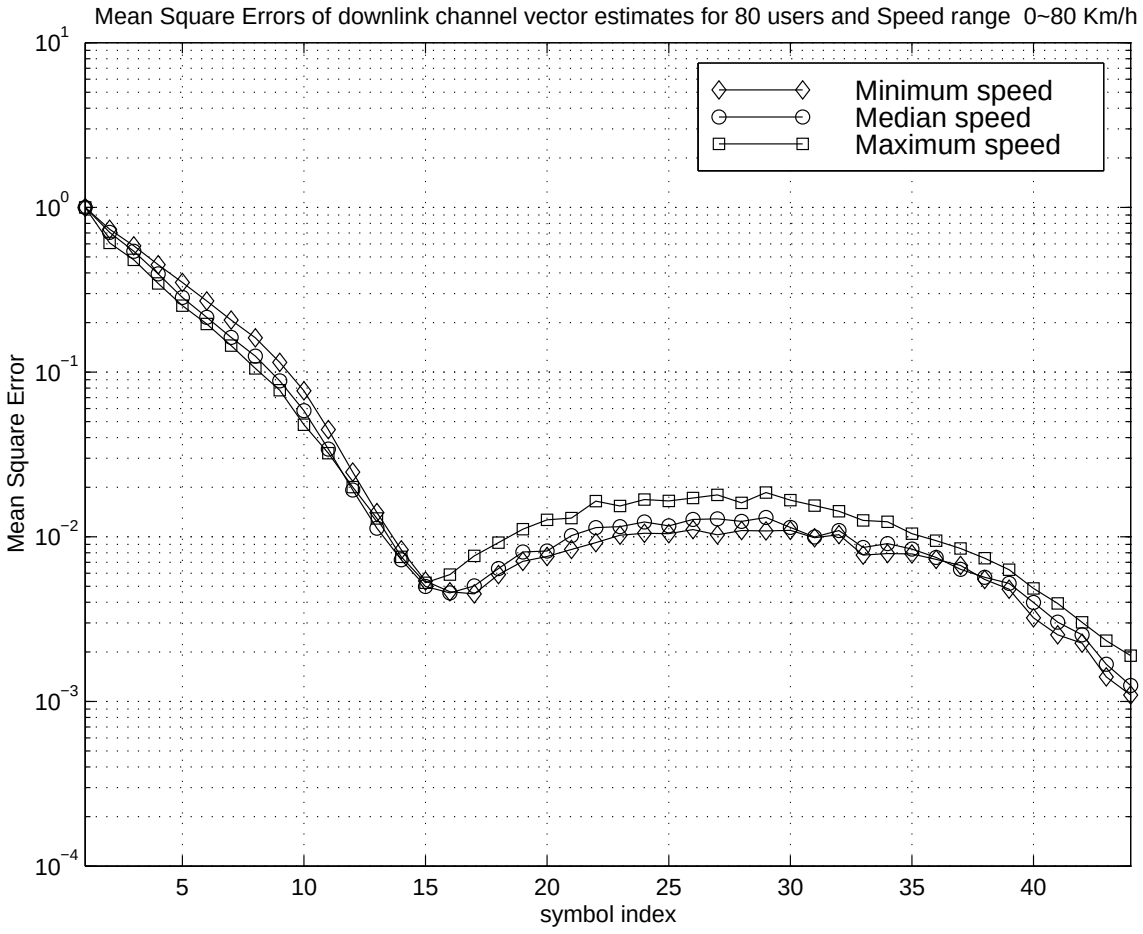

Figure 5.18: Using the PRLS algorithm to estimate the channel vector for 80 users and the speed range $0 \sim 80$ Km/h

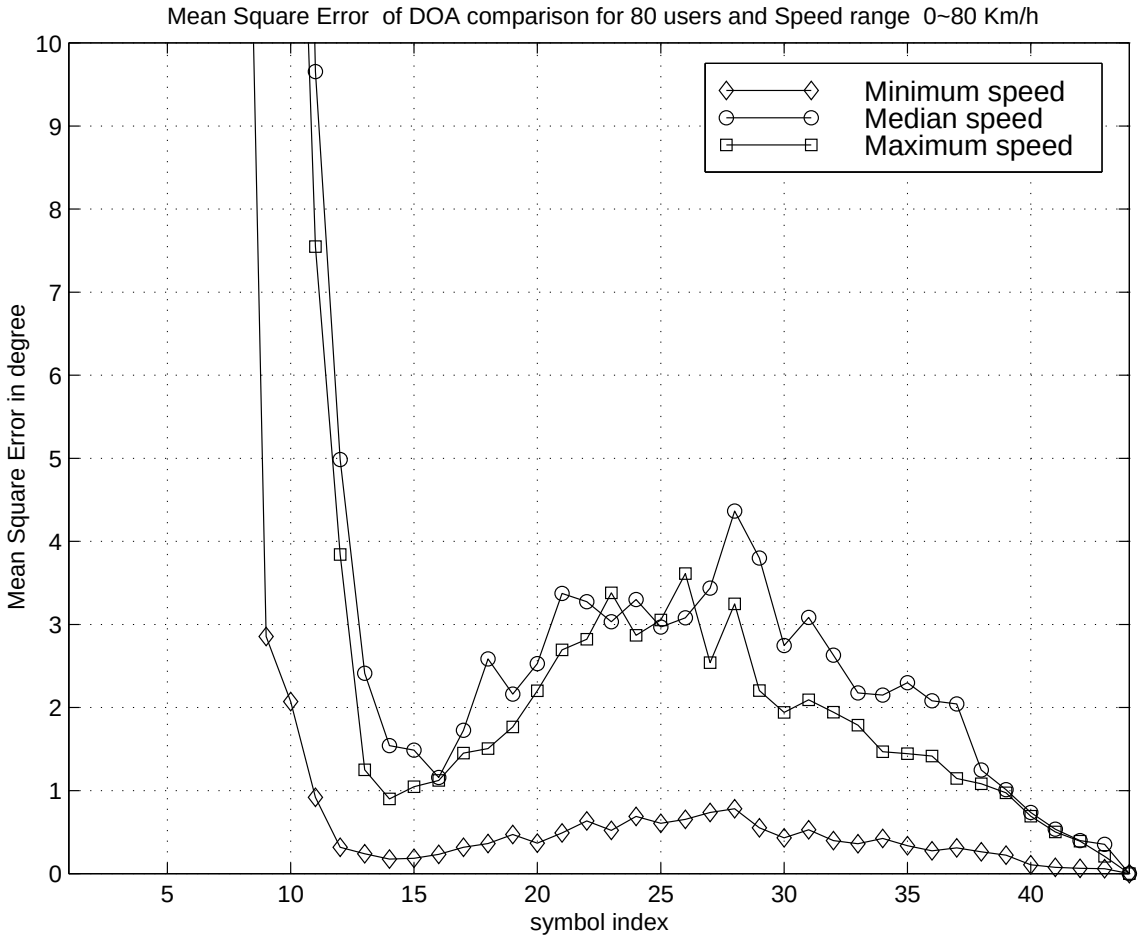

Figure 5.19: Using the PRLS algorithm to estimate the channel vector for 80 users and the speed range $0 \sim 80$ Km/h

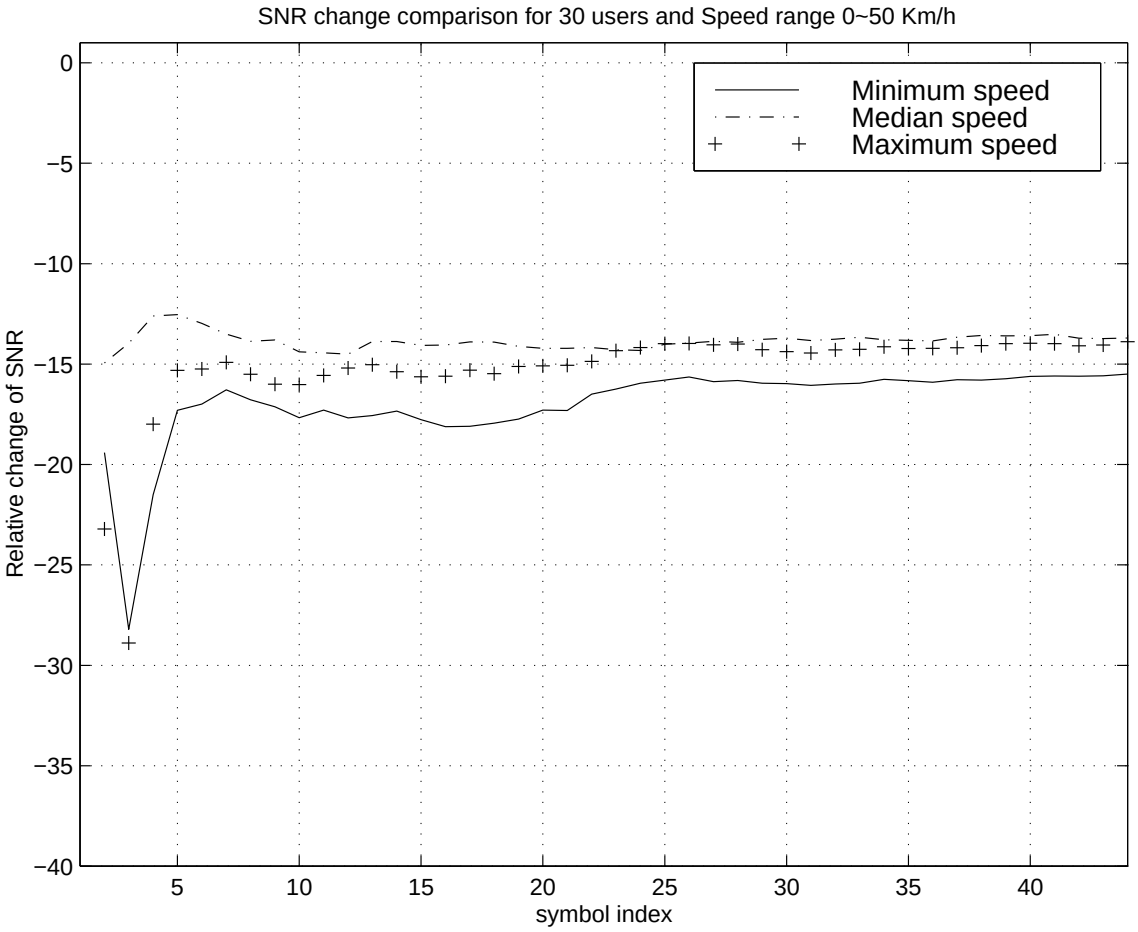

Figure 5.20: Using the PRLS algorithm to estimate the channel vector for 30 users and the speed range $0 \sim 50$ Km/h

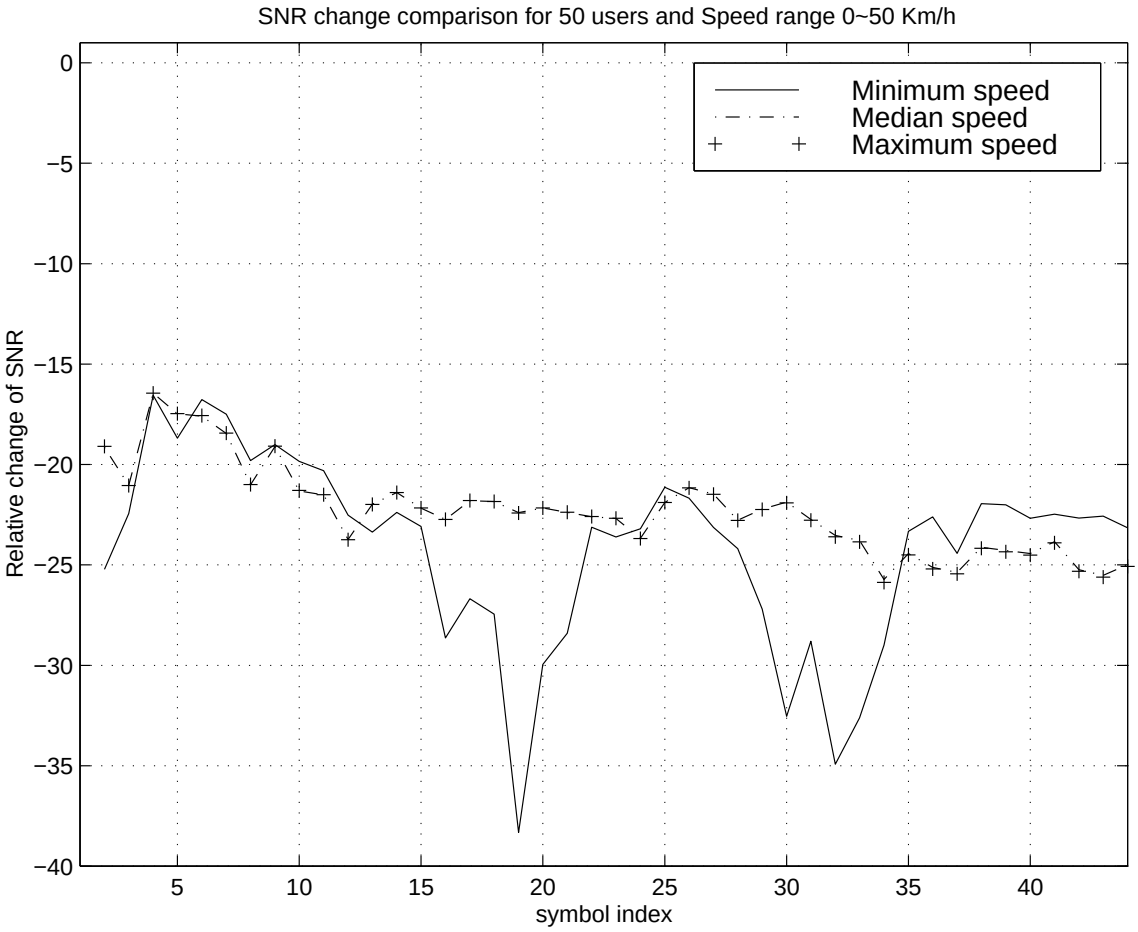

Figure 5.21: Using the PRLS algorithm to estimate the channel vector for 50 users and the speed range $0 \sim 50$ Km/h

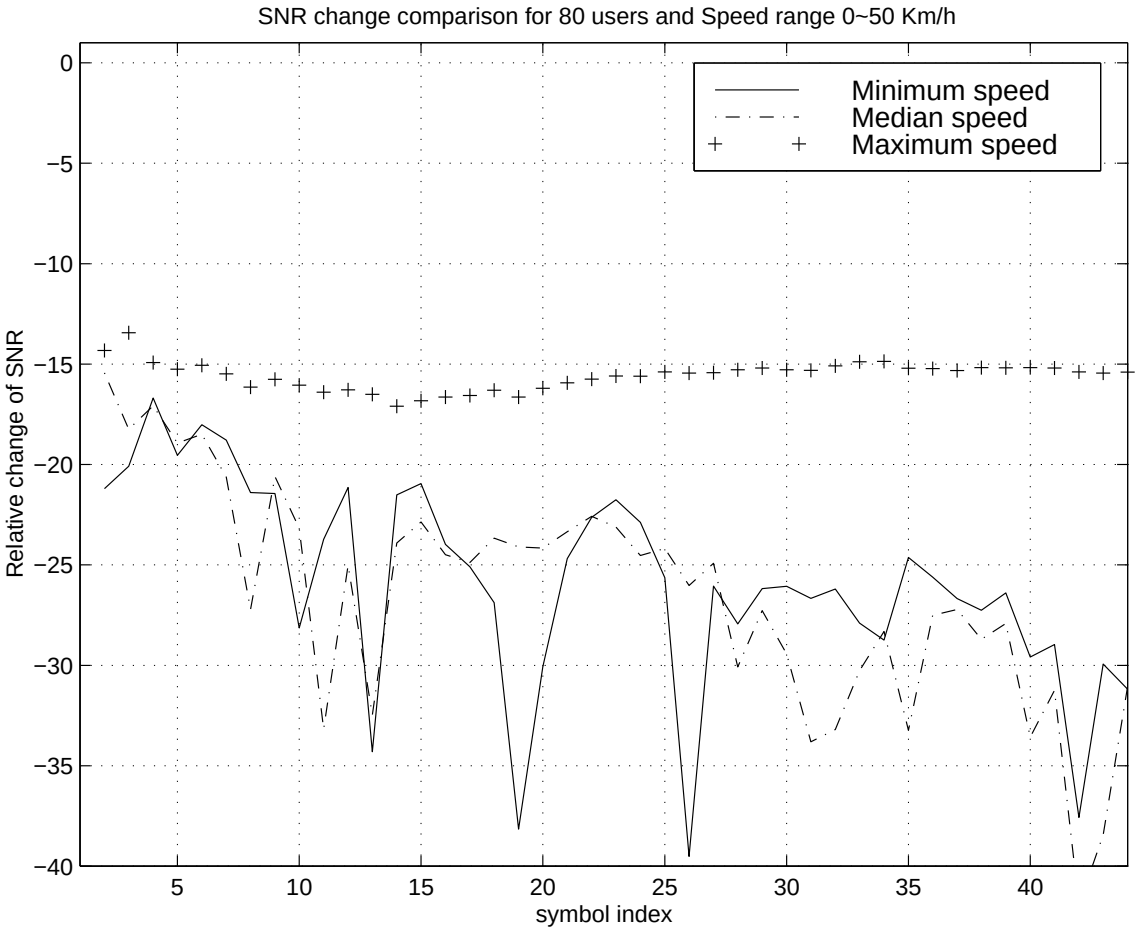

Figure 5.22: Using the PRLS algorithm to estimate the channel vector for 80 users and the speed range $0 \sim 50$ Km/h

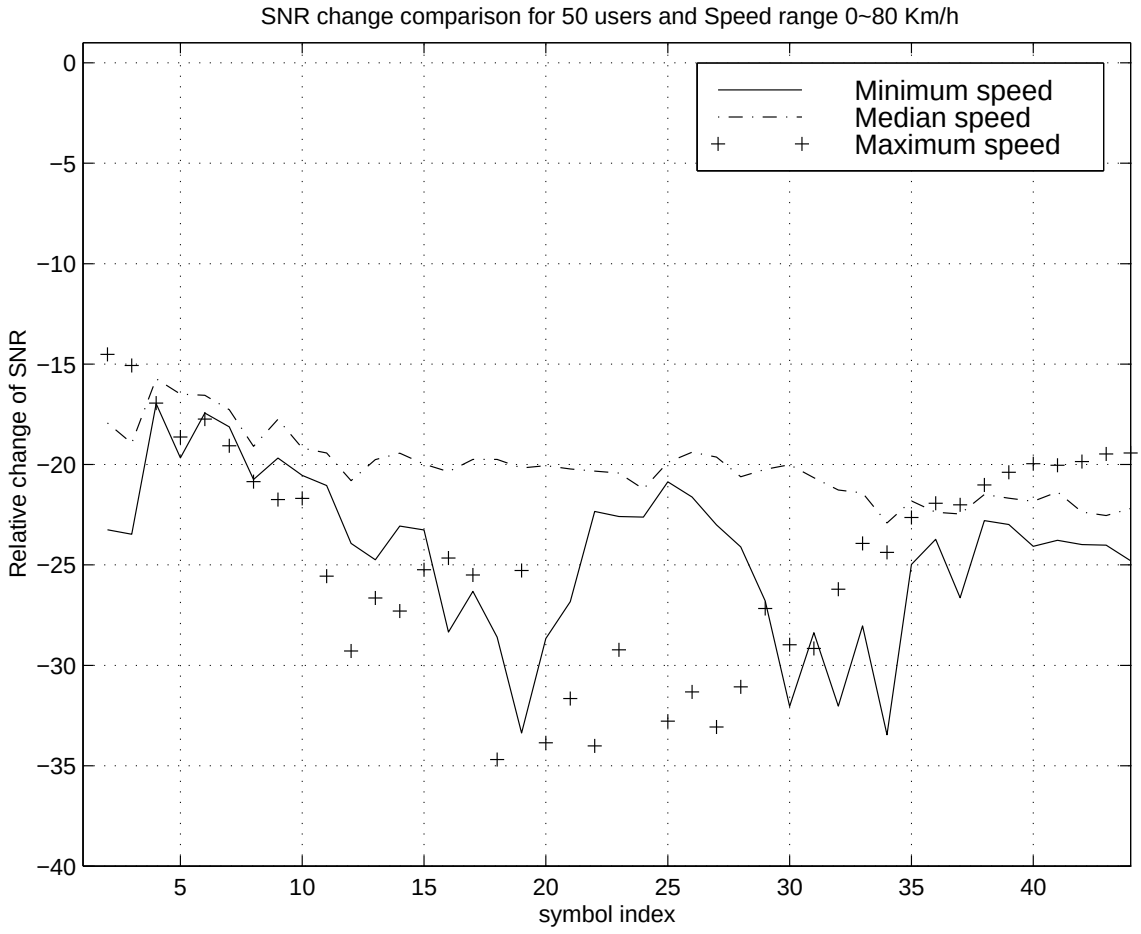

Figure 5.23: Using the PRLS algorithm to estimate the channel vector for 50 users and the speed range $0 \sim 80$ Km/h

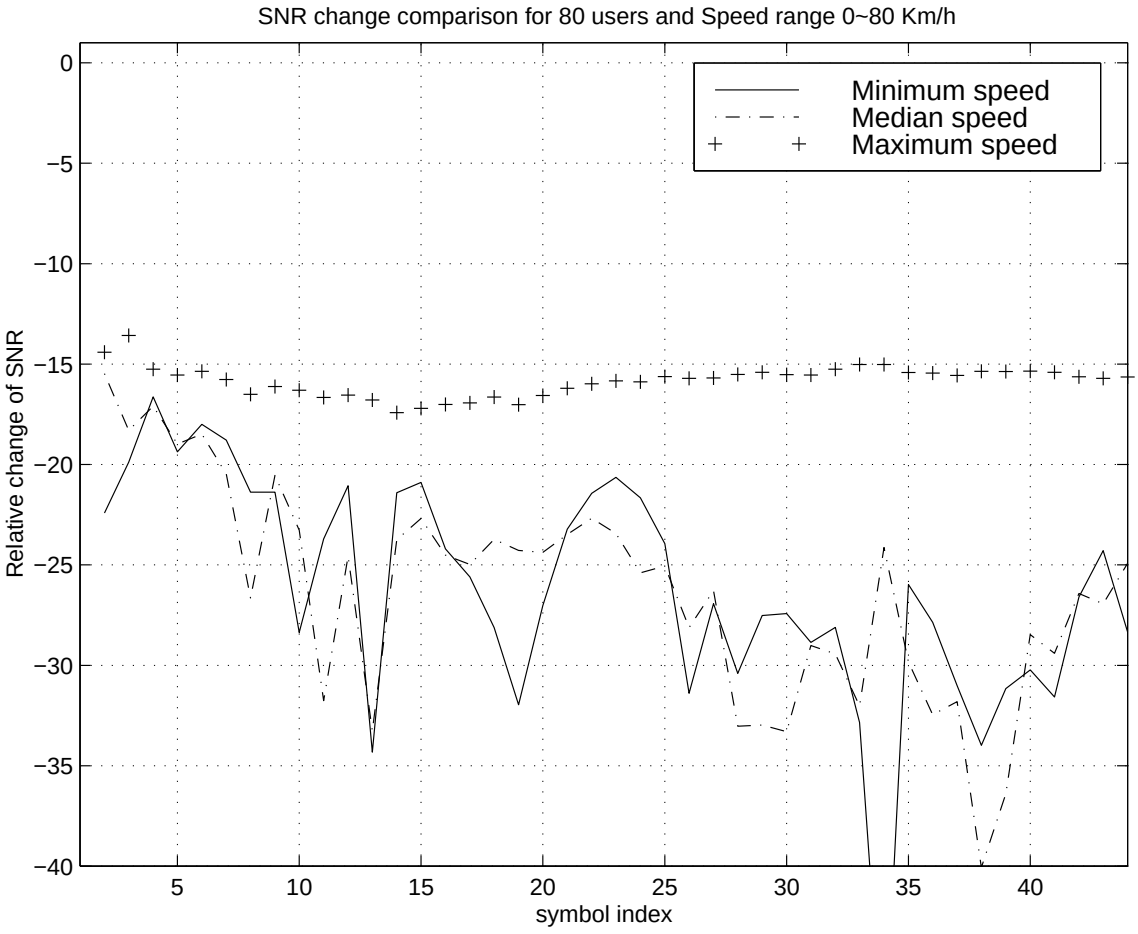

Figure 5.24: Using the PRLS algorithm to estimate the channel vector for 80 users and the speed range $0 \sim 80$ Km/h

Step #	Number of Flops
1	M
2	$2M^2+2M$
3	M
4	M
5	$4M^2$

Table 5.1: Computational complexity of the PRLS algorithm

5.6.5 Computation complexity of the PRLS algorithm

Here we examine the computation complexity of the PRLS algorithm. The PRLS algorithm is summarized in Figure 5.25. Table 5.1 gives the number of floating point operations(flops) for each step of the PRLS algorithm in Figure 5.25. The overall complexity of the PRLS algorithm is $6M^2 + 5M$. Compared with the standard RLS algorithm, the PRLS algorithm requires M more flops in Step 1 in Figure 5.25. The number of flops is the number of multiplication operation involved. We note that we make no distinction between real and complex numbers. As in Step 1, 2, 5, the product of a complex vector and a real scalar α will be require M complex flops.

Initialize the RLS algorithm:

$\hat{L} = 0$;

$\mathbf{W}(0) = \zeta \mathbf{I}$ $\quad (\mathbf{S}(0) = \zeta^{-1}\mathbf{I})$ and

set $\hat{\mathbf{w}}(0) = \mathbf{w}$ which is fed forward by the base station;

For each instant of time, $\hat{L}$=1,2,..., compute

{

1. Updating the perturbed weight vector $\hat{\mathbf{w}}(l)$

   $\hat{\mathbf{w}}(\hat{L}) = \hat{\mathbf{w}}(0) + \varpi ||\mathbf{w}|| \delta_{\mathbf{w}_L}$

2. Updating $\mathbf{u}(\hat{L})$

   $\mathbf{u}(\hat{L}) = \frac{\alpha^{-1}\mathbf{S}(\hat{L}-1)\hat{\mathbf{w}}(\hat{L})}{1+\alpha^{-1}\hat{\mathbf{w}}^{\mathbf{H}}(\hat{L})\mathbf{S}(\hat{L}-1)\hat{\mathbf{w}}(\hat{L})}$

3. Updating $\chi(\hat{L})$

   $\chi(\hat{L}) = g_k(\hat{L}) - \hat{\mathbf{w}}^{\mathbf{H}}(\hat{L})\mathbf{a}_k(\hat{L}-1)$

4. Updating $\mathbf{a}_k(\hat{L})$

   $\mathbf{a}_k(\hat{L}) = \mathbf{a}_k(\hat{L}-1) + \mathbf{u}(\hat{L})\chi^*(\hat{L})$

5. Updating $\mathbf{S}(\hat{L})$

   $\mathbf{S}(\hat{L}) = \alpha^{-1}\mathbf{S}(\hat{L}-1) - \alpha^{-1}\mathbf{u}(\hat{L})\hat{\mathbf{w}}^{\mathbf{H}}(\hat{L})\mathbf{S}(\hat{L}-1)$

}

Figure 5.25: Summary of the PRLS algorithm for estimating the kth mobile's downlink channel vector

5.7 Application and Comparison

5.7.1 Application to TDMA and FDMA system

The proposed method may be applied to TDMA or FDMA communication systems. We only need a downlink channel to feedforward weight information to the mobiles. As all mobiles share this downlink channel, the overhead entailed by adding this extra channel is small. In a FDMA system we do not need the frequency of the feedforward channel to lie in or near the frequency band of the information signals. This gives us a flexible choice. In a TDMA system we have flexible choice of the time slot. In addition, we have to estimate the scalar channel gain of the mobile stations. This may be done using the known 14 synchronization symbols in each user slot of 162 symbols in an IS-54 system [78]. In FDMA we may use a pilot tone to estimate the scalar channel gain.

5.7.2 Comparison of feedforward and feedback downlink channel estimation

Here we compared the downlink channel estimation methods in terms of overhead entailed by the probe and feedback [19, 20, 17] and the feedforward and feedback methods presented in this thesis. In the following part of this chapter, we refer to the probe/feedback method as the *feedback* method, and the feedforward/ feedback method as the *feedforward* method. As both methods use feedback from the mobiles to the base station, we compare them first.

5.7.2.1 Uplink comparison

In Gerlach's method [19, 20, 17], the mobile quantizes the channel response of r probing signals sent from the base station and feeds them back through the uplink channel. As the channel response of a specific probing signal is a complex number, we need to quantize each real/imaginary component of the channel response to b bits of resolvability, therefore the number of bits for transmitting these response vectors

	Gerlach's Method	Proposed Method
Uplink overhead	$> 2Mb$	$2Mb$
Downlink overhead	Dedicated Analog Channel	$2Mb$

Table 5.2: Comparison between Gerlach's method and proposed method

at each time is $2rb$. However, the feedback method requires

$$r \geq M \tag{5.102}$$

to uniquely determine the channel vectors at the M-element base station. In the feed-forward method, we quantize the estimated channel vector for that user and send it back through the uplink channel. As the dimension of the channel vector is M, the number of bits for transmitting the channel vector each time is $2Mb$. Obviously, the feed-forward method saves uplink bandwidth.

5.7.2.2 Downlink comparison

It is not possible to compare these two methods directly because in the feed-forward method, we need not interrupt the transmission of information signals. However, in the feedback method, the base station must stop transmitting information signals to transmit the probing signals because the probing signals lie in or near the frequency band of the information signals. We therefore examine the overhead due to feed-forward or probing. In the feedback method, the base station transmits r probing signals to all users sharing the same channel (frequency or time slot) in the same cell. In contrast, the feed-forward method quantizes the weights $\mathbf{w}$ and then broadcasts them through the pilot channel since the weights are common to all users in the same cell site. Analogous to the uplink, we obtain the number of bits for transmitting the quantized weights at each time is $2Mb$. The comparison is shown in Table 5.2.

5.8 Conclusion

This chapter presented a novel approach for downlink channel estimation in a cellular CDMA system and applied a RLS algorithm to update the channel estimates continuously. A maximum SNR downlink beamforming scheme was proposed and analyzed. We discussed implementation issues and the simulation results show the weights change smoothly at a smooth change in the MAI environment. Further, a perturbed RLS (PRLS) algorithm was proposed and analyzed and the simulation results show we can estimate downlink channel vectors very accurately. Finally, we indicated how our method may be extended to TDMA and FDMA communication systems.

Chapter 6

Summary and Conclusions

6.1 Introduction

This thesis began with a brief description of the motivation behind the problems investigated here. Then the background information for the thesis including DS-CDMA system data models, fading channel models and array signal processing techniques was examined in detail. An optimum uplink beamforming algorithm was proposed and analyzed. Further, an error analysis of uplink optimum beamforming was conducted and applied to the proposed optimum uplink beamforming algorithm. Finally, a new technique for downlink beamforming was proposed and analyzed.

This chapter first summarizes the contributions formulated in the thesis. Then conclusions are made in Section 6.3 from the research results in the thesis. Finally, Section 6.4 presents several future research directions based on the thesis.

6.2 Summary of contributions

- An original optimum uplink beamforming algorithm employing signal cancellation method, was proposed. It used direct PN sequence signal cancellation to obtain a signal-free IN covariance matrix. This directly estimated interference-noise covariance was applied to optimum beamforming. A finite-sample analysis of the algorithm was conducted and compared with the well known code-filtering approach [49] [51]. The proposed algorithm showed significant improvement

both in output $SINR$ and DOA estimation.

- The combined effect of estimation error from finite-sample covariance data, interference and thermal noise was analytically determined. We quantified how finite-sample errors in the estimation in both the array response and covariance matrices affect system SINR. As an application of the above results, we have applied this analysis to the optimum beamforming algorithm using signal cancellation proposed in Chapter 3. We showed that finite-sample estimation errors in the array response vector are independent of multi-access interference errors in this algorithm.

- A feedforward approach for downlink beamforming was proposed and analyzed. This algorithm reduces the amount of transmission overhead since channel estimates are obtained at the same time as data is being transmitted. We applied the RLS algorithm to estimate downlink channel vectors which are used to form the downlink beamforming weight vector. A perturbation version of the RLS algorithm was then proposed and analyzed to track the channel vector in a non-stationary environment. Finally, the application of feedforward approach to other multi-access wireless communication systems, TDMA and FDMA, was briefly discussed.

6.3 Conclusions

We propose a new algorithm to directly estimate the interference-noise covariance matrix using PN signal cancellation. We obtain improved DOA estimation and an average increase of 2.5dB in output SINR compared with [51] [49]. In addition, the computational complexity is less than that of [51] [49].

We presented the effect of antenna array beamforming errors on DS-CDMA communication systems. We have considered the situation where the errors in estimating the array response are independent from the errors in estimating the MAI. We have shown that the degradation of the output **SINR** increases as the number of antennas increases. When the variance of the errors in both the array response and the MAI matrix are the same, such as -15dB, there is nearly no degradation in the output

$SINR$ due to array errors but there is a 0.5dB $SINR$ degradation due to MAI matrix errors in the case of a 7-element array. We also show that as we increase the number of antennas to increase the $SINR$, the sensitivity to array response error does not change while the sensitivity to MAI matrix estimates increases proportionally. This analysis has been applied to the signal cancellation algorithm presented in Chapter 3, where Monte-Carlo simulation results and analytical calculation agreed quite closely.

A new approach for downlink channel estimation in a cellular CDMA system is proposed and a RLS algorithm was applied to update the channel estimates continuously. The results show the weights change smoothly with a smooth change in the MAI environment. With the help of weight perturbations, we may estimate downlink channel vectors much more accurately and use them for downlink beamforming.

6.4 Future directions

In Chapter 4, we have analyzed the effects of array response and covariance errors on the output SINR. An analysis of error in DOA estimation and its effect on the SINR of the downlink may be useful in downlink beamforming in a rural enviroment where the estimated DOA from the uplink data was used for downlink beamforming.

In Chapter 5, we have proposed a feedfward approach for downlink channel vector estimation for the case of a single cell case. Generalization to the multi-cell and multi-path case is a future research topic.

Bibliography

[1] Y. Akaiwa. "Antenna selection diversity for framed digital signal transmission in mobile radio channel". In *1989 IEEE 39th Vehicular Technology Conference*, pages 470–473, 1989.

[2] A. Baier. "An open multi-rate radio interface based on ds-cdma-the radio interface concept of codit". In *1993 RACE Mobile Telecommunication Workshop*, pages 123–128, 1993.

[3] A. Baier, U.C. Fiebig, W. Granzow, W. Koch, P. Teder, and J. Thieleche. "Design study of a CDMA-based third-generation mobile radio system". *IEEE Journal on Selected Areas in Communications*, 12(4):733–743, 1994.

[4] M. Benthin and K. Kammeryer. "Influence of channel estimation on the performance of coherent DS-CDMA system". *IEEE Transactions on Vehicular Technology*, 46(2):262–268, 1997.

[5] I. Chiba, T. Takahashi, and Y. Karasava. "Transmitting null beam forming with beam space adaptive array antennas". In *1994 IEEE 44th Vehicular Technology Conference*, pages 1498–1502, 1994.

[6] R.T. Compton. "The effect of random steering vector errors in the applebaum adaptive array". *IEEE Transactions on Aerospace and Electronic Systems*, 18(5):392–400, 1982.

[7] H. Cox. "Resolving power and sensitivity to mismatch of optimum array processors". *Journal of the Acoustical Society of America*, 54(3):771–785, 1973.

[8] R.C. Dixon. *Spread Spectrum Systems with Commercial Applications.* John Wiley & Sons, Inc., 1994.

[9] A.M. Earnshaw. *An Investigation into Improving Performance of Cellular CDMA Communication Systems with Digital Beamforming.* PhD thesis, Dept. of Electrical and Computer Engineering, Queen's University, 1997.

[10] A.M. Earnshaw and S.D. Blostein. "A chip-level IS95-compliant cellular CDMA simulator: Design, implementation, and analysis". Technical report, Department of Electrical and Computer Engineering, Queen's University, 1996. Available from `http://ipcl.ee.queensu.ca`.

[11] A.M. Earnshaw and S.D. Blostein. "Investigating the effects of imperfect digital beamforming on cell capacity in a cellular CDMA communication system". In *1996 International Conference on Universal Personal Communications*, pages 458–462, 1996.

[12] J.S. Engel. "The effects of cochannel interference on the parameters of a small-cell mobile telephone system". *IEEE Transactions on Vehicular Technology*, 18(3):110–116, 1969.

[13] C. Farsakh and J.A. Nossek. "Channel allocation and downlink beamforming in an SDMA mobile radio system". In *The Sixth Internation Symposium on Personal, Indoor and Mobile Radio Communications*, pages 687–691, 1995.

[14] C. Farsakh and J.A. Nossek. "A real time downlink channel allocation scheme for an sdma mobile radio system". In *The 7th Internation Symposium on Personal, Indoor and Mobile Radio Communications*, pages 1216–1220, 1996.

[15] Federal communications Commission. "Docket 18262, FCC report 14", 1968.

[16] P.G. Flikkema. "Spread-spectrum techniques for wireless communications". *IEEE Signal Processing Magazine*, 14(3):26–36, 1997.

[17] D. Gerlach. *Adaptive transmitting antenna arrays at the base station in mobile radio networks.* PhD thesis, Dept. of Electrical Engineering, Stanford University, 1995.

[18] D. Gerlach and A. Paulraj. "Base-station transmitting antenna arrays with mobile to base feedback". In *27th Asilomar Conference on Signals, Systems and Computers*, pages 1432–1436, 1993.

[19] D. Gerlach and A. Paulraj. "Adaptive transmitting antenna arrays with feedback". *IEEE Signal Processing Letters*, 1(10):150–152, 1994.

[20] D. Gerlach and A. Paulraj. "Base station transmitting antenna arrays for multipath environments". *Signal Processing*, 54(1):59–73, 1996.

[21] G.G.Raleigh and V.K.Jones. "Adaptive antenna transmission for frequency duplex digital wireless communication". In *1997 International Conference on Communications*, pages 641–646, 1997.

[22] L.C. Godara. "The effect of phase shifter errors on the performance of an antenna a rray beamformer". *IEEE Journal of Oceanic Engineering*, 10(3):278–284, 1985.

[23] L.C. Godara. "Error analysis of the optimal antenna array processors". *IEEE Transactions on Aerospace and Electronic Systems*, 22(4):395–409, 1986.

[24] J. Goldberg and J.R Fonollosa. "Downlink beamforming for saptially distributed sources in cellular mobile communications". In *ACTS Mobile Communications Summit*, pages 510–516, 1996.

[25] S.W. Golomb. *Shift Register Sequences.* Aegean Park Press, 1967.

[26] S. Haykin. *Adaptive Filter Theory.* Prentice-Hall, Inc., 1996.

[27] J.E. Hudson. *Adaptive Array Principles.* Peter Peregrinus Ltd., 1989.

[28] G.T. Irvine and P.J. McLane. "Symbol-aided plus decision-directed reception for PSK/TCM modulation on shadowed mobile satellite fading channels". *IEEE Journal on Selected Areas in Communications*, 10(8):1289–1299, 1992.

[29] W.C. Jakes. *Microwave Mobile Communications.* John Wiley & Sons, Inc., 1974.

[30] D.H. Johnson and D.E. Dudgeon. *Array Signal Processing – Concepts and Techniques.* Prentice-Hall, Inc., 1993.

[31] H.J. Schulte Jr. and W.A. Cornell. "Multi-area mobile telephone system". *IRE Trans. on Vehic. Commun.*, 9(1):49–53, 1960.

[32] B.C. Kuo. *Automatic Control Systems.* Prentice-Hall, 1987.

[33] I.D. Landau. *System identification and control design.* Prentice Hall, Inc., 1990.

[34] W.C.Y. Lee. *Mobile Communications Engineering.* McGraw-Hill Book Company, 1982.

[35] W.C.Y. Lee. "Overview of cellular CDMA". *IEEE Transactions on Vehicular Technology*, 40(2):291–302, 1991.

[36] J.W. Liang and A.J. Paulraj. "Forward link antenna diversity using feedback for indoor communication systems". In *1995 International Conference on Acoustics, Speech, and Signal Processing*, pages 1753–1755, 1995.

[37] C. Loo. "A statistical model for a land mobile satellite link". *IEEE Transactions on Vehicular Technology*, 34(3):122–127, 1985.

[38] T. Luo and S.D. Blostein. "Using signal cancellation for optimum beamforming in a cellular CDMA system". 1997. To appear in *1998 International Conference on Acoustics, Speech, and Signal Processing.*

[39] M.T. Ma. *Theory and Application of Antenna Arrays.* John Wiley & Sons, Inc., 1974.

[40] P.E. Mogensen and J. Wigard. "On antenna and frequency diversity in gsm related systems (GSM-900, DCS-1800,PCS-1900)". In *The Sixth Internation Symposium on Personal, Indoor and Mobile Radio Communications*, pages 1272–1276, 1996.

[41] R.A. Monzingo and T.W. Miller. *Introduction to Adaptive Arrays.* John Wiley & Sons, Inc., 1980.

[42] A.F. Naguib. *Adaptive Antennas for CDMA Wireless Networks.* PhD thesis, Dept. of Electrical Engineering, Stanford University, 1995.

[43] A.F. Naguib and A. Paulraj. "Base-station antenna array receiver for cellular DS/CDMA with M-ary orthogonal modulation". In *28th Asilomar Conference on Signals, Systems and Computers*, pages 858–862, 1994.

[44] A.F. Naguib and A. Paulraj. "Effects of multipath and base-station antenna arrays on uplink capacity of cellular CDMA". In *1994 Global Communication Conference*, pages 395–399, 1994.

[45] A.F. Naguib and A. Paulraj. "Performance of CDMA cellular networks with base-station antenna arrays". In *1994 International Zurich Seminar on Digital Communications*, pages 87–100, 1994.

[46] A.F. Naguib and A. Paulraj. "Performance enhancement and trade-offs of smart antennas in CDMA cellular networks". In *1995 IEEE 45th Vehicular Technology Conference*, pages 40–44, 1995.

[47] A.F. Naguib and A. Paulraj. "Performance of DS/CDMA with M-ary orthogonal modulation cell site antenna arrays". In *1995 International Conference on Communications*, pages 697–702, 1995.

[48] A.F. Naguib and A. Paulraj. "Recursive adaptive beamforming for wireless CDMA". In *1995 International Conference on Communications*, pages 1515–1519, 1995.

[49] A.F. Naguib and A. Paulraj. "Performance of wireless CDMA with M-ary orthogonal modulation and cell site antenna arrays". *IEEE Journal on Selected Areas in Communications*, 14(9):1770–1783, 1996.

[50] A.F. Naguib, A. Paulraj, and T. Kailath. "Capacity improvement of base-station antenna arrays: Cellular CDMA". In *27th Asilomar Conference on Signals, Systems and Computers*, pages 1437–1441, 1993.

[51] A.F. Naguib, A. Paulraj, and T. Kailath. "Capacity improvement with base-station antenna arrays in cellular CDMA". *IEEE Transactions on Vehicular Technology*, 43(3):691–698, 1994.

[52] A.F. Naguib, A. Paulraj, and T. Kailath. "Performance of CDMA cellular networks with base-station antenna arrays: The downlink". In *1994 International Conference on Communications*, pages 795–799, 1994.

[53] R. Nitzberg. "Effect of errors in adaptive weights". *IEEE Transactions on Aerospace and Electronic Systems*, 12(3):369–373, 1976.

[54] T. Ohgane. "Spectral efficiency evaluation of adaptive base station for land mobile cellular systems". In *1994 IEEE 44th Vehicular Technology Conference*, pages 1470–1474, 1994.

[55] A. Papoulis. *Probability, Random Variables, and Stochastic Processes*. McGraw-Hill, Inc., 1984.

[56] J.D. Parsons. *The mobile Radio Propagation Channel*. Halsted Press, 1992.

[57] R.L. Peterson, R.E. Ziemer, and D.E. Borth. *Introduction to Spread Spectrum Communications*. Prentice Hall, Inc., 1995.

[58] R.L. Pickholtz, L.B. Milstein, and D.L. Schilling. "Spread spectrum for mobile communications". *IEEE Transactions on Vehicular Technology*, 40(2):313–322, 1991.

[59] R.L. Pickholtz, D.L. Schilling, and L.B. Milstein. "Theory of spread-spectrum communications – A tutorial". *IEEE Transactions on Communications*, 30(5):855–884, 1982.

[60] S.U. Pillai. *Array Signal Processing*. Springer-Verlag, 1989.

[61] J.G. Proakis and M. Salehi. *Communication Systems Engineering*. Prentice-Hall, Inc., 1994.

[62] Qualcomm Inc. "Mobile station-base compatibility standard for dual-mode wide-band spread system", 1993.

[63] G. Raleigh, S.N. Diggavi, V.K. Jones, and A Paulraj. "A blind adaptive transmit antenna algorithm for wireless communication". In *1995 International Conference on Communications*, pages 1494–1499, 1995.

[64] G. Raleigh, S.N. Diggavi, A.F. Naguib, and A. Paulraj. "Characterization of fast fading vector channels for multi-antenna communication systems". In *28th Asilomar Conference on Signals, Systems and Computers*, pages 853–857, 1994.

[65] Jr. R.T. Comptoon. *Adaptive Arrays – Concepts and Performance.* Prentice Hall, Inc., 1988.

[66] L.L. Scharf. *Statictical Signal Processing.* Addison-Wesley, 1991.

[67] S. Souissi and S.B. Wicker. "A diversity combining DS/CDMA system with convolutional encoding and Viterbi decoding". *IEEE Transactions on Vehicular Technology*, 44(2):304–312, 1995.

[68] S. Soussi and S.B. Wicker. "A diversity combining DS/CDMA system with convolutional encoding and Viterbi decodings". In *1994 International Conference on Communications*, pages 1412–1416, 1994.

[69] G.W. Stewart and J.G. Sun. *Matrix Perturbation Theory.* Academic Press, 1990.

[70] B. Suard, A.F. Naguib, G. Xu, and A. Paulraj. "Performance of CDMA mobile communication systems using antenna arrays". In *1993 International Conference on Acoustics, Speech, and Signal Processing*, volume VI, pages 153–156, 1993.

[71] S. C. Swales, M.A. Beach, D.J. Edwards, and J.P. McGeehan. "The performance enhancement of multibeam adaptive base-station antennas for cellular land mobile radio systems". *IEEE Transactions on Vehicular Technology*, 39(1):56–67, 1990.

[72] D.J. Torrieri. "Performance of direct-sequence systems with long pseudonoise sequences". *IEEE Journal on Selected Areas in Communications*, 10(4):770–781, 1992.

[73] G.L. Turin. "The effects of multipath and fading on the performance of Direct-sequence CDMA systems". *IEEE Journal on Selected Areas in Communications*, 2(4):597–603, 1984.

[74] B.D. Van Veen and K.M. Buckley. "Beamforming: A versatile approach to spatial filtering". *IEEE ASSP Magazine*, pages 4–24, April 1988.

[75] R.G. Vaughan. "On optimum combining at the mobile". *IEEE Transactions on Vehicular Technology*, 37(4):181–188, 1988.

[76] M. Viberg and A.L. Swindlehurst. "Analysis of the combined effects of finite samples and model errors on array processing performance". *IEEE Transactions on Signal Processing*, 42(11):3073–3083, 1994.

[77] A.J. Viterbi. *CDMA: Principles of Spread Spectrum Communication.* Addison-Wesley, 1995.

[78] A.J. Weiss and B. Friedlander. "Fading effects on antenna arrays in cellular communications". *IEEE Transactions on Signal Processing*, 45(5):1109–1117, 1997.

[79] B. Widrow and J. McCool. "A comparasion of adaptive algorithm based on the methods of steeptest descent and random search. *IEEE Transactions on Antennas and Propagation*, 24(9):615–37, 1976.

[80] J.H. Winters. "Optimum combining in digital mobile radio with cochannel interference". *IEEE Journal on Selected Areas in Communications*, 2(4):528–539, 1994.

[81] J.H. Winters. "The diversity gain of transmit diversity in wireless systems with rayleigh fading". In *1994 International Conference on Communications*, pages 1121–1125, 1994.

[82] J.H. Winters, J. Salz, and R.D. Gitlin. "The impact of antenna diversity on the capacity of wireless communication systems". *IEEE Transactions on Communications*, 42(2/3/4):1740–1751, 1994.

[83] P. Zetterberg. *Mobile Cellular Communication with Base Station Antenna Arrays: Spectrum Efficiency, Algorithms and Propagation Models.* PhD thesis, Dept. of Signals, Sensors and Systemss, Royal Institute of Technology, Stockholm, Sweden, 1997.

[84] P. Zetterberg and B. Ottersten. "The spectrum efficiency of a base station antenna array system for spatially selective transmission". *IEEE Transactions on Vehicular Technology*, 44(3):651–660, 1995.

Vita

Tao Luo

EDUCATION

1996.9–1998.2	M.Sc (Engineering) Electrical Engineering, Kingston, Ontairo, Canada
1988.9–1992.7	B.S Electrical Engineering, Shanghai Jiao Tong University, Shanghai , P.R.China

AWARDS

1997–1998	Queen's Graduate Awards
1996–1997	Queen's Graduate Awards
1988–1992	Academic Awards in Shanghai Jiao Tong University

EXPERIENCE

1997–1998	Teaching Assistant Electrical and Computer Engineering, Queen's University
1996–1998	Research Assistant Electrical and Computer Engineering, Queen's University
1995–1996	Professional Engineer ABC Communications Co.Ltd
1994–1995	Senior Engineer AT&T Paradyne Far East Co.Ltd
1992–1994	Wireless Engineer Sunluck Communications Co.Ltd

PUBLICATIONS

T.Luo and Steven D. Blostein (1997), "Using Signal Cancellation for Optimum Beamforming in a Cellular CDMA system" to appear in *1998 International Conference on Acoustics, Speech, and Signal Processing*

T.Luo and Steven D. Blostein (1997), "Using Signal Cancellation for Optimum Beamforming in a Cellular CDMA system" , *Proceeding of the CITR Annual Research Conference*, Toronto, Canada, August, 1997